Continuous DPM Monitoring in Underground Mine Environments: Demonstration of Potential Options in the Laboratory and Field

Chelsea Anne Barrett

Thesis submitted to the faculty of the Virginia Polytechnic Institute and State University in partial fulfillment of the requirements for the degree of

Master of Science
In
Mining Engineering

Emily A. Sarver, Chair
Kray D. Luxbacher
Gerald H. Luttrell

February 2, 2018
Blacksburg, VA

Keywords: Diesel Particulate Matter, DPM, Elemental Carbon, Black Carbon, Continuous Monitoring

Continuous DPM Monitoring in Underground Mine Environments: Demonstration of Potential Options in the Laboratory and Field

Chelsea Anne Barrett

ACADEMIC ABSTRACT

Diesel particulate matter (DPM) is the solid portion of diesel exhaust. DPM occurs primarily in the submicron range, and poses a number of respiratory and other health hazards including cardiovascular and pulmonary disease. Underground miners typically have the highest DPM exposures compared to other occupations. This is because many mines are characterized by confined work spaces and large diesel equipment fleets. Exposures can be a particularly high hazard in large opening mines where ventilation can be challenging. As such, DPM monitoring is critical to protecting miner health and informing a range of engineering decisions.

DPM is primarily composed of two components, elemental carbon (EC) and organic carbon (OC), which are often summed to report total carbon (TC). The ratio of EC to OC, and presence of a number of other minor constituents such as sorbed metals, can vary with many factors such as engine operating conditions, maintenance, fuel types and additives, and the level and type of exhaust after-treatments used. Given its complexity, DPM cannot be measured directly, and either TC or EC are generally used as a surrogate. Currently, the Mining Safety and Health Administration (MSHA) limits personal exposures of underground metal/non-metal miners to 160 µg TC/m^3 on an 8-hr time weighted average basis. Compliance is demonstrated by collecting full-shift personal filter samples, which are later analyzed using the NIOSH 5040 Standard Method. For engineering purposes, area samples can also be collected and analyzed. The typical lag time between sample collection and reporting of results is on the order of weeks, and this presents a real problem for identifying and remediating conditions that led to overexposures or high DPM in area samples. The handheld FLIR Airtec monitor was developed to provide real-time DPM data and allow immediate decision making. The monitor works on a laser extinction principle to measure EC, the black component of DPM, as mass accumulates on a filter. The Airtec has proven useful for personal monitoring and short-term DPM surveying. However, capabilities are needed for continuous, long-term monitoring. Continuous DPM monitoring would be highly valuable for applications such as design and operation of ventilation on demand systems, or engineering studies of new ventilation, exhaust treatment or other DPM controls.

The work presented in this thesis considers three continuous monitors, two of which are already commercially available: Magee Scientific's AE33 black carbon (BC) Aethalometer and Sunset Laboratory's Semi-Continuous OCEC Field Analyzer. The third monitor, called the Airwatch, is still in development. The AE33 and Airwatch effectively operate on the same principle as the Airtec, but include a self-advancing filter tape to allow autonomous operation over relatively long periods of time. The OCEC field monitor is essentially a field version of the laboratory analyzer used for traditional 5040 Method analysis. The AE33 has been briefly demonstrated in mine environments in a couple of other studies, but further testing is needed. The current prototype of the Airwatch and the OCEC field monitor have never been mine-tested.

Two separate studies are reported here. The first is a field study in an underground stone mine that tested the Airwatch prototype and AE33 head-to-head under relatively high DPM conditions. Results demonstrated that both instruments could track general trends, but that further work was needed to identify and resolve issues associated with use of both instruments in high-DPM environments – and with basic design elements of the Airwatch. Additionally, the need to calibrate the monitors' output data to the standard measure of EC (i.e., 5040 Method EC) was made clear.

In the second study, laboratory testing was conducted under very controlled conditions to meet this need, and another round of field testing was also done. The second study also included the OCEC field monitor. The laboratory tests yielded data to allow interpretation of the AE33 and Airwatch results with respect to 5040 EC. These tests also shed light on the current range EC concentrations over which these monitors can provide reliable data – which is indeed a primary range of interest for mines. As expected, the OCEC field monitor was shown to produce lab-grade results across a wide range of concentrations. The field testing in the second study demonstrated that all three monitors could operate autonomously in a mine environment over extended periods of time (i.e., weeks to months). Overall, it can be concluded that the AE33 and OCEC field monitor represent off-the-shelf options for DPM monitoring in mines, and the Airwatch might be another option if fully developed in the future. Selection of a

particular monitoring tool should include careful consideration of specific factors including data quality needs, conditions in the intended monitoring location(s), and general user friendliness of the monitor.

Continuous DPM Monitoring in Underground Mine Environments: Demonstration of Potential Options in the Laboratory and Field

Chelsea Anne Barrett

GENERAL AUDIENCE ABSTRACT

Diesel particulate matter (DPM) is the solid portion of diesel exhaust. DPM occurs primarily in the submicron range (i.e., below 0.8 μm), and poses a number of respiratory and other health hazards including cardiovascular and pulmonary disease. Underground miners typically have the highest DPM exposures compared to other occupations. This is because many mines are characterized by confined work spaces and large diesel equipment fleets. Exposures can be a particularly high hazard in large opening mines where ventilation can be challenging. As such, DPM monitoring is critical to protecting miner health and informing a range of engineering decisions.

DPM is primarily composed of two components, elemental carbon (EC) and organic carbon (OC), which are often summed to report total carbon (TC). The ratio of EC to OC, can vary with many factors such as engine operating conditions, maintenance, fuel types and additives, and the level and type of exhaust after-treatments used. Given its complexity, DPM cannot be measured directly, and either TC or EC are generally used as a surrogate. Currently, the Mining Safety and Health Administration (MSHA) limits personal exposures of underground metal/non-metal miners to 160 μg TC/m^3 on an 8-hr time weighted average basis. Compliance is demonstrated by collecting full-shift personal filter samples, which are later analyzed using the NIOSH 5040 Standard Method. For engineering purposes, area samples can also be collected and analyzed. The typical lag time between sample collection and reporting of results is on the order of weeks, and this presents a real problem for identifying and remediating conditions that led to overexposures or high DPM in area samples. The handheld FLIR Airtec monitor was developed to provide real-time DPM data and allow immediate decision making. The monitor works on a laser extinction principle to measure EC, the black component of DPM, as mass accumulates on a filter. The Airtec has proven useful for personal monitoring and short-term DPM surveying. However, capabilities are needed for continuous, long-term monitoring. Continuous DPM monitoring would be highly valuable for applications such as design and operation of ventilation on demand systems, or engineering studies of new ventilation, exhaust treatment or other DPM controls.

The work presented in this thesis considers three continuous monitors, two of which are already commercially available: Magee Scientific's AE33 black carbon (BC) Aethalometer and Sunset Laboratory's Semi-Continuous OCEC Field Analyzer. The third monitor, called the Airwatch, is still in development. The AE33 and Airwatch effectively operate on the same principle as the Airtec, but include a self-advancing filter tape to allow autonomous operation over relatively long periods of time. The OCEC field monitor is essentially a field version of the laboratory analyzer used for traditional 5040 Method analysis. The AE33 has been briefly demonstrated in mine environments in a couple of other studies, but further testing is needed. The current prototype of the Airwatch and the OCEC field monitor have never been mine-tested.

Two separate studies are reported here. The first is a field study in an underground stone mine that tested the Airwatch prototype and AE33 head-to-head under relatively high DPM conditions. Results demonstrated that both instruments could track general trends, but that further work was needed to identify and resolve issues associated with use of both instruments in high-DPM environments – and with basic design elements of the Airwatch. Additionally, the need to calibrate the monitors' output data to the standard measure of EC (i.e., 5040 Method EC) was made clear.

In the second study, laboratory testing was conducted under very controlled conditions to meet this need, and another round of field testing was also done. The second study also included the OCEC field monitor. The laboratory tests yielded data to allow interpretation of the AE33 and Airwatch results with respect to 5040 EC. These tests also shed light on the current range EC concentrations over which these monitors can provide reliable data – which is indeed a primary range of interest for mines. As expected, the OCEC field monitor was shown to produce lab-grade results across a wide range of concentrations. The field testing in the second study demonstrated that all three monitors could operate autonomously in a mine environment over extended periods of time (i.e., weeks to months). Overall, it can be concluded that the AE33 and OCEC field monitor represent off-the-shelf options for DPM monitoring in mines, and the Airwatch might be another option if fully developed in the future. Selection of a

particular monitoring tool should include careful consideration of specific factors including data quality needs, conditions in the intended monitoring location(s), and general user friendliness of the monitor.

ACKNOWLEDGEMENTS

First and foremost, I would like to extend my utmost gratitude to my advisor Dr. Emily Sarver for the continuous support and guidance she has offered throughout my career as a graduate student. I am extremely grateful and appreciative for the time, effort, and knowledge she brought forth to help me achieve my goals and conclude my studies.

I would also like to thank my committee members, Dr. Gerald Luttrell and Dr. Kray Luxbacher for their insight and encouragement.

I would like to thank CDC/NIOSH for funding this work under contract no. 200-2014-59646. I am extremely appreciative of the support and technical advice given by Mr. Christopher Pritchard, Dr. James Noll, Dr. Emanuele Cauda, and Mr. Shawn Vanderslice.

I would like to express my thanks to Magee Scientific for the extended loaning of the AE33 Aethalometer, as well as the technical support provided during this process. I would especially like to thank Dr. Jon Volkwein and Dr. Tony Hansen for their technical insight and support.

A very special thank you to all of the miners and personnel at the study mine that supported, encouraged, and taught me valuable lessons while gathering data. Their insight, knowledge, and hospitality was incredibly helpful and heartening.

Finally, I would like to thank my friends and family for supporting me through my graduate experience. I'm especially thankful of Kody Musick, Sallie Gaillard, and Lauren English for their unconditional support and friendship during this time. I am incredibly thankful for my parents, Ryan and Deanne Harrison, my grandmother, Elsie Carr, and my sister, Lauren Jones for their encouragement and patience over the past year and a half.

TABLE OF CONTENTS

TABLE OF CONTENTS vii
LIST OF FIGURES viii
LIST OF TABLES xi
PREFACE xii

Chapter 1. Review of Continuous DPM Monitoring Capabilities for Underground Mining Applications 1
1. Background. 1
2. DPM Sampling and Analysis by 5040 2
3. Continuous Monitoring 3
4. DPM Monitoring using the Laser Extinction Principle 3
4.1 Airtec Monitor 5
4.2 Airwatch Monitor 5
4.3 AE33 Aethalomter 6
4.4 Filter Loading Effect and Consumption 6
5. Semi-Continuous OCEC Field Monitor 7
6. Conclusions 7
7. References. 8
Chapter 2. Demonstration of Continuous Monitors for Tracking DPM Trends over Prolonged Periods in an Underground Mine 10
Abstract 10
1. Introduction 10
1.1 DPM Monitoring 10
2. Experimental Site and Methods 11
2.1 Study Site 11
2.2 Monitoring Schedule and Equipment 12
2.3 Airwath Calibration and Data Processing 13
3. Results and Discussion 13
3.1 Continuous Monitoring Over Extended Peiods 13
3.2 Filter Tape Loading and Sample Dilution 16
4. Conclusions 17
5. Acknowledgements 18
6. Works Cited 18
Chapter 3. Comparison of Several DPM Field Monitors for Use in Underground Mining Applications 19
Abstract 19
1. Introduction 19
2. Experimental Details 21
2.1 Laboratory Testing 21
2.2 Field Testing 22
2.3 Data Analysis 23
3. Results and Discussion 25
3.1 Laboratory Testing 25
3.2 Field Testing 29
3.3 Discussion 32
4. Conclusions 32
5. Acknowledgements 32
6. References 33
Summary and Conclusions 35
Appendix A. Chapter 3 Supplemental Data 36

LIST OF FIGURES

Figure 1.1: Example thermogram from analysis of a DPM sample analyzed by the 5040 Standard Method. The sample was collected in a controlled laboratory experiment where DPM was the only particulate present in the sampling chamber. 3
Figure 1.2: Illustrative plot showing idealized decay of optical sensor voltage with increasing blackness on a DPM sample filter. 4
Figure 1.3: Illustrative plot of voltage decay where filter loading effect is evident. 6
Figure 2.1. Airwatch calibration curve. The data point shown as an x was not used in generating a best-fit line. 13
Figure 2.2: 5-minute rolling average EC or BC concentration ($\mu g/m^3$) data collected using the AE33, Airwatch, and Airtecs in monitoring periods 1-5 (plots a-e, respectively). TWA EC concentration ($\mu g/m^3$) derived from 5040 sample analysis is also shown 15
Figure 2.3: Data illustrating Airwatch and AE33 filter loading effect, corresponding to Figure 2(b). Close-up image inset taken from Thursday evening. ..... **Error! Bookmark not defined.**
Figure 3.1: Example test data (high concentration lab test). TWA EC concentrations are shown for 5040 and OCEC field monitor, EC concentration is shown for Airtec, (raw) BC concentration is shown for AE33, and calculated absorbance values are shown for Airwatch. ..... **Error! Bookmark not defined.**
Figure 3.2: TWA EC concentration measured by OCEC field monitor versus 5040 Method for laboratory tests. Error bars represent 95% confidence intervals for replicate 5040 samples results; confidence intervals were not computed for OCEC field monitor data since individual samples collected within each test had variable collection times. ..... **Error! Bookmark not defined.**
Figure 3.3: TWA EC concentration measured by Airtec monitors versus 5040 Method for laboratory tests. Error bars represent 95% confidence intervals for replicate 5040 samples and Airtec (5 monitors) results. Data points for tests 10,11, and 19 are labeled, and these tests had relatively high sample masses of 98.71, 111.73, and 122.67 μg, respectively. 27
Figure 3.4: Corrected AE33 BC concentration versus 5040 EC concentration for low DPM laboratory tests. Error bars represent 95% confidence intervals for replicate 5040 samples; confidence intervals were not computed for AE33 data since individual filter spots within each tests had variable collection times. 27
Figure 3.5: First-minute AE33 BC concentration versus 5040 EC concentration for laboratory tests. Error bars represent 95% confidence intervals for replicate 5040 samples and first-minute data from all AE33 filter spots in each tests. 28
Figure 3.6: Airwatch calibration curve showing EC mass accumulated on filter versus laser absorbance. 29
Figure 3.7: Bias plots for OCEC field monitor, Airtec, AE33, and Airwatch monitors (a-d respectively) as compared to 5040 EC concentrations. 31
Figure 3.8: EC concentration measured by the OCEC field monitor, AE33, and Airwatch over six consecutive days (Thursday to Wednesday) in an underground stone mine. Airwatch concentrations were determined on a 5-minute rolling average for this plot. 32
Figure 3.9: Comparison of AE33 and Airwatch EC concentrations to OCEC EC concentration for duration of 8-week field study. 32
Figure A.1: AE33 BC uncorrected concetration as a function of 5040 EC concentration. Error bars represent 95% confidence in replicate 5040 values. 39
Figure A.2: Time series data for an 8-week field study divided into 8 separate weeks. Airwatch data was analyzed on a minute by minute basis for this plot. AE33 BC data was used. 41
Figure A.3: Sample 1-A thermogram. Second punch analysis used 43
Figure A.4: Sample 1-B thermogram. Second punch analysis used 43
Figure A.5: Sample 1-C thermogram. Second punch analysis used 43
Figure A.6: Sample 1-D thermogram. Second punch analysis used 44
Figure A.7: Sample 1-E thermogram. Second punch analysis used 44
Figure A.8: Sample 2-A thermogram. 44
Figure A.9: Sample 2-B thermogram. 45
Figure A.10: Sample 2-C thermogram. 45
Figure A.11: Sample 2-D thermogram. 45
Figure A.12: Sample 2-E thermogram. 46
Figure A.13: Sample 3-A thermogram. Second punch analysis used 46
Figure A.14: Sample 3-B thermogram. Second punch analysis used 46
Figure A.15: Sample 3-C thermogram. Second punch analysis used 47

Figure A.16: Sample 3-D thermogram. Second punch analysis used 47
Figure A.17: Sample 3-E thermogram. Second punch analysis used 47
Figure A.18: Sample 4-A thermogram. 48
Figure A.19: Sample 4-B thermogram. 48
Figure A.20: Sample 4-C thermogram. 48
Figure A.21: Sample 4-D thermogram. 49
Figure A.22: Sample 4-E thermogram. 49
Figure A.23: Sample 5-A thermogram. Second punch analysis used 49
Figure A.24: Sample 5-B thermogram. Second punch analysis used 50
Figure A.25: Sample 5-C thermogram. Second punch analysis used 50
Figure A.26: Sample 5-D thermogram. Second punch analysis used. 50
Figure A.27: Sample 5-E thermogram. Second punch analysis used. 51
Figure A.28: Sample 6-A thermogram. Second punch analysis used. 51
Figure A.29: Sample 6-B thermogram. Second punch analysis used. 51
Figure A.30: Sample 6-C thermogram. Second punch analysis used. 52
Figure A.31: Sample 6-D thermogram. Second punch analysis used. 52
Figure A.32: Sample 6-E thermogram. Second punch analysis used. 52
Figure A.33: Sample 7-A thermogram. Second punch analysis used. 53
Figure A.34: Sample 7-B thermogram. Second punch analysis used. 53
Figure A.35: Sample 7-C thermogram. 53
Figure A.36: Sample 7-D thermogram. 54
Figure A.37: Sample 7-E thermogram. Second punch analysis used. 54
Figure A.38: Sample 8-A thermogram. 54
Figure A.39: Sample 8-B thermogram. 55
Figure A.40: Sample 8-C thermogram. 55
Figure A.41: Sample 8-E thermogram. 55
Figure A.42: Sample 9-A thermogram. Second punch analysis used. 56
Figure A.43: Sample 9-B thermogram. Second punch analysis used. 56
Figure A.44: Sample 9-C thermogram. Second punch analysis used. 56
Figure A.45: Sample 9-D thermogram. Second punch analysis used. 57
Figure A.46: Sample 9-E thermogram. 57
Figure A.47: Sample 10-A thermogram. Second punch analysis used. 57
Figure A.48: Sample 10-B thermogram. Second punch analysis used. 58
Figure A.49: Sample 10-C thermogram. Second punch analysis used. 58
Figure A.50: Sample 10-D thermogram. Second punch analysis used. 58
Figure A.51: Sample 10-E thermogram. 59
Figure A.52: Sample 11-A thermogram. 59
Figure A.53: Sample 11-B thermogram. 59
Figure A.54: Sample 11-C thermogram. 60
Figure A.55: Sample 11-D thermogram. 60
Figure A.56: Sample 11-E thermogram. 60
Figure A.57: Sample 12-A thermogram. 61
Figure A.58: Sample 12-B thermogram. 61
Figure A.59: Sample 12-C thermogram. 61
Figure A.60: Sample 12-D thermogram. 62
Figure A.61: Sample 12-E thermogram. 62
Figure A.62: Sample 13-A thermogram. 62
Figure A.63: Sample 13-B thermogram. 63
Figure A.64: Sample 13-C thermogram. 63
Figure A.65: Sample 13-D thermogram. 63
Figure A.66: Sample 14-A thermogram. 64
Figure A.67: Sample 14-B thermogram. 64
Figure A.68: Sample 14-C thermogram. 64
Figure A.69: Sample 14-D thermogram. 65
Figure A.70: Sample 14-E thermogram. 65
Figure A.71: Sample 15-A thermogram. Second punch analysis used. 65

Figure A.72: Sample 15-B thermogram. Second punch analysis used. 66
Figure A.73: Sample 15-C thermogram. 66
Figure A.74: Sample 15-D thermogram. Second punch analysis used. 66
Figure A.75: Sample 15-E thermogram. 67
Figure A.76: Sample 16-A thermogram. Second punch analysis used. 67
Figure A.77: Sample 16-B thermogram. Second punch analysis used. 67
Figure A.78: Sample 16-C thermogram. Second punch analysis used. 68
Figure A.79: Sample 16-D thermogram. Second punch analysis used. 68
Figure A.80: Sample 16-E thermogram. Second punch analysis used. 68
Figure A.81: Sample 17-A thermogram. Second punch analysis used. 69
Figure A.82: Sample 17-B thermogram. Second punch analysis used. 69
Figure A.83: Sample 17-C thermogram. Second punch analysis used. 69
Figure A.84: Sample 17-D thermogram. 70
Figure A.85: Sample 17-E thermogram. 70
Figure A.86: Sample 18-A thermogram. 70
Figure A.87: Sample 18-B thermogram. 71
Figure A.88: Sample 18-C thermogram. 71
Figure A.89: Sample 18-D thermogram. 71
Figure A.90: Sample 18-E thermogram. 72
Figure A.91: Sample 19-A thermogram. 72
Figure A.92: Sample 19-B thermogram. 72
Figure A.93: Sample 19-C thermogram. 73
Figure A.94: Sample 19-D thermogram. 73
Figure A.95: Sample 19-E thermogram. 73
Figure A.96: 9.29.2017 unit 1 field sample thermogram. 74
Figure A.97: 9.29.2017 unit 2 field sample thermogram. 74
Figure A.98: 10.02.2017 unit 1 field sample thermogram. 74
Figure A.99: 10.02.2017 unit 2 field sample thermogram. 75
Figure A.100: 10.02.2017 unit 3 field sample thermogram. 75
Figure A.101: 10.09.2017 unit 1 field sample thermogram. 75
Figure A.102: 10.09.2017 unit 2 field sample thermogram. 76
Figure A.103: 10.09.2017 unit 3 field sample thermogram. 76
Figure A.104: 10.27.2017 unit 1 field sample thermogram. 76
Figure A.105: 10.27.2017 unit 2 field sample thermogram. 77
Figure A.106: 10.27.2017 unit 3 field sample thermogram. 77
Figure A.107: 10.30.2017 unit 1 field sample thermogram. 77
Figure A.108: 10.30.2017 unit 2 field sample thermogram. Second punch anlaysis used. 78
Figure A.109: 10.30.2017 unit 3 field sample thermogram. 78
Figure A.110: 11.02.2017 unit 1 field sample thermogram. 78
Figure A.111: 11.02.2017 unit 2 field sample thermogram. Second punch anlaysis used. 79
Figure A.112: 11.02.2017 unit 3 field sample thermogram. 79
Figure A.113: 11.06.2017 unit 1 field sample thermogram. 79
Figure A.114: 11.06.2017 unit 2 field sample thermogram. 80
Figure A.115: 11.06.2017 unit 3 field sample thermogram. Second punch analysis used. 80
Figure A.116: 11.10.2017 unit 1 field sample thermogram. 80
Figure A.117: 11.10.2017 unit 2 field sample thermogram. 81
Figure A.118: 11.10.2017 unit 3 field sample thermogram. 81
Figure A.119: 11.13.2017 unit 1 field sample thermogram. 81
Figure A.120: 11.13.2017 unit 2 field sample thermogram. 82
Figure A.121: 11.13.2017 unit 3 field sample thermogram. 82
Figure A.122: 11.17.2017 unit 1 field sample thermogram. 82
Figure A.123: 11.17.2017 unit 2 field sample thermogram. 83
Figure A.124: 11.17.2017 unit 3 field sample thermogram. 83
Figure A.125: 11.20.2017 unit 1 field sample thermogram. 83
Figure A.126: 11.20.2017 unit 2 field sample thermogram. 84
Figure A.127: 11.20.2017 unit 3 field sample thermogram. 84

LIST OF TABLES

Table 1.1: Summary of monitors that utilize the laser extinction principle. 5
Table 2.1: Monitoring dates and equipment used/samples collected. 12
Table 3.1: Summary of tests run during calibration study. 22
Table 3.2: Summary of calibration equipment, cut size, size selector, and operational flow rates used. 22
Table A.1: Monitoring dates and equipment used for sample collection. 36
Table A.2: Summary of all used 5040 samples raw EC data. Highlighted values were identified as outliers. NA indicates that no data was available because the sample filter was not seated properly in the cassette. 36
Table A.3: Summary of all calibration data results for various analysis methods. NA indicates 95% confidence internval could not be calculated due to test only having one sample. 37
Table A.4: Summary of outlier data points identified for each instrument. Outliers were determined as points over three σ away from the mean instrument to 5040 ratio. 37
Table A.5: Summary of field 5040 EC concentrations and number of samples used in analysis. Highlighted values represent outliers. 38
Table A.6: Summary of all TWA values for each monitor during field testing. 39

PREFACE

This thesis includes three main chapters, which address the need and current options for continuous diesel particulate matter (DPM) monitoring in a underground mine settings. The research was conducted as part of a capacity building project "DPM Research: Monitoring Responses to Ventilation and Control by Water Sprays, and Capacity Building for Mine Ventilation Expertise", which is funded by CDC/NIOSH (contract No. 200-2014-59646). All field work was conducted in the same underground stone mine, which has partnered with Virginia Tech and graciously offered access to the operation as support and for this research.

Chapter 1 provides a brief review of DPM as an occupational hazard in underground mine settings and the conventional strategy for sampling and monitoring (i.e., the NIOSH 5040 Standard Method). It then lays out underlying principles for continuous monitoring, which are either based on thermo-optical analysis or the laser extinction, and summarizes current options in terms of off-the-shelf and in-development monitors – all of which have seen limited or no previous testing in underground mines.

In Chapter 2, the prototyped Airwatch monitor and the commercially-available Magee Scientific AE33 Aethalometer were used to continuously track DPM trends over multi-day periods of time at a single location within the study mine. These results were periodically compared to the standard measure of DPM (i.e., 5040 Method) to determine general accuracy of the instruments. Chapter 2 was presented at the 16th North American Mine Ventilation Symposium and included in the peer-reviewed proceedings from that meeting. It has been reproduced here with written permission from the publisher.

In Chapter 3, the Airwatch, AE33, and Sunset Laboratories' Semi-continuous OCEC Field Analyzer were all tested head-to head in both the laboratory and field. The lab tests were conducted in the diesel research laboratory at NIOSH's Office of Mine Safety and Health Research facility near Pittsburgh, PA, and covered a wide range of DPM concentrations in an effort to evaluate the monitors' reliability against the 5040 Method results. Following the lab testing, the monitors were deployed underground for a duration of approximately eight weeks, and again periodic measurements were made with the 5040 Method for comparison. Chapter 3 will be submitted for peer-review and publication in a research journal.

In conjunction with the work presented here, Chelsea Barrett and Emily Sarver co-authored an additional paper with J. Volkwein and A. Hansen (Magee Scientific). The paper "Application of an Environmental 'Black Carbon' Particulate Sensor for Continuous Measurement of DPM in Three Underground Mines" was presented at the 2017 Australian Mine Ventilation Conference and published in the peer-reviewed proceedings (paper 96). It included a series of separate data sets collected by Ms. Barrett using the AE33 monitor in the same partner mine as studied in Chapters 2 and 3. These data were used to demonstrate the general utility of the AE33 for tracking DPM trends in several key locations of the mine.

Review of Continuous DPM Monitoring Capabilities for Underground Mining Applications

Chelsea Barrett[1], Emily Sarver[1]
[1]*Virginia Tech*

Background

Diesel exhaust is generated due to the combustion of fuel within an engine. It is composed of a gaseous portion and a solid portion known as diesel particulate matter (DPM). DPM generally occurs within the submicron range and is primarily composed of elemental carbon (EC) and organic carbon (OC) [1,2]. Due to the small size of DPM, the particles are easily respired and can deposit deep within the lung tissue. This deposition can lead to a range of health problems such as respiratory irritation, cardiovascular damage, and lung tissue inflammation [3]. While whole diesel exhaust has been classified as a carcinogen, it has yet to be determined what role the DPM itself plays in cancer and other disease [4,5].

In general, underground miners face the highest occupational exposures to DPM due to frequent use of large diesel-powered equipment in confined work spaces [6]. In mines with challenging ventilation conditions (e.g., mines with very large openings, very deep mines), DPM levels can be particularly high. To protect underground miners, the US Mine Safety and Health Administration (MSHA) regulates personal exposures to DPM in metal/non-metal mines[1]. DPM cannot be measured directly due to its varying composition (i.e. ratio of OC and EC) and the tendency to co-occur with dust particles that are often carbonaceous in composition [8]. To account for these variances, MSHA uses total carbon (TC), which is the sum of EC and OC, as a surrogate to determine exposure levels in metal and non-metal mines [7]. Currently, the regulatory limit for personal exposures is set at 160 μg TC/m^3 on the basis of an 8-hr time period TWA (time weighted average) [9].

To demonstrate regulatory compliance, the NIOSH 5040 Standard Method is used to measure EC and OC (summed to TC) in personal filter samples. For engineering purposes, it can also be used to analyze filter samples collected for area monitoring. The 5040 Method is typically conducted in a centralized, certified facility using a Laboratory OCEC Aerosol Analyzer (Sunset Laboratory Inc., Tigard, OR). The lag time between sample collection and analysis can be lengthy, which prohibits immediate corrective actions. Rather, overexposures and/or undesirable conditions are only identified well after-the-fact, and correlation to specific activities or events may be difficult.
To address this issue, the handheld Airtec monitor (FLIR Industries, Nashua, NH) was designed to aid mine operators in monitoring DPM concentrations in near real time [10,11]. The instrument can be used to track personal exposures over several hours or for the entire duration of a shift, and can also act as a valuable engineering tool (e.g., for "spot checking" certain areas of interest) [12]. The units are commercially available and have been calibrated to 5040 EC. They can estimate TC through an assumed correction factor (i.e., a TC to EC ratio of 1.3, which is based on a comprehensive study of TC and EC in many underground metal/non-mental mines [13]).

Even with the development of the Airtec, there still exist needs for continuous and autonomous DPM monitoring systems. Mines could benefit from the ability to track DPM trends to discover and monitor problem areas, monitor concentrations continuously to protect miners, and incorporate DPM monitoring instruments into ventilation on demand (VOD) systems to help improve environmental conditions and lower operating costs. To meet these needs, a continuous version of the Airtec called the Airwatch was initially designed and prototyped by Nomadics Inc. (later bought by FLIR, Inc.) Following some preliminary testing, Actinica Inc. (Boston, MA) built several second-generation prototypes of the Airwatch [14], which were designed to be more rugged and address several technical issues observed in the original units. Unlike its handheld counterpart, the Airwatch is built to run on mine power (or long term battery) and it uses a self-advancing filter tape rather than a single filter which much be manually replaced after several hours or days of use.

---

[1] DPM is also regulated in coal mines, but not as a personal exposure limit. Currently, the 5040 method cannot determine between DPM and submicron coal dust. [7]

There are also two commercially-available monitors that were developed for environmental DPM but may have great potential for underground mining applications. The first of these is the Magee Scientific AE33 Aethalometer (Berkeley, CA), which is analogous to the Airwatch in terms of its operating principle. The AE33 has seen limited testing in mines to date [15]. The second available monitor of interest is the Semi-Continuous OCEC field monitor (Sunset Laboratory Inc., Tigard, OR), which is effectively a field version of the laboratory OCEC analyzer used for the 5040 Standard Method. It has never been tested in a mine setting. It should be noted that there are other commercially-available monitors advertised for DPM applications. These monitors are designed to monitor ultrafine particles rather than DPM as an analyte [16]. Application of these may pose problems, especially in dusty environments, as not all ultrafine particulates will be DPM.

The following sections provide more information about the NIOSH 5040 Method and all of these DPM monitors.

DPM Sampling and Analysis by 5040

As mentioned previously, to demonstrate regulatory compliance, the NIOSH 5040 Standard Method is used to measure EC and OC. Samples are obtained using a field apparatus composed of a personal air pump and a 37mm quartz fiber filter. When sampling occurs in environments prone to high dust content, size selectors such as cyclones and impactors are used upstream of the filter to avoid interferences in DPM analysis [17]. A cut size of approximately 0.8 μm is used to separate DPM and dust. It has been found that to generally work well to capture DPM while discarding mineral dust [17]. A Dorr-Oliver cyclone can be used to remove relatively large dust particles. At a standard flow rate of 1.7 L/min, this cyclone has a d_{50} cut size of about 5 μm. When coupled with a diesel particulate matter impactor (DPMI, placed downstream of the cyclone), the remaining particles greater than about 0.8 μm are removed before being deposited on the sample filter.

In addition to the primary sample filter, a secondary filter is usually also collected and analyzed [18]. The secondary filter is collected in order to quantify vapor-phase OC in the DPM sample. The basic idea is that both vaporous and particulate OC will collect on the primary filter; but since only the particulate OC is considered to contribute to TC in DPM, the vapor-phase OC needs to be removed from the primary filter OC result. The secondary filter should only collect vaporous OC. Thus, the particulate OC can be determined by difference (i.e., primary filter OC minus secondary filter OC).

Once collected, the sample filters are analyzed, most commonly using a Laboratory OCEC Aerosol Analyzer (Sunset Laboratory Inc., Tigard, OR) [18]. The analyzer operates via a thermal-optical analysis method to analyze carbon-based aerosols such as DPM, by quantitating EC and OC [18]. Where applicable, carbonate carbon (CC, i.e., from mineral dust included in the sample) can also be determined. The analysis is performed in two phases, to separately determine OC and EC. The sample is first heated in inert atmosphere to drive off OC, and the evolved carbon dioxide is reduced to methane, which is detected using flame ionization in order to stoichiometrically quantitate the OC. The sample is then reheated in oxidizing atmosphere to oxidize the EC, which is again quantitated via methane detection. A portion of the OC might convert to EC (called “char”) during the first phase of the thermal analysis, which can interfere with apportionment of OC and EC mass fractions. To correct for this, laser transmittance through the sample is also monitored throughout the analysis such that the char can be measured and apportioned back to the OC result [17]. These phases are labeled in Figure 1.1, which displays a 5040 Method thermogram. CC was not present in the sample shown in Figure 1.1. But, if CC is present, a distinct peak will also be observed near the end of the inert stage before the OC/EC split. The analyst can manually integrate this peak to quantitate CC and remove this from the OC result.

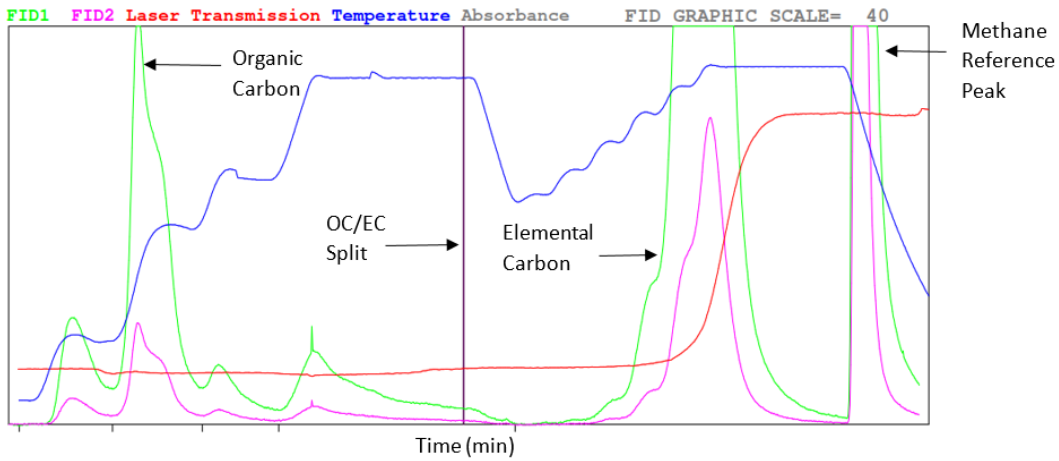

Figure 1.1: Example thermogram from analysis of a DPM sample analyzed by the 5040 Standard Method. The sample was collected in a controlled laboratory experiment where DPM was the only particulate present in the sampling chamber.

Continuous Monitoring

Due to the complexity of the 5040 analysis and its frequent use in compliance monitoring, the analysis is typically done by centralized, certified labs. This means that following sample collection, it may be weeks or more before analytical results are available. This is highly problematic with respect to identifying and correcting hazardous conditions. For instance, overexposures indicated in personal samples are not determined until well after the exposure occurred, and it can be difficult to correlate contributing factors after the fact. Likewise, in cases where a mine operator is collecting DPM samples for engineering purposes, it can be difficult to relate results to specific variables due to the dynamic nature of mine conditions. Continuous monitoring capabilities that yield near real-time data would be of significant value for protecting worker health and allowing efficient engineering in mines where DPM is a serious concern. Determining periods of minimum and maximum area concentrations could be utilized to restructure shift times or worker locations and overall trends can be used to determine the impact of ventilation or engineering controls. Such capabilities could also support larger efforts such as VOD and other integrated atmospheric monitoring systems. Operations could have the opportunity to save energy and money by being better equipped to monitor overall air quality in near real time.

There are currently two main categories of DPM monitors available or in development: those that work on a laser extinction principle and one that operates using the thermal-optical analysis method (i.e., a field version of the laboratory OCEC analyzer).

DPM Monitoring using the Laser Extinction Principle

The laser extinction principle is often used as the analytical technique by near real time monitors for determining DPM concentrations. The technique utilizes the collection of particles and an optical sensor to determine a voltage decay over time. The voltage decay occurs due to the decreased laser transmittance through a filter medium as particle mass accumulates. DPM contains black carbon (BC) which causes the collection filter to slowly darken overtime. The relationship between voltage decay, laser absorbance and filter darkening can be seen in Figure 1.2 for an idealized case where the sample collection is occurring in a constant-concentration environment.

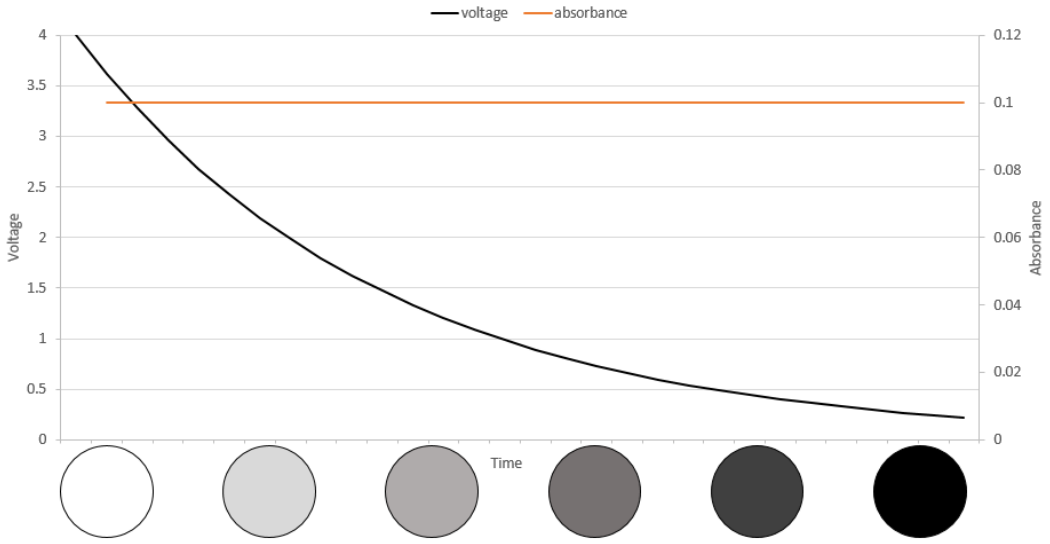

Figure 1.2: Illustrative plot showing idealized decay of optical sensor voltage and resultant laser absorbance with consistently increasing blackness on a DPM sample filter collected in a constant-concentration environment.

Since compliance is measured by the concentration of DPM a miner is exposed to, the voltage decay must be converted to prove useful. This can be done by first calculating the absorbance, as seen in Equation 1.

$$Absorbance = -\log\left(\frac{v_f}{v_i}\right) \qquad \text{(Equation 1)}$$

where v_i is the initial voltage and v_f is the final voltage. Once the absorbance is calculated, mass can be determined by using Equation 2.

$$Mass = Absorbance * slope \qquad \text{(Equation 2)}$$

where slope refers to the slope of the calibration curve (which must be created by comparison to the 5040 standard) for the monitor. Since the 5040 method quantitates EC rather than BC, the mass is effectively converted to EC, which can be used to calculate the overall concentration using Equation 3.

$$Concentration = \frac{m}{Q*t} \qquad \text{(Equation 3)}$$

where m is the mass determined previously, Q is the flow rate in liters per minute, and t is time in minutes.
The Airtec, Airwatch, and AE33 are all monitoring instruments that utilize the laser extinction principle to determine either EC or BC. However, these monitors have various differences such as functionality, portability, and power source. These similarities and differences are summarized in Table 1.1.

Table 1.1: Summary of monitors that utilize the laser extinction principle.

Monitor	Application	Analyte	Data Collection Rate and Output	Filter	Power Supply	Portability
Airtec	Personal exposure monitoring; short-term area monitoring or spot checking	BC (calibrated to EC)	1 point per minute; reports 5-minute rolling average EC concentration ($\mu g/m^3$)	37-mm PTFE, replaced after 8-12 hours sampling	Battery	Portable, handheld
Airwatch	Long-term area monitoring	BC (calibrated to EC)	1 point per 5 seconds; reports optical sensor voltage value (mV)	PTFE on polyester/ polyethylene filter tape, self-advancing	Mine Power Plug-in	Semi-portable
AE33	Long-term area monitoring	BC	1 point per minute; reports 1-minute BC concentration (ng/m^3)	Self-advancing filter tape	Mine Power Plug-in	Semi-stationary

Airtec Monitor

Prompted by the need to monitor personal DPM exposures in real-time, the Airtec monitoring units were developed by NIOSH and are now commercially available from FLIR, Inc. (Nashua, NH) for near real-time monitoring [11]. The Airtec is a portable, handheld unit containing an air pump, a sample filter housed in a cassette for collection, and recommended to be used with size selectors (i.e. Dorr Oliver cyclone coupled with a DPMI). Since the Airtec was designed for personal exposure monitoring, it is generally powered by its internal, rechargeable battery; it can also be plugged in for stationary monitoring. While the Airtec fundamentally measures BC mass accumulation per unit time, it has been calibrated to 5040 EC. Using its flow rate and sampling time, it reports EC mass concentration ($\mu g/m^3$) every minute as a 5-minute rolling average value. The Airtec converts the EC to a TC concentration using an assumed correction factor (i.e., TC = 1.3*EC), which is based on a comprehensive survey of EC and TC concentrations in underground metal/nonmetal mines [13]. While the Airtec is not accepted for demonstration of regulatory compliance, it represents a valuable tool for both occupational health protection and some mine engineering purposes (e.g., for "spot checking" problem areas) [12]. For more robust and long-term engineering needs, monitoring capabilities that offer continuous and autonomous data collection are required.

Airwatch Monitor

The Airwatch monitor was envisioned as a continuous and autonomous version of the Airtec [14]. It was conceptualized by NIOSH specifically for mining applications as a rugged and relatively inexpensive instrument. The first prototypes were built by Nomadics Inc. (now FLIR Inc.). To allow extended run-time, the Airwatch was designed to plug into mine power or run on a large (e.g., military) battery. It also utilizes a self-advancing filter tape to avoid the need for frequent filter replacement. Following very limited field testing to demonstrate proof-of-concept, a second-generation of the Airwatch was prototyped by Actinica (Boston, MA) [14]. The new prototype included several improvements to address technical issues observed in the initial design and to make the instrument more rugged for the mining environment.

The Airwatch outputs raw data in the form of an optical sensor voltage value every 5 seconds. As DPM mass accumulates on the filter, the voltage decays. Once the voltage has decayed to a certain degree, the monitor advances the tape to a clean filter spot and sample collection resumes. To translate the Airwatch output data into a usable format, laser absorbance values must first be determined from the voltage decay per Equation 1. Given that the Airwatch is still development, choosing appropriate time increments for this is tasked to the user. To guide this work and determine how the instrument's absorbance measurements correlate to DPM mass accumulation, calibration testing is required. Such testing must be done in a controlled environment and ideally the Airwatch absorbance should be calibrated to 5040 EC.

AE33 Aethalometer

While the Airwatch has been envisioned as a continuous, autonomous and DPM-specific monitor for mine environments, a very similar monitor is already commercially available for BC monitoring in ambient environmental applications. The AE33 Aethalometer (Magee Scientific, Berkeley, CA) is a rack-mounted monitor that also operates on plug-in power and utilizes a self-advancing tape. The AE33 reports BC concentration on a 1-minute time basis, and depending on conditions in the sampling environment, its filter tape can last for months. For deployment in remote locations, the instrument has wireless internet capabilities which allow the user to access data at any time. The AE33 can be fitted with an environmental enclosure designed to protect the instrument from dust, humidity, and other potential damage.

The AE33 has been tested on a limited basis in several underground mines with promising results [15,19,20].). However, it has not been calibrated to any standard measure of EC to date. This would be highly beneficial for future applications in mine settings in order to allow interpretation of data within the context familiar to the mining industry. Data available in the literature suggests that the ratio between BC and EC should be somewhere around 1.5 [9].

Filter Loading Effect and Consumption

One common problem with monitoring instruments that operate on the laser extinction principle is a filter loading effect [21]. This occurs when mass accumulation on the sample filter reaches the point where the optical sensor is no longer able to accurately measure incremental additions. As particles are collected they initially deposit on clean areas of the filter such that with each unit of mass addition, the optical sensor voltage response yields a consistent change in absorbance (e.g., as shown in Figure 1.2). At some point, particles begin to significantly deposit on top of one another, such that the same unit of mass addition produces a smaller change in voltage, which yields a smaller change in absorbance (Figure 1.3).

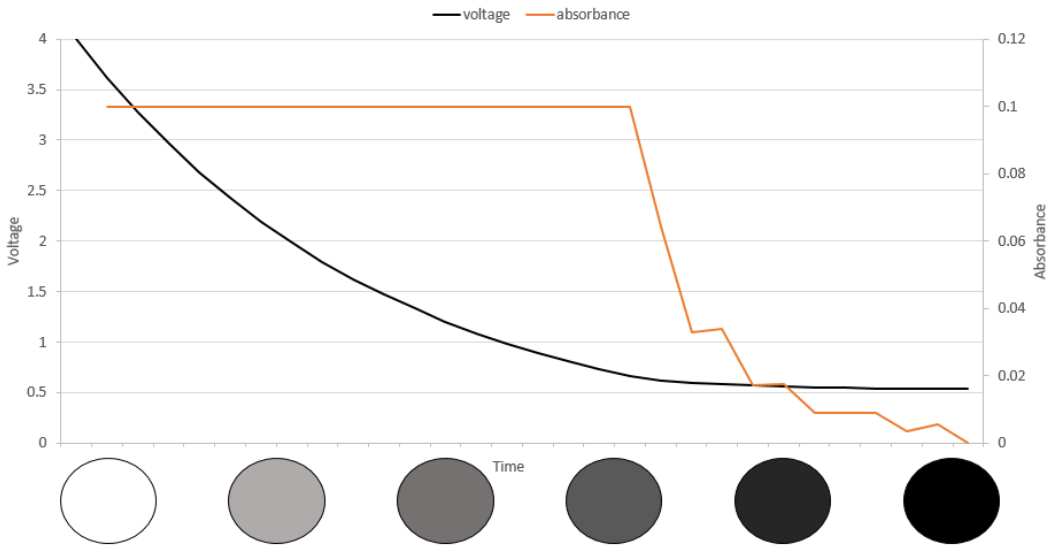

Figure 1.3: Illustrative plot of voltage decay where filter loading effect is evident.

The Airtec, Airwatch and AE33 data are all subject to the sort of filter loading effect shown in Figure 1.3, since they all utilize the laser extinction principle. The range of linearity (i.e., in terms of mass accumulation and monitor response) is undoubtedly dependent on a number of factors, including the properties of the filter tape, laser wavelength, optical sensor sensitivity, and absorbance properties of the whole sample (i.e., all particulates deposited on the filter). Practically, the result is that for a given BC concentration in the sampling environment and sampling flow rate, there will be some period of time (i.e., mass accumulation) after which monitoring results become less accurate. The Airtec's design (i.e., filter size, material, sensor, etc.) limits this issue fairly well for the typical DPM

concentration ranges and sampling times for which the monitor was designed. Noll and Jansiko (2013) showed that the Airtec bias (i.e., versus 5040 EC) is sufficiently small across a wide range of mass accumulation on the sample filter [22].

Magee Scientific has also sought to deal with the filter loading effect on the AE33 monitoring results. The latest models of the instrument use a dual filter spot ("dual spot") sample collection mode, which effectively splits the sample stream between two filter spots that collect simultaneously [23,24]. One spot collects at a significantly lower flow rate than the other, producing a different mass accumulation rate and hence a different rate of change in the laser absorbance. The instrument uses the difference in the laser absorbance change rates on the two spots and the proportionality of their flow rates (i.e., mass accumulation) to compute a compensation factor (in real-time) that is used to correct the measured BC concentration. The underlying algorithm has been described in detail and demonstrated in an urban air monitoring study by Drinovec et al. (2015) [24].

In addition to the filter loading effect shown in Figure 1.3, which manifests relatively late in the loading process, some types of filter tape can exhibit another effect early in the loading process. Fibrous filters, for instance, may show large differences in absorbance values between initial and later loading. This behavior is fundamentally due to different phases of loading, dominated by different mechanisms. On a clean filter, the mass begins to accumulate first within the pore spaces in the filter; but as the filter continues loading, mass begins accumulating on top of the filter. In a constant-concentration sampling environment, a plot of laser absorbance over time may show these phases of loading as relatively large drops in absorbance early on, followed by relatively stable absorbance later – and then another drop in absorbance when the aforementioned filter loading effect becomes significant.

Beyond filter loading effects, filter tape consumption may also pose a problem for continuous monitoring in mines. The tape advance rate for the Airwatch and AE33 is directly related to DPM concentration in the sampling environment; higher concentration results in higher mass accumulation rate for a given sampling flow rate, requiring the instrument to advance to a new filter spot more frequently.

To address this issue, several options exist including a simple reduction in sampling flow rate. In this case, careful consideration must be given to the impact of flow rate on the sampling size selector. The Airwatch and AE33 are intended for use with a cyclone size separator, which can generally operate for very long periods of time without cleaning or other maintenance (i.e., unlike a DPMI). However, the operating principle for the cyclone is flow dependent. Reduction in sampling flow rate will increase the effective particle cut size of the cyclone, which may allow excessive mineral dust to deposit on the filter with DPM. Another option, which could maintain the total sampling flow rate and thus not affect use of a cyclone size selector, is to combine a small flow of raw mine air with a flow of clean (i.e., filtered) air that balances the total desired flow rate. This option would effectively dilute the sampled mine air, and the dilution factor could be used as a multiplier to correct the measured BC or EC concentration. Aside from these, the monitors could also be operated semi-continuously – meaning that they could be programmed to sample over relatively short time periods but with sufficient frequency to meet the practical monitoring needs. For instance, a monitor might be programmed to sample for 5 minutes on a 30-minute cycle (i.e., twice per hour).

Semi-Continuous OCEC Field Monitor

Sunset Laboratories Inc. (Tigard, OR) offers a Semi-Continuous OCEC field monitor, which is essentially a field version of the laboratory OCEC analyzer commonly used for the 5040 Standard Method. This monitor works by sampling directly onto a small quartz fiber filter that is housed within the furnace chamber. The sample collection time and flow rate are set by the user, and a particle size separator can be inserted into the sampling train to cut out oversized particles. At the end of the sample collection period, the monitor runs the same 5040 thermal-optical method used by the laboratory OCEC analyzer. The primary output data are TWA EC and OC (and CC when programmed accordingly) masses that correspond to the time period of sample collection, and these can be translated into mass concentrations based on the sampling time and flow rate. Additionally, the monitor reports a real-time estimation of BC mass, which is determined by tracking laser transmittance through the sample filter as the sample is collected – similar to the way that laser extinction monitors discussed above operate.

The sample analysis time is about 20 minutes, which makes the monitor a semi-continuous instrument. During the analysis, the sample filter is effectively regenerated since carbon is completely burned off; however, the presence of

any refractory mineral dusts can gradually result in residue buildup and so the filter should be periodically replaced. Analysis and calibration gases for the OCEC field monitor are typically supplied by bottles in the field, which must also be replaced as needed. The monitor comes fully equipped with a laptop to run the analysis software, and this means that the instrument can be remotely accessed and controlled.

To date, the OCEC field monitor has never been tested in an underground mine. While it may offer lab-grade data in a field setting, it is a relatively complex instrument as compared to the monitors that operate only on the laser extinction method.

Conclusions

Capabilities for continuous and autonomous DPM monitoring in underground mines would support both protection of worker health and advanced engineering projects (e.g., VOD). At present, the Magee Scientific AE33 Aethalometer and the Sunset Laboratories semi-continuous OCEC field monitor represent two available technologies that might serve DPM monitoring needs in mines. The Airwatch monitor, which is still currently in development, may be another option. Each of these appear to have some particular benefits and challenges with respect to data quality versus costs, ease of use, readiness for mine application, etc. – and these must be weighed in the context of specific mine needs. Field demonstration and head-to-head testing of the monitors would provide valuable information to mine operators and other interested stakeholders.

References

[1] D. B. Kittelson, "Engines and Nanoparticles: A Review", J. Aerosol Sci. Vol. 29, 1997.

[2] M.E. Birch, "Monitoring of diesel particulate exhaust in the workplace", NIOSH Manual of Analytical Methods, 4th Edition., 2003.

[3] Z.D. Ristovski, B. Miljevic, N.C. Surawski, L. Morawska, K.M. Fong, F. Goh, I. Yang, "Respiratory health effects of diesel particulate matter", Asian Pacific Society of Respirology Volume 17, Issue 2, 2011.

[4] International Agency for Research on Cancer, "IARC: Diesel Engine Exhaust Carcinogenic", 2012.

[5] NIOSH, "Carcinogenic effects of exposure to diesel exhaust", Current Intelligence Bulletin No 50, DHHS (NIOSH) Publication No. 88-116, 1988.

[6] R.H. Grau III, S.B. Robertson, T.P. Mucho, F. Garcia, A.C. Smith, "NIOSH Ventilation Research Addressing Diesel Emissions and Other Air Quality Issues in Nonmetal Mines", SME Annual Meeting, Phoenix, AZ, 2002.

[7] Department of Labor, "30 CFR Part 72 Diesel Particulate Matter Exposure of Underground Coal Miners; Final Rule", Federal Register Vol. 66, No. 13, 2001.

[8] J. Noll, Timko, R., McWilliams, L., Hall, P., and R. Haney, "Sampling results of the improved SKC diesel particulate matter cassette", Journal of Occupational and Environmental Hygiene 29-37, 2010.

[9] OSHA – MSHA, "Diesel Exhaust/Diesel Particulate Matter", 2012.

[10] L. Takiff, G. Aiken, "A real-time, wearable elemental carbon monitor for use in underground mines", 13th United States/North American Mine Ventilation Symposium, 2010.

[11] J. Noll, S. Janisko, S.E. Mischler, "Real-time diesel particulate monitor for underground mines". (NIOSH) Publication No. 2004804, 2013.

[12] S. Gaillard, E. McCullough, E. Sarver, "Area Monitoring and Spot-Checking for DPM in an Underground Mine" Mining Engineering, Vol. 68, No. 12 pg. 57-63, 2016.

[13] Janisko, S., and Noll, J.D., "Near real time monitoring of diesel particulate matter in underground mines," Proceedings of the 12th U.S./North American Mine Ventilation Symposium, pp. 509-513, 2008.

[14] Nomadics, Inc., "Autonomous Networked EC Monitor Final Report", Contract: 200-2010-36901.

[15] Volkwein, J C, Robertson, K and Hansen, A D A, “Long-term continuous measurement of diesel particulate matter patterns in a large underground metal mine”, Proceedings 16th North American Mine Ventilation Symposium (ed: J Brune), pp 5–19, (Society for Mining, Metallurgy, and Exploration: Littleton, CO), 2017.

[16] Yu, Chang Ho, Patton, Allison P., Zhang, Andrew, Fanac, Zhi-Hua (Tina), Weisel, Clifford P., and Lioy, Paul J. “Evaluation of Diesel Exhaust Continuous Monitors in Controlled Environmental Conditions”, Journal of Occupational and Environmental Hygiene, 2015.

[17] Cantrell, Bruce K. and Rubow, Kenneth L., “Diesel Exhaust Aerosol Measurements in Underground Metal and Nonmetal Mines”. Diesels in underground mines: measurement and control of particulate emissions proceedings. Bureau of Mines Information and Technology Transfer Seminar, Minneapolis, MN, September 29-30, 1992.

[18] NIOSH, “Elemental Carbon (Diesel Particulate): Method 5040”, Issue 3, March 15, 2003.

[19] C. Pritchard, J. Hill, J. Volkwein, J. Noll, A. Miller, “Reduction in diesel particulate matter through advanced filtration and monitoring techniques”, SME Annual Conference and Expo, 2016.

[20] J. Volkwein, A. Hansen, J. Hill, “New sensor for continuous tracking of diesel particulate matter in mines to optimize mine ventilation systems”, SME Annual Conference and Expo, 2016.

[21] J. Jimenez, C. Claiborn, T. Larson, T. Gould, T.W. Kirchstetter, L. Gundel “Loading Effect Correction for Real-Time Aethalometer Measurements of Fresh Diesel Soot”, Journal of the Air and Waste Management Association, 57:7, 868-873, 2007.

22] J. D. Noll, S. Janisko, “Evaluation of a Wearable Monitor for Measuring Real-Time Diesel Particulate Matter Concentrations in Several Underground Mines”, Journal of Occupational and Environmental Hygiene, 10: 716-722, 2013.

[23] Magee Scientific, “Aethalometer® Model AE33”, User Manual Version 1,54, 2016.

[24] L. Drinovec, G. Mocnik, P. Zotter, A. S. H. Prévôt, C. Ruckstuhl, E. Coz, M. Rupakheti, J. Sciare, T. Müller, A. Wiedensohler, and A. D. A. Hansen, “The “dual-spot” Aethalometer: an improved measurement of aerosol black carbon with real-time loading compensation” Atmos. Meas. Tech. Discuss.: 30 September 2014.

Demonstration of Continuous Monitors for Tracking DPM Trends over Prolonged Periods in an Underground Mine

Chelsea Barrett[1*], S. Gaillard[1], E. Sarver[1]
[1]*Virginia Tech, United States*
*Corresponding author: chelsea9@vt.edu

Paper peer reviewed and originally published in the proceedings of the 16th North American Mine Ventilation Symposium, June 17-22, 2017. Golden, Colorado.

The solid fraction of diesel exhaust is called diesel particulate matter (DPM), of which elemental carbon (EC) is a major component. Particularly in confined environments like underground mines, DPM is a significant occupational health concern. Development of a hand-held, near real-time EC monitor has provided miners and engineers an important tool in tracking personal DPM exposures and general trends. The capability to monitor DPM continuously and over prolonged periods within a mine represents a logical next step. Coupled with knowledge of ventilation and other mine variables, such capability would be highly valuable for improving both occupational health conditions and operational efficiencies. For this, the AE33 aethalometer is a commercially available technology that has seen limited demonstration in mine environments; and another monitor called the Airwatch has been prototyped but not yet demonstrated. Both operate on a laser extinction principle, and include a self-advancing filter-tape and power plug-in capability to allow autonomous operation. In this study, we tested these instruments in a relatively high-DPM mine environment, while collecting comparative data from established short-term monitoring methods.

Introduction

Diesel particulate matter (DPM) is the solid fraction of diesel exhaust, commonly referred to as "soot". It is produced by the incomplete combustion of fuel and is generally accepted to have two primary components: elemental carbon (EC) and organic carbon (OC) [1,2]. DPM occurs predominantly in the submicron range [1]. In this range, inhaled particles are able to penetrate the respiratory system and deposit deep within the lungs [3]. As of June 2012, the International Agency for Research on Cancer classified whole diesel exhaust as a human carcinogen [4]. While the potential carcinogenic effects of DPM itself have not been elucidated [5], the US National Institute for Occupational Health and Safety (NIOSH) has made precautionary recommendations that diesel exhaust exposures be minimized to decrease cancer risks [5]. Exposures have also been linked to other acute and chronic health risks such as respiratory irritation, cardiovascular complications, and lung inflammation [3].

Relative to ambient levels and even other occupational environments, DPM concentrations can be particularly high in underground mines – especially large-opening mines, where supply of ventilation air is challenging [6]. This is attributed to the operation of large fleets of diesel-powered vehicles in confined spaces. Currently, the US Mine Safety and Health Administration (MSHA) regulates personnel exposures to DPM in metal and non-metal mines using total carbon (TC) as a surrogate [7]. TC is defined as the sum of EC and OC, and personal exposures are limited to an 8-hr time weighted average (TWA) of 160 $\mu m/m^3$ [8].

DPM Monitoring

To demonstrate compliance, filter samples are analyzed per the NIOSH 5040 method, which quantitates EC and OC (between 1 and 105 µg per filter portion) [7]. The samples are collected by individual miners using a personal dust pump and size selector(s) (i.e., if supra-micron dust is present at concentrations which may interfere with sample analysis). They must then be sent to a certified lab for the 5040 analysis. This time lapse between sampling and results means that overexposures are only known after the fact – and so mitigation efforts are retroactive in nature.

To promote more proactive decision-making, a near real-time monitor called the Airtec was developed by NIOSH and is now commercially available from FLIR, Inc. (Nashua, NH) [9,10]. The Airtec is a handheld instrument, which measures EC mass concentration. It does this by collecting airborne particulate on a filter (again using a size selector if necessary), and tracking the change in laser absorbance. Since the black component of DPM is considered

to be EC, laser light is increasingly absorbed as EC accumulates on the filter. (It should be noted that other instruments working on the same principle, generally report black carbon (BC), but the Airtec was calibrated against the 5040 method and so has been operationally devised to report EC.) Because the Airtec only measures EC, and must approximate TC via a generic ratio (i.e., see [10,11]), it is not acceptable for demonstrating regulatory compliance; however, it can serve as very valuable engineering tool. The Airtec was designed for monitoring personal exposures, recent work has shown it can also be modified for relatively quick "spot-checking" surveys [12].

Beyond real-time monitoring over relatively short time periods (i.e., a few minutes or over a work shift), the capability to monitor DPM continuously (i.e., over days to months) would be very helpful – particularly in mines that are challenged to meet DPM exposure limits or may be considering operational changes which could impact exposures (e.g., production locations or schedules, ventilation schemes, equipment re-assignment, etc.) For this, autonomous monitoring equipment such as an aethalometer could be used. Magee Scientific (Berkeley, CA) currently offers an aethalometer called the AE33, which again works on the laser extinction principle (measuring BC), but it has a self-advancing filter tape and plugs to central power supply. The filter tape advances to begin sample collection on a clean area when the monitor detects that the current area is loaded enough to degrade laser extinction data. The AE33 was developed for BC monitoring in environmental applications (e.g., urban air quality monitoring optical attenuation values between 75 to 125), where BC levels are generally much lower than in some underground mines. However, the instrument has seen limited testing as a continuous monitor for DPM in underground mine environments, and overall good performance was observed [13, 14].

Another continuous monitor called the Airwatch was designed and prototyped by Nomadics, Inc. (now FLIR, Inc.) in collaboration with NIOSH [15]. The Airwatch is intended to be calibrated to the NIOSH 5040 method to measure EC, and was envisioned as a relatively simple and low-cost autonomous DPM monitor for use in mines (i.e., where DPM levels can be relatively high). Like the AE33, the Airwatch uses a self-advancing filter tape and is meant to plug into mine power. Aside from a brief 2-day test that the original prototypes saw in an underground limestone mine, the Airwatch has not been previously demonstrated in the field (i.e. detection limits not known).

In this paper, we present field-monitoring results for the AE33 and Airwatch in an underground stone mine with relatively high DPM concentrations. The results of the continuous monitors are compared to the Airtec and to samples analyzed by the NIOSH 5040 method.

Experimental Site and Methods

Study Site

Monitoring for this study was completed in an underground stone mine during the summer of 2016. The mine generally operates five days per week on two 8-hour shifts. The day shift is production-focused, and the evening shift includes a smaller production crew and blasting.

This is a large-opening mine, and air speeds are generally very low (i.e., less than 100 ft./min) in most locations [9]. Ventilation is provided by both natural and forced airflow, with most natural ventilation occurring through the main ramp to the mine [9]. The main fan is located underground in the belt slope, which extends from the primary crusher and terminates at the surface. This serves as the main exhaust from the mine. A smaller fan also pushes air into the mine, and several auxiliary fans are located along the main ventilation path to continue ventilation. Additionally, several booster and portable fans, along with ventilation tubing and significant use of curtains, assist in delivering fresh air where needed and directing dirty air toward the main exhaust.

DPM is generally the only airborne contaminant of concern in this mine [12]. The mobile fleet consists of all diesel-operated equipment such as haul trucks, loaders, drills, and light-duty trucks. Despite a significant focus on ventilation, EC concentrations in some areas can be very high and EC can linger during non-production periods (i.e., over nights or weekends) [12]. Some inactive areas in the mine likely serve as sinks for DPM, such that at least low levels diffuse into the mine even when emission sources are not present.

All data for this study was collected adjacent to the primary crusher. In addition to seeing airflow toward the main exhaust, this location is affected by intermittent vehicle traffic. Previous research by the authors during June – August 2015 and December 2015 – January 2016 showed that under typical mine operating conditions, EC levels

near the crusher can range between about 50-200 µg/m^3 [12]. During data collection for the current study, EC levels near the crusher were expected to be somewhat higher due to temporary use of additional diesel equipment.

Monitoring Schedule and Equipment

Monitoring was conducted during five separate periods in Summer 2016 (Table 1), all of which started late in one work-week (i.e., Thursday or Friday) and ended early in the next (i.e., Monday, Tuesday or Wednesday). This schedule was chosen such that, since the mine does not produce during weekends, a characteristic decline in EC or BC is expected at the monitoring location after production ends on Friday, and the level should rise again following the start of production on Monday. However, use of additional diesel equipment in the mine at times during Summer 2016 (including over nights and weekends) may obscure this trend in some cases.

Table 2.1. Monitoring dates and equipment used/samples collected.

Monitoring Period	Dates (Days)	Equipment/Samples
1	Jun 9 (Th) - Jun 13 (M)	Airwatch, Airtecs (3 Th, 3 M), 5040 (3 T, 3 M)
2	Jun 23 (Th) - Jun 27 (M)	Airwatch, AE33[1], Airtecs (3 Th, 3 M), 5040 (3 Th, 3 M)
3	July 1 (F) - July 5 (Tu)	Airwatch, AE33[1], Airtecs (3 F), 5040 (3 F)
4	July 8 (F) - July 11 (M)	Airwatch, AE33, 5040 (3 F, 3 M)
5	July 15 (F) - July 19 (Tu)	Airwatch[2], AE33

[1] AE33 ran out of tape during test.

[2] New brand of tape was installed in Airwatch.

For a given monitoring period, the continuous monitors (AE33 and Airwatch) were intended to collect data over the entire time; and the short-term equipment (Airtecs and 5040 sample pumps) were intended to be used for the first and last 5 hours in order to gather comparative data. For all monitoring periods, all equipment was set up so that the airflow inlets were side-by-side and oriented in the same direction. Equipment was started and stopped simultaneously, per the above description. All monitoring with the Airtecs and 5040 sample collection occurred during the day shift.

The AE33 was loaned by Magee Scientific. It was not installed in the monitoring location until just before the second monitoring period. The standard flow rate on this instrument is 2.0 L/min, and a sharp-cut cyclone (SCC) was used to provide a particulate cut-size of approximately 0.8 µm [16]. The AE33 collected data (i.e., BC in µg/m^3 each minute, which was later used to calculate a 5-minute rolling average to match data from the Airwatch and Airtec.

The Airwatch was provided by NIOSH. This device is an upgraded, more rugged version of the original prototype (see [15]), and was built by Actinica, Inc. (Boston, MA) on a separate contract with NIOSH. It should be noted the current unit was previously tested briefly in both the laboratory and the field by the authors, and several minor issues (e.g., intermittent problems with clamping around the filter tape) were corrected by Actinica prior to the field-testing described here – and calibration of the unit to 5040 method EC data (see below). The Airwatch flow rate is 2.2 L/min. It also used a SCC, resulting in an approximate cut-size of 0.8 µm. The Airwatch was programmed to collect data (i.e., raw optical sensor voltage in mV) every 5 seconds. Using the calibration curve shown in Figure 1, this data was used to calculate EC (in µg/m^3) on a 5-minute rolling average.

Three Airtec units belonging to the research team were used with standard filter cassettes and SKC DPM impactors (Eighty Four, PA). The Airtecs' flow rate was set to the standard 1.7 L/min that the instrument uses to calculate EC (in µg/m^3) on a 5-minute rolling average. Flow rate on each unit was measured before and after each use; and for flow rates differing significantly from the standard, EC data was corrected.

To collect 5040 samples, three Escort ELF personal sampling pumps belonging to the research team were used with Dorr-Oliver cyclones and SKC DPM impactors. Samples were collected on pre-burned quartz filters per the 5040 standard method [17]. The pump flow rates were calibrated to 1.7 L/min, and checked before and after each use. The 5040 method results in a single EC value (µg per cm^2 of filter analyzed), which was converted to an EC concentration (µg/m^3) using the pump flow rate, sample collection time and total filter area.

Airwatch Calibration and Data Processing

Calibration of the Airwatch monitor used in this study was conducted in March 2015. Like other instruments that operate on a laser extinction principle, the raw data gathered by the Airwatch is simply a time series of optical sensor voltages measured as laser light is transmitted through the filter tape. When there is a voltage differential between two measurements, laser absorbance on the filter can be calculated by Equation 1:

$$Absorbance = -\log\left(\frac{v_f}{v_i}\right) \qquad \text{(Equation 1)}$$

where v_f is the final voltage and v_i is the initial voltage. And, the laser absorbance for the time period in question is proportional to the mass of light-absorbing substance on the filter – in this case EC.

To construct a calibration curve for the Airwatch, a series of 13 tests were conducted in which the instrument recorded optical sensor voltage while DPM was simultaneously being collected on a filter for 5040 analyses. The tests were conducted in a Marple chamber at the NIOSH Office of Mine Safety and Health Research facility near Pittsburgh, PA. This chamber allows for highly controlled, and highly uniform DPM concentrations. Absorbance values for the Airwatch sensor were calculated from the initial and final voltage values in each test; which coincided with the start and stop times, respectively, for DPM sample collection in that test. The resulting data is shown in Figure 1, along with the best-fit trend line. The single data point shown as an x appears to be in error and was excluded. However, the best-fit trend line including this point is y = 26.04x – 1.4443 with an R^2 value of .5584.

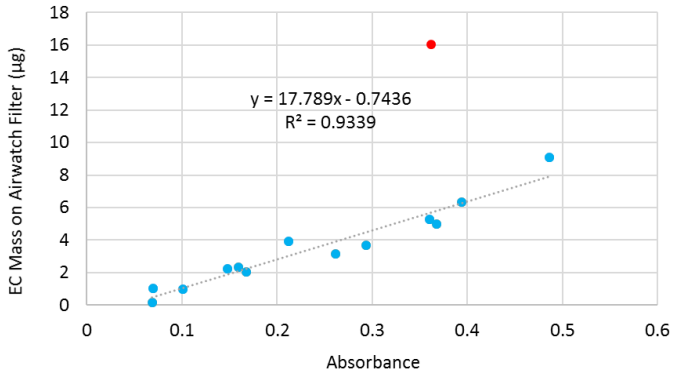

Figure 2.1. Airwatch calibration curve. The data point shown as an x was not used in generating a best-fit line.

Using the equation of the trend line in Figure 1, EC mass collected on the Airwatch filter (m, in µg) over a given time interval can be calculated from the associated absorbance value for that period (i.e., via Equation 1). Further, knowing the length of the time interval (t, in minutes) and the flow rate of the Airwatch pump (Q, in L/min), the EC concentration (C, in µg/m^3) in the monitoring environment can be calculated by Equation 2:

$$C = \frac{m*1000}{Q*t} \qquad \text{(Equation 2)}$$

As mentioned above, the Airwatch used in this study is programmed to gather optical sensor voltage values every 5 seconds. Practically, before calculating the EC concentration from the raw voltage values, this means that some processing is needed to reduce the number of data points. For this, a program was written to extract one voltage value per minute. The program also flags "tape change" events (i.e., when the filter advances to a clean spot) such that absorbance values can be properly calculated (i.e., initial and final voltage values must be recorded on the same filter spot.) Following data reduction, EC concentrations are calculated on 5-minute rolling average.

Results and Discussion

Continuous Monitoring Over Extended Periods

Figures 2a-e show the data collected for all five monitoring periods. Before discussing the specific trends, several points should be made about the different data types. First, upon careful inspection, frequent breaks in the Airwatch and AE33 data can be seen. These are associated with tape change events, during which the monitor is not collecting valid EC/BC data. Next, intervals in the Airwatch (e.g., Friday-Monday in Figure 2a) and AE33 data (e.g., Friday to Monday in Figure 2b) showing no EC concentration are associated with times where the filter tape ran out. Lastly,

with respect to the short-term data, the 5040 results are all plotted as a horizontal line, which represents the average (i.e., of triplicate samples) of the TWA EC concentration measured over the sample collect period. The TWA EC concentration of each 5040 sample is shown in Table 2; results between triplicate samples generally agreed well. Similarly, the data shown in Figure 2 for the Airtecs represents the average of three units running side-by-side. Again, the results between individual units generally agreed well (data not shown).

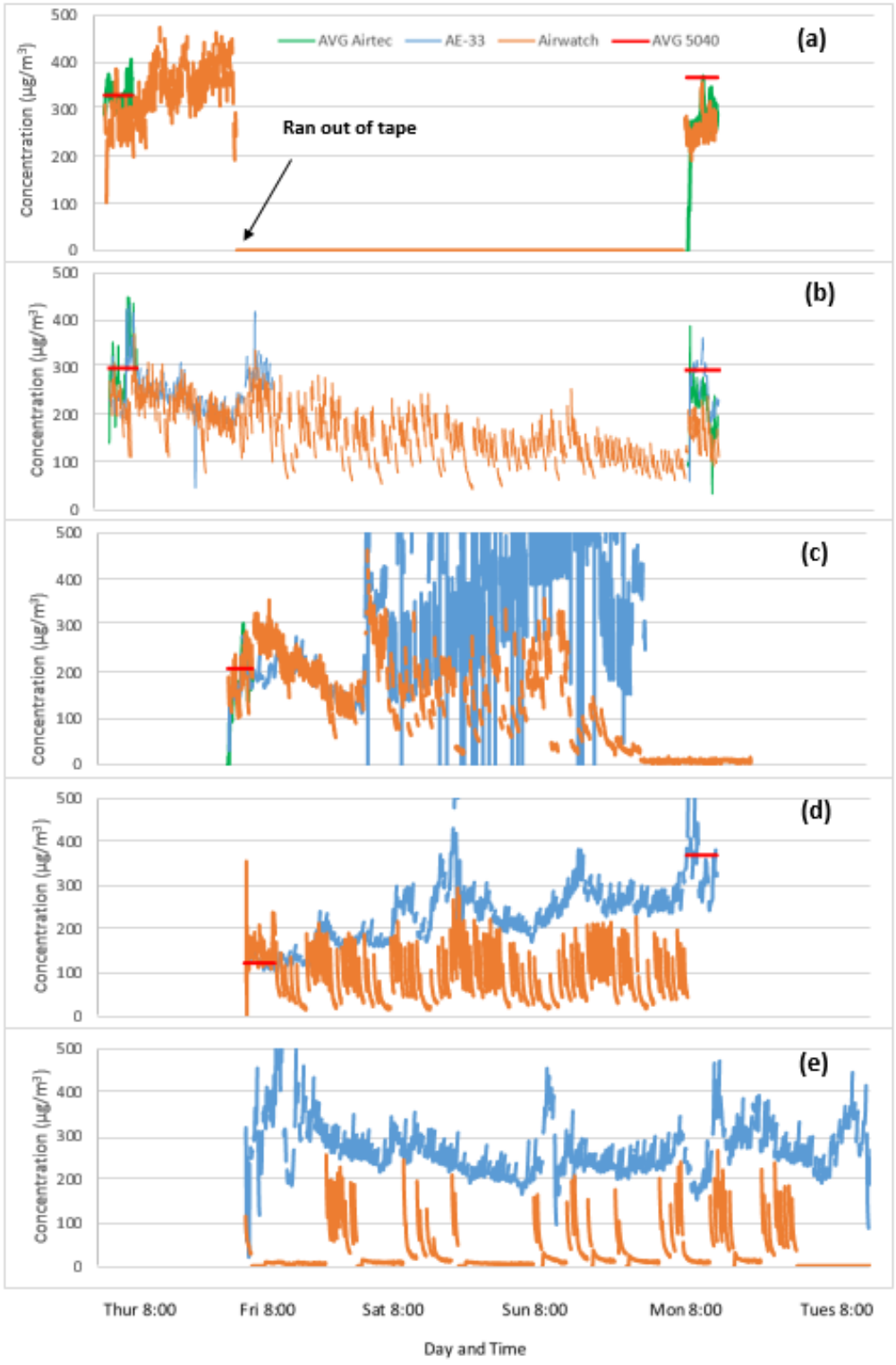

Figure 2.2. 5-minute rolling average EC or BC concentration (µg/m^3) data collected using the AE33, Airwatch and Airtecs in monitoring periods 1-5 (plots a-e, respectively). TWA EC concentration (µg/m^3) derived from 5040 sample analysis is also shown.

Examining the data trends in Figures 2a-e, some key observations can be made about the AE33 and Airwatch. In general, it is clear that both monitors can run continuously and are capable of gathering useful data in a relatively high DPM environment – as indicated by their correlation with the 5040 and Airtec data. (Oscillations in continuous data, particularly the Airwatch, are likely due to a filter loading affect, which is discussed further below.) During monitoring periods 1 (Airwatch only), 2 and the first part of 3, these instruments appear to match fairly well with the Airtec and 5040 data, and follow expected trends. For example, Figure 2b shows a decline in EC concentration over Thursday night, a rise on Friday, a decline again from Friday night through early Monday morning, and then a rise again later on Monday. This is consistent with expectations based on production activity in the mine. The characteristic trend is also clear in Figure 2c between Friday morning and Saturday mid-day.

However, later on the Saturday in Figure 2c and throughout the remainder of that monitoring period, both the Airwatch and AE33 exhibit unexpected behavior – the cause for which is not definitively known. The Airwatch data suggests that EC rose quickly on Saturday evening, which is possible due to use of temporary diesel equipment in the mine. Around the same time, the AE33 data begins to oscillate severely and eventually the Airwatch data also has significantly more oscillation than it did previously. This may indicate that DPM levels were simply out of range for the monitors, although they seem to handle similar levels without such issues in other monitoring periods. Another possibility is that fine water drops in the monitoring location (e.g., due to high enough relative humidity to form condensation or some other source of mist) may have been sampled. Magee Scientific notes that water condensate can affect measurements [18], and the Airtec is also known to produce erroneous EC data if condensation forms on the optical sensor [19]; condensation should affect the Airwatch sensor similarly.

In monitoring period 4 (Figure 2d), both the Airwatch and AE33 appear to initially perform well; and the AE33 continues performing without any indication of issues for the entire period. The resulting BC data suggests that, again, DPM levels actually increased over the weekend; but again this is possible given the use of temporary diesel equipment in the mine for this time interval. The BC rose higher on Monday, consistent with normal production activity, and the 5040 data on that day supports the AE33 measurements. While the Airwatch data in this monitoring period generally tracks with the AE33 (i.e., they rise and fall together), the Airwatch EC values become increasingly smaller than the AE33 BC values over time (i.e., the EC to BC ratio decreases). This divergence in the two data sets may be related to decreased flow through the Airwatch. At the end of this monitoring period, the instrument was found to be very dirty, with visible buildup of black-colored particulate around the flow inlet and the filter tape clamp and optical sensor components. Care was taken to clean the instrument and check its flow rate prior to the next monitoring period.

In monitoring period 5 (Figure 2e), the AE33 appears to generally perform well. Occasional spikes or abrupt falls in the data may again be associated with water condensation, or whatever phenomena contributed to the unexpected behavior observed in monitoring period 3. Between periods 4 and 5, the original stock of filter tape for the Airwatch ran out and new tape was ordered based on the original specifications. However, as evident in the data, the Airwatch does not perform with the new tape. For some spots on the filter, the instrument never records a change in optical sensor voltage, and for others the tape does not advance properly as the voltage decays. Further work is required to determine the differences in filter media properties that may be responsible for this behavior responsible.

Filter Tape Loading and Sample Dilution

As mentioned above, the Airwatch and AE33 both appear to exhibit a filter loading effect, which results in the characteristic oscillatory shape of the data. The effect is more pronounced in the Airwatch data (e.g., Figure 3), and occurs when incremental accumulation of EC mass on the filter no longer results in the expected proportional optical sensor voltage decay. In other words, EC particles start to load the filter by depositing on top of one another such that the optical sensor cannot detect all of the new mass [20]. Over time, the effect becomes worse as there is increasingly less uncovered area for the EC to deposit on. For each filter spot (i.e., before the tape advances), the resulting data appears to show relatively high EC concentrations early on, followed by continually decreasing values. Assuming the instrument calibration is accurate, the early data should thus be most accurate. This phenomenon is well established for instruments that work on the laser extinction principle [20], and can often be resolved to some extent [20]. Any plans for commercializing the Airwatch should include a correction, which might be achieved in various ways (e.g., variable flow rate for different DPM ranges, so long this does not interfere adversely with particle size selection; larger filter area; diluted sample stream; etc.)

The AE33 has been designed to reduce the loading effect the instrument experiences by using a "dual spot" correction, which has been described in detail elsewhere [21]. While the AE33 exhibits significantly less oscillation

than the Airwatch, it does still appear to be affected by rapid filter loading in the high-DPM monitoring location. Upon careful examination of Figure 3, the shape of the AE33 data on each filter spot is quite interesting; it often appears as an "S" of "V" shape. The cause for this is not known, but is currently under investigation.

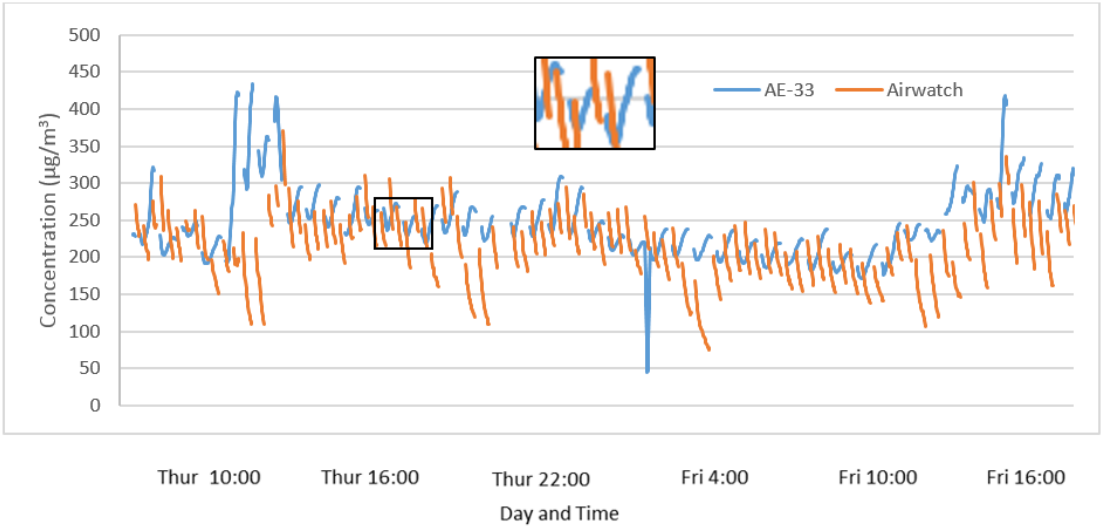

Figure 2.3. Data illustrating Airwatch and AE33 filter loading effect, corresponding to Figure 2(b). Close-up image inset taken from Thursday evening.

In an effort to test the idea of a diluted sample stream for further reducing the filter loading effect seen with the AE33 – and to prolong filter tape life – monitoring with this instrument was continued in the same location following collection of the five datasets shown above. In collaboration with Magee Scientific, a basic device was built to provide a dilution ratio of 4:1. Still operating at a total sample flow rate of 2.0 L/min, a regulated pressure pump was used to set the intake of ambient mine air into the AE33 at 0.5 L/min; and the other 1.5 L/min was HEPA-filtered mine air. (Laboratory testing confirmed the HEPA filter removed 99% of diesel particulate from a concentrated stream.) Due to the dynamic DPM conditions in the mine, conducting a controlled test of the dilution device was not possible. However, a basic comparison of BC measurements before and after the device installation showed that it is generally performing well (i.e., BC concentration just after installation of the device was about 4x lower than just before). It should be noted that this result was only achieved upon using a finely controlled flow regulator. Careful control of the dilution ratio is indeed a critical requirement for using such a dilution device long. term. That said, this modification may make the AE33 a more viable option for continuous monitoring in high-DPM environments like underground mines. In the study mine described here, it has significantly reduced the filter tape consumption rate. One tape roll lasts 19-28 days vs. 5-7 days with no dilution.

Conclusions

Underground miners and mine operators would benefit from real-time monitoring capabilities that can track DPM trends over prolonged periods. The AE33 aethalometer is already commercially available from Magee Scientific, but has seen only limited demonstration underground; and the prototype-stage Airwatch is currently still in development and has not yet been demonstrated. Both of these instruments were recently tested in a relatively high-DPM stone mine. While they performed well overall, several issues were observed. Most notably, a clear filter loading effect was evident – and was severe in the case of the Airwatch. This will require attention if the Airwatch is destined for widespread use. While the AE33 already includes a filter tape correction, it may also benefit from further improvement targeted at very high DPM ranges. Also, filter tape consumption rate could be problematic in mine environments. A basic dilution device could resolve this issue, although other options should also be investigated (e.g., reduced flow rate and compatible particle size selector) that could be incorporated into the monitoring instrument and may not require additional consumables. Finally, entrainment of very fine water drops and/or water condensation within the monitors may present problems in mine applications. Drying of the sample stream (e.g., via a diffusion dryer) may be a viable solution, but this should be field tested over a range of possible conditions.

Acknowledgements
The authors thank NIOSH/CDC for funding this work (contract 200-2014-59646) and James Noll, Emanuele Cauda, and Shawn Vanderslice, in particular for their guidance and help with data analysis. We gratefully acknowledge all personnel at the study mine for their cooperation and interest in this work. At Virginia Tech, we also thank Mohammad Rezaee for help with data collection, and Chreston Miller for help with Airwatch data processing. Finally, we thank Jon Volkwein, Tony Hansen and Jim Morton at Magee Scientific for assistance with the AE33.

Works Cited

[1] D. B. Kittelson, "Engines and Nanoparticles: A Review", J. Aerosol Sci. Vol. 29, 1997

[2] M.E. Birch, "Monitoring of diesel particulate exhaust in the workplace", NIOSH Manual of Analytical Methods, 4th Edition., 2003.

[3] Z.D. Ristovski, B. Miljevic, N.C. Surawski, L. Morawska, K.M. Fong, F. Goh, I. Yang, "Respiratory health effects of diesel particulate matter", Asian Pacific Society of Respirology Volume 17, Issue 2, 2011

[4] International Agency for Research on Cancer, "IARC: Diesel Engine Exhaust Carcinogenic", June 2012

[5] NIOSH, "Carcinogenic effects of exposure to diesel exhaust"., Current Intelligence Bulletin No 50, DHHS (NIOSH) Publication No. 88-116, 1988.

[6] R.H. Grau III, S.B. Robertson, T.P. Mucho, F. Garcia, A.C. Smith, "NIOSH Ventilation Research Addressing Diesel Emissions and Other Air Quality Issues in Nonmetal Mines".

[7] J. Borak, G. Sirianni, H.J. Cohen, S. Chemerynski, R. Wheeler, "Comparison of NIOSH 5040 method versus Aethalometer to monitor diesel particulate in school buses and at work sites.

[8] OSHA – MSHA, "Diesel Exhaust/Diesel Particulate Matter", November 2012.

[9] L. Takiff, G. Aiken, "A real-time, wearable elemental carbon monitor for use in underground mines", 13th United States/North American Mine Ventilation Symposium, 2010.

[10] J. Noll, S. Janisko, S.E. Mischler, "Real-time diesel particulate monitor for underground mines".

[11] J.D. Noll, S.E. Mischler, G.H. Schnakenberg, Jr., A.D. Bugarski, "Measuring diesel particulate matter in underground mines using submicron elemental carbon as a surrogate", 11th U.S./North American Ventilation Symposium, 2006.

[12] S. Gaillard, E. McCullough, E. Sarver, "Area Monitoring and Spot-Checking for DPM in an Underground Mine", 2016.

[13] C. Pritchard, J. Hill, J. Volkwein, J. Noll, A. Miller, "Reduction in diesel particulate matter through advanced filtration and monitoring techniques", SME Annual Conference and Expo, 2016.

[14] J. Volkwein, A. Hansen, J. Hill, "New sensor for continuous tracking of diesel particulate matter in mines to optimize mine ventilation systems", SME Annual Conference and Expo, 2016.

[15] Nomadics, Inc., "Autonomous Networked EC Monitor Final Report", Contract: 200-2010-36901.

[16] BGI, Inc., "Instructions: SCC 0.695 Cyclone", May, 2013.

[17] NIOSH, "Elemental Carbon (Diesel Particulate)", 5040 Method.

[18] Magee Scientific, "Sample Steam Dryer", User's Manual Part Number: 5610 Manual 1.7, September, 2016.

[19] FLIR Systems, "Airtec Diesel Particulate Monitor", Rev. 9, March, 2011.

[20] J. Jimenez, C. Claiborn, T. Larson, T. Gould, T.W. Kirchstetter, L. Gundel "Loading Effect Correction for Real-Time Aethalometer Measurements of Fresh Diesel Soot", Journal of the Air and Waste Management Association, 57:7, 868-873, 2007.

[21] L. Drinovec, G. Mecnik, P. Zotter, A.S.H. Prévôt, C. Ruckstuhl, E. Coz, M. Rupakheti, J. Sciarre, T. Müller, A. Wiedensohler, A. D. A. Hansen, "The "dual-spot" Aethalometer: an improved measurement of aerosol black carbon with real-time loading compensation", Atmos. Meas. Tech. Discuss., September, 2014.

Comparison of Several DPM Field Monitors for Use in Underground Mining Applications

Chelsea Barrett[1], E. Sarver[1*], E. Cauda[2], J. Noll[2], S. Vanderslice[2], J. Volkwein[3], B. Cary[4], J. Dixon[4]
[1]*Virginia Tech,* [2]*NIOSH,* [3]*Science Consultant,* [4]*Sunset Laboratory Inc.*
*Corresponding author: esarver@vt.edu

Monitoring diesel particulate matter (DPM) in underground mines is important for protecting worker health. The NIOSH 5040 Standard Method is a thermal-optical method that is well established for laboratory analysis of filter samples. It is commonly used for determining personal exposures to total or elemental carbon (TC or EC), which may serve as surrogates for DPM. For near real-time monitoring over short periods (e.g., a single work shift), the FLIR Airtec handheld monitor is also available. It measures black carbon (BC) using a laser extinction principle and has been calibrated to the 5040 EC. However, the capability to monitor DPM continuously are still needed to support a range of mine engineering endeavors, such as ventilation on-demand. At present, only a few instruments may offer such capability. The continuous Magee Scientific AE33 Aethalometer was designed to monitor BC using laser extinction in ambient environmental applications. It has undergone limited mine testing, but has not been calibrated to the 5040 EC. A similar but more basic monitor called the Airwatch has also been prototyped. Additionally, the Sunset Laboratory Semi-Continuous OCEC field monitor was designed as a field version of laboratory analyzer used for the 5040 Method, but it has never been tested in a mine environment. In this study, the AE33, Airwatch and OCEC field monitor were tested head-to-head in a controlled laboratory setting and compared against 5040 EC. The monitors were also tested in an underground stone mine. Results indicate that all three have potential for mine monitoring, though they vary in terms of suitability for specific applications. The OCEC field monitor provides lab-grade results across a wide range of conditions, but it is a relatively complex instrument that requires special considerations for installation and consumables. The AE33 can provide reliable BC data, which can be interpreted in the context of more standard EC data, in DPM concentrations that are relatively low, but within a primary range of interests for mines. Its range might be extended with some simple modifications. The Airwatch has several issues that still must be addressed, including its susceptibility to a filter loading effect, but the fundamental operating principle was demonstrated here. If fully developed, it may represent a basic, rugged option for DPM monitoring in mines.

Introduction

Diesel particulate matter (DPM) is the solid portion of diesel exhaust. The particulates occur primarily in the submicron range, and pose serious health hazards [1]. Underground miners generally experience the highest exposures of any occupational group due to operation of heavy diesel equipment in confined spaces [2]. DPM is heterogeneous in nature and cannot be measured directly, but total or elemental carbon (TC or EC) are often used as surrogate analytes because they represent primary DPM constituents [3]. In metal/non-metal mines in the US, personal exposures to DPM are regulated using a permissible limit of 160 µg TC/m^3 on the basis of an 8-hr time weighted average (TWA) [4]. For compliance purposes, TC is measured in filter samples using the NIOSH 5040 Standard Method. This is a thermal-optical method that results in quantitative measures of EC and organic carbon (OC), which can then be summed to determine TC [5]. Samples are collected onto quartz fiber filters using a personal air pump, which is generally equipped with particle size selector(s) to limit collection of larger mineral dust particles. The sample analysis is then performed in a certified laboratory. This approach can also be used for non-compliance monitoring.

With respect to personal protection and mine engineering, however, the significant lag time (i.e., on the order of weeks) between sample collection and 5040 results is problematic. Miners cannot take immediate action to limit their exposures, and it may be difficult to identify the circumstances surrounding overexposures retrospectively [5]. Engineering decisions related to DPM abatement are also delayed. Moreover, due to the nature of mining operations, DPM conditions may be very dynamic. This means that many data points, preferably on a higher-resolution time basis (e.g., one data point per minute or per hour as opposed to a point per day), are generally needed to correlate DPM trends with other conditions in the mine. Field monitoring capabilities that are (or near) continuous and real-time are needed to address these issues.

The Airtec handheld DPM monitor (FLIR, Nashua, NH) was specifically developed for tracking personal exposures in occupational environments like mines [5]. It uses a laser extinction principle to measure black carbon (BC) as DPM accumulates on a filter. As the filter darkens during a given time increment, the decay in light transmittance can be correlated to the incremental increase in BC mass. The Airtec has been calibrated against the 5040 EC, and it uses an assumed EC to TC ratio (i.e., TC = 1.3EC) to report TC. The Airtec reports TC ($\mu g/m^3$) as a cumulative TWA and EC as a 5-minute rolling average [6]. While it represents a very useful tool for personal monitoring and periodic DPM surveying, the Airtec's design (e.g., with a filter that must be replaced regularly) is really not compatible with long-term continuous monitoring needs.

Long term monitoring can provide insight into overall DPM behavior within an area, or after a ventilation change. The first of three monitors which could be used for long term area sampling that were investigated is the AE33 Aethalometer (Magee Scientific, Berkeley, CA). It is another commercially available instrument. It was developed for continuous environmental monitoring applications, but has been demonstrated in a limited number of field tests in underground mines [7, 8, 9]. It also utilizes the laser extinction principle and reports BC ($\mu g/m^3$) on a 1-minute basis. Rather than a single filter that must be replaced, the AE33 uses a self-advancing filter to allow autonomous operation over relatively long time periods (e.g., weeks to months). It has heretofore not been directly calibrated to 5040 EC. However, given that the few field tests using this monitor have shown different BC to EC ratios (i.e., between about 1.0 – 1.7, a direct calibration is important for interpreting AE33 field data against the standard EC measure [9].

The Airwatch was originally designed and prototyped as a field monitor intended specifically for high-DPM environments [10]. It was conceived as a continuous version of the Airtec handheld monitor, and operates similarly to the AE33 with a self-advancing filter tape. The Airwatch outputs raw optical sensor voltage values, which can be translated into incremental or cumulative laser absorbance values, and then used to calculate an EC concentration ($\mu g/m^3$) using an absorbance to EC mass calibration curve. Following brief testing of the original prototypes, several new and more rugged prototypes were built by Actinica (Boston, MA). One unit was recently calibrated to EC mass and field-tested in an underground stone mine [7]. That testing indicated that the Airwatch could at times correlate well with EC mass concentration, however its long-term performance has not been evaluated.

A Semi-continuous OCEC field monitor (Sunset Laboratory Inc., Tigard, OR) is another potential option for DPM monitoring in mines – though it has never been field-tested in such a setting. This instrument is essentially a field version of the Laboratory OCEC Aerosol Analyzer used for the 5040 Standard Method. It collects a sample on a filter that is housed within the analyzer furnace chamber, and then it runs the 5040 thermal-optical analysis to determine OC and EC mass on that filter, which can be converted to mass concentration values ($\mu g/m^3$) using the sample collection time and flow rate [11]. The OCEC field monitor is considered semi-continuous as it produces one data point for every sample collection and analysis time increment. The sample collection time and flow rate are user defined, and the analysis time is about 20 minutes. Like for the laboratory OCEC analyzer, the OCEC field monitor requires high-purity gases for the thermal analysis and instrument calibration; in a field setting, these are supplied from cylinders. Since the same sample filter is used repetitively, build-up of refractory material can occur (e.g., due to collection of mineral dust particles, which do not burn off like EC or OC) and thus the sample filter must be periodically replaced [11]. Despite the more complex nature of OCEC field monitor (versus the laser-based monitors), its principle of measurement is effectively identical to the that of the 5040 Standard Method.

Notably, there are other instruments that have been used or suggested for DPM monitoring – including particle counters with capabilities in the submicron size range [12]. Such instruments are not specific to DPM, however, and the propensity for relatively high dust concentrations in mines may limit their general applicability in these environments. In order to evaluate and compare the available/in-development options for continuous DPM monitoring, this study tested the AE33, Airwatch and OCEC field monitor side-by-side in both the laboratory and the field. Standard 5040 samples and Airtec data were also collected in all laboratory tests and periodically during the field testing for comparison with the AE33, Airwatch and OCEC field monitor results.

Experimental Details

Laboratory Testing

A total of 19 laboratory tests were conducted in a Marple chamber at the NIOSH/PMRD/DVTSB Diesel Aerosol lab in Pittsburgh, PA. The Marple chamber is a large (roughly 1.8 m^3) calm-air chamber specially designed to limit

spatial variability in aerosol distributions, such that measurements can be conducted under carefully controlled and stable conditions [13]. It has been used for a variety of experiments investigating dust and DPM, and for calibration of monitoring equipment. Particulates are generally fed to the chamber from the top along with dilution/make up air and exhausted from the bottom, with flow through the chamber being very slow. Due to its geometry, it acts as a well-mixed reactor at mid-height where sampling occurs.

For this study, the DPM source was a Genset Tier-4 diesel engine (Kubota model D1703-M-BG-ET01) operated at either high (i.e. 80%) or low (i.e., 20%) load. The ratio of EC to OC is expected to be somewhat higher under high loading conditions versus low loading. Both types of conditions are frequently present in mine environments due to varying operating cycles for equipment (i.e., from idling to climbing steep grades with heavy material loads). A bleed-off of the engine exhaust was piped directly into the Marple chamber to achieve a relatively high (~800 $\mu g/m^3$), medium (~500 $\mu g/m^3$) or low (~200 $\mu g/m^3$) DPM concentration. High concentrations might represent peak DPM concentrations in an active section of a mine environment, and low concentrations might represent more typical background concentrations. Within each concentration range, tests were run for varying times to vary the amount of DPM mass sampled (Table 3.1). For 5040 analysis, the total sample mass is the important parameter. It is used to determine a TWA EC mass concentration for the entire test period, and the sample mass must be within the limits of quantification per the 5040 Method [14]. This is also true for the semi-continuous OCEC monitor, except that it can be used to take a series of samples during a given a test – each of which can be used to determine a TWA EC concentration over the respective sample collection time. For the continuous monitors using laser-extinction (i.e., AE33, Airwatch and Airtec), the mass concentration inside the chamber is the important parameter. It determines the incremental mass accumulation on the monitor filter, which is being measured at a particular frequency.

The concentration in the chamber was estimated using a single ambient particulate monitor that utilizes a tapered-element oscillating microbalance (TEOM), which was sampling from the same position as all monitoring equipment. Since the only source of particulates for these tests was the engine exhaust, the TEOM measurements served as direct proxy for total mass concentration of DPM. Once the TEOM concentration stabilized near the desired concentration, no further adjustments were made in the exhaust to make up air ratio and a specific test could begin. TEOM data during the tests indicated that DPM concentrations were generally stable within a given test period (i.e., within 5%), although some fluctuations were observed in particularly long tests, tests at low engine load, or those conducted at high DPM concentration.

During each of the 19 tests, an AE33, Airwatch, OCEC field monitor, and five Airtec monitors were used to sample the DPM inside the chamber. All instruments were equipped with a size selector (i.e., sharp-cut cyclone or combination of Dorr-Oliver cyclone and diesel particulate matter impactor, DPMI) in order to limit collection of any oversized particles, which could significantly impact mass/laser absorbance measurements. Based on the instrument flow rates, the size selectors used here should produce a consistent cut size of around 0.8 µm (Table 3.2). Standard filters/filter tape were used for the Airtecs, AE33 and OCEC field monitor. The Airwatch tape has a PTFE membrane on polyester/polyethylene. The AE33 and Airwatch units tested here were the same units previously tested together in an underground stone mine [7], and both were thoroughly cleaned prior to the experiments described here. The OCEC field monitor and all Airtecs were also cleaned prior to testing. Additionally, before and after each ~300 total minutes of testing, the flow rate of each instrument was measured in order to allow for data adjustment where necessary (e.g., in case flow rate of any instrument drifted). For each test, sample collection by each monitor was started/stopped simultaneously and sample collection always began on a clean filter/filter spot. All sampling tube inlets were positioned at the same height in the chamber and in relatively close proximity to one another (i.e., no more than 7 cm apart).

For each test, a total of five 5040 samples were collected – again using sharp-cut cyclones and with tube inlets positioned near those of the monitoring instruments. The 5040 sample collection was done using a single air pump with a five-way manifold to ensure precise sample collection times, which started/stopped simultaneously with those of the monitoring instruments. The 5040 samples were collected onto pre-burned 37-mm quartz fiber filters per the Standard Method [14]. They were later analyzed per the method using a Laboratory OCEC Aerosol Analyzer (Sunset Laboratory Inc., Tigard, OR) in order to determine EC mass concentration ($\mu g/m^3$) inside the chamber during each test.

Table 3.1: Summary of tests run during calibration study.

Test	Target Mass Concentration ($\mu g/m^3$)	Target 5040 EC Sample Mass (µg)	OCEC Field Analyzer Test Times (min)	Total Test Time (min)
1	Low	15	40	40
2	Low	170	50, 50, 50, 53, 52	350
3	Low	75	60, 60, 12	170
4	Low	125	60, 60, 60, 48	285
5	Low	50	50, 50, 12	150
6	Low	10	30	30
7	Low	75	60, 60, 12	170
8	Low	170	60, 60, 60, 60, 44	360
9	Med	10	10	10
10	Med	50	4, 19	41
11	Med	125	22, 14, 8, 22	120
12	Med	170	25, 25, 25, 22	154
13	Med	125	25, 25, 25	113
14	Med	75	25, 26	70
15	Med	50	30	45
16	Med	25	22	22
17	Med	170	11, 11, 11	92
18	High	25	14	14
19	High	170	20, 30, 4	90

Table 3.2: Summary of calibration equipment, cut size, size selector, and operational flow rates used.

Instrument	Number of Units	Flow Rate (L/min)	Particle Cut Size (µm)	Sample Train Components
Escort ELF pump (5040 samples)	5-port manifold	2.2	0.8	Sharp Cut Cyclone
Airtec	5	1.7	0.8	Dorr-Oliver Cyclone, *SKC DPMI
Airwatch	1	2.2	0.8	Sharp Cut Cyclone
AE33	1	2.0	0.89	Sharp Cut Cyclone
OCEC Field Monitor	1	2.2	0.8	Sharp Cut Cyclone

*SKC DPMI – Diesel Particulate Matter Impactor (Eighty Four, PA)

Field Testing

The field portion of this study was conducted in a large-opening underground stone mine. The mine generally operates on a 5-day workweek (i.e., Monday through Friday), with a limited workforce on the weekends as needed. There are two eight-hour work shifts. Currently, maintenance and activities such as roof scaling and blast hole drilling are performed on the first shift, whereas most production activities occur on the second shift. Blasting is done following the second shift, such that gases are able to clear overnight.

Due to the large openings in the mine, air velocities are generally low (less than 100 ft./min in most locations) [15]. Ventilation is provided by both natural and mechanical means. Natural ventilation forces fresh air into the mine primarily via the main ramp, and a blower fan also pushes fresh air into the mine through a dedicated airway. The main exhaust is through the belt slope, which extends from a mid-level of the mine just below the primary crusher to the surface. Various auxiliary and booster fans, along with curtains and ventilation tubing, are also used to direct air as needed.

The primary airborne contaminant of concern in the mine is DPM [15]. The mine's equipment fleet consists of several haul trucks, loaders, scalers, drills, and support equipment such as light duty trucks. Historically, EC concentrations in the mine have been relatively high, although they are much lower recently due to a number of factors (i.e., revised production schedule, replacement or retrofitting of older engines with new exhaust treatments, and improved ventilation). Even so, inactive workings in the mine can serve as DPM sinks and this, combined with the slow turnover rate of air, can allow significant background concentrations for hours or days after engine emissions are halted. Previous monitoring studies near the main exhaust have shown a slow decline in EC over nights and weekends [7,8,15].

Because trends in EC near the main mine exhaust do tend to follow characteristic and expected patterns, all monitoring for the current study was performed in this location. Field data was collected over a period of approximately eight weeks using the same AE33, Airwatch and OCEC field monitor accompanied by the same operating conditions and size selectors used in the laboratory tests (Table A.1). For comparative data, 5040 samples were periodically collected over short time periods (i.e., about 5 hours) on either Thursday or Friday and Monday of most study weeks; and Airtec monitors were generally also used during these times. The late-week samples were expected to have relatively high EC concentrations as compared to those collected just after the weekend, since there is typically minimal activity in the mine over weekends. As another attempt to ensure a range of EC concentrations were covered by the 5040 samples, the samples were collected on first shift sometimes and on second shift other times.

The field 5040 samples were collected in triplicate using Escort ELF personal sampling pumps with Dorr-Oliver cyclones and DPMIs. The sampling flow rate was 1.7 L/min in order to achieve the desired 0.8 µm cut size to match that of the monitoring instruments. The samples were again collected onto pre-burned quartz fiber filters, and later analyzed by the same laboratory OCEC analyzer described above. When used, generally three Airtec monitors were operated to provide this data in triplicate also. These were again operated at a flow rate of 1.7 L/min, with the Dorr-Oliver cyclones and DPMIs. Flow rates for the ELF pumps and Airtecs were measured before and after each sampling period.

Data Analysis

As mentioned earlier, the monitors used in this study have different output variables based on their analytical techniques. Like the 5040 Standard Method, the OCEC field monitor reports a sample EC mass (µg), which can be converted to a mass concentration (µg/m^3) using the sample collection time and flow rate. The Airtec reports EC mass concentration (µg/m^3) as a 5-minute rolling average; and since multiple Airtecs were generally used for testing in this study, their data was averaged before comparing to other data. The AE33 reports BC concentration (ng/m^3, converted to µg/m^3 here) as both a raw and corrected value, which is discussed further below. Finally, the Airwatch reports optical sensor voltage (mV). For any time increment on a given filter spot, the voltages can be translated into a laser absorbance value using Equation 1, where v_f is the final voltage and v_i is the initial voltage. To determine EC mass accumulated on the filter (or mass concentration in the environment) for that same time increment, a calibration curve correlating absorbance to EC mass must be used.

$$Absorbance = -\log\left(\frac{v_f}{v_i}\right) \quad \text{(Equation 1)}$$

In addition to having different output variables, the monitors used in this study collect data at different rates. Thus, some work was required to allow comparison of time-series and TWA data. Figure 3.1 shows example data from all instruments for one of the laboratory tests to demonstrate several key points. First, the AE33, Airwatch and Airtec data all appear as continuous over the test period shown. The AE33 and Airtec both record data on a 1-minute time basis, and the Airwatch records on a 5-second basis. In this study, the Airwatch data was condensed (by data extraction) to a 1-minute basis to match the output from the AE33 and Airtec. In contrast, the OCEC field monitor data appears as semi-continuous – meaning the monitor produces a series of short TWA values corresponding to the individual samples collected during the test period. And the 5040-sample value appears as a single TWA value, which is applied over the entire test period (i.e., sample collection time).

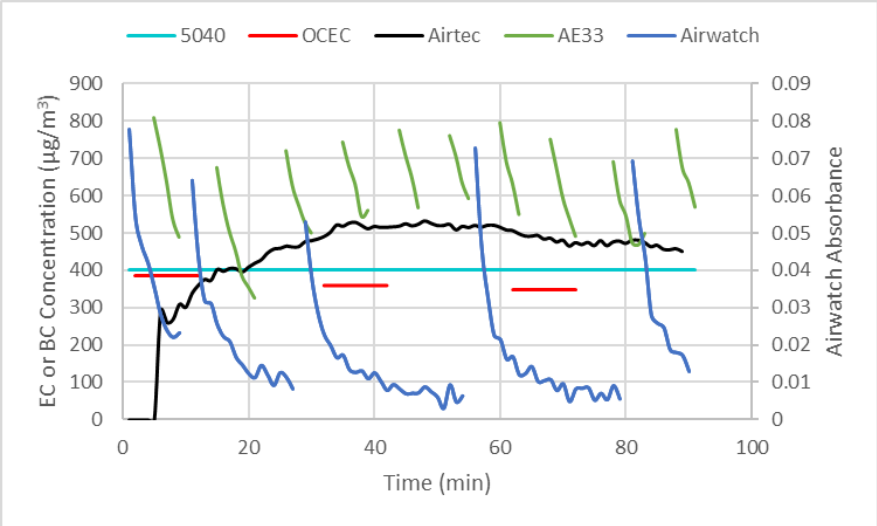

Figure 3.1: Example test data (high concentration lab test). TWA EC concentrations are shown for 5040 and OCEC field monitor, EC concentration is shown for Airtec, (raw) BC concentration is shown for AE33, and calculated absorbance values are shown for Airwatch.

Figure 3.1 also illustrates breaks in data that correspond to filter tape advancement (AE33 and Airwatch) or sample analysis (OCEC field monitor). The tape advance takes about 6 minutes for the AE33 and about 15 seconds for the Airwatch; sample analysis takes about 20 minutes for the OCEC field monitor. To calculate a single TWA value for each laboratory test or each 5040 sample collection period during the field testing, data from these monitors was interpolated between breaks (or extrapolated to the end of a test). For the Airtec, Figure 3.1 shows that some time is required at the beginning of the test to reach a relatively stable value. This is partially because it reports data on a 5-minute rolling average (i.e., only zero values are reported before minute 6). Moreover, the optical sensor in the monitor is also limited in detecting very small changes in laser absorbance (i.e., incremental mass accumulation), which means that data stabilization can take longer in relatively low DPM concentrations [15]. Thus, TWA values for the Airtec were determined for the time period following data stabilization (i.e., after non-zero values were continually registered).

A final observation from Figure 3.1 is that the monitors which operate on a laser extinction principle can exhibit filter loading effects. One type of effect is clearly visible in the Airwatch absorbance data, which declines sharply at the beginning of each filter spot and then begins to stabilize. This effect is attributed to a fibrous filter media, which experiences two distinct phases of loading. In the first phase, mass is loaded in the spaces between fibers and this produces a rapid decay in voltage and thus laser absorbance. In the second phase, mass begins to load on top of the filter and produces a consistent unit laser absorbance per unit of mass accumulated – which is the ideal behavior for a laser-based monitor in a constant-concentration sampling environment. This type of loading effect can be avoided by using a non-fibrous filter, but unfortunately it appears that the PTFE coating on the Airwatch filter in this study was degraded. The impact on study results is discussed in detail below.

Another and very common type of filter loading effect is also evident in the Figure 3.1 in the AE33 data. It is that he monitors which operate on the laser extinction principle (AE33, Airwatch, Airtec) may exhibit a filter loading effect. The effect is observed as an apparent decay in BC or EC mass concentration in the sampling environment as data is

collected on a given filter/filter spot. This effect is well established and happens because even using a non-fibrous filter, particles eventually start to load on top of one another, which reduces the unit laser absorbance expected per unit of mass accumulation [16,17]. In the figure, despite the EC concentration being relatively constant throughout the test, the AE33 concentration sharply declines on each filter spot. In a lower concentration environment, this effect might manifest as a relatively constant BC concentration at the beginning of a filter spot, followed by a sharp decline toward the end. This type of effect can also impact the Airtec and Airwatch, though neither of those instruments appear to be affected in the test shown in Figure 3.1. For the Airtec, the filter loading effect is generally not significant over the range of EC masses expected to be loaded on a sample filter during a full shift of mine monitoring (i.e., about 35-250 μg) [5]. In Figure 3.1, the total EC mass sampled was about 80 μg.

For the AE33, Magee Scientific has sought to address the filter loading effect using a patented compensation method based on real-time tracking of the change in laser absorbance on two filter spots collected simultaneously but at different flow rates [18]. Using this "dual spot" method, the AE33 reports both a raw and corrected BC concentration value. While this method has been shown to yield accurate corrected data in relatively low DPM environments (e.g., urban air monitoring) [18], in the current study the AE33 did not consistently report corrected data in the medium and high DPM laboratory tests (i.e., tests 9-19 in Table 3.1). Thus, corrected AE33 data was analyzed for the low DPM tests (and field testing), and uncorrected (raw) data was analyzed for the other tests.
Regarding the 5040 data, since the 5040 Standard Method is conducted using only a small punch from the sample filter, non-uniform DPM loading on the filter might yield significantly different results amongst replicate samples. For each data set in this study, the 5040 sample results were evaluated to identify statistical outliers (i.e., a sample value more than three σ away from the average). Where outliers were identified, samples were re-analyzed (using a second punch from the original filter) to rule out errors associated with the sample preparation or laboratory OCEC analyzer. Ultimately, 4 of the 19 laboratory tests had five samples that were not statistically significantly different, 6 tests had 4 samples that were not statistically significantly different, and 9 tests had 3 samples that were not statistically significantly different (see Table A.2 in Appendix). Samples determined to be in agreement were averaged to obtain a TWA 5040 EC concentration (μg/m^3 and 95% confidence interval) for each test, which was compared to the TWA value derived from each monitor.

Results

Laboratory Testing

The 5040 sample results confirmed that low DPM tests (1-8) had EC concentrations between 100-200 μg/m^3, medium DPM tests (9-17) had concentrations between 450-550 μg/m^3, and high DPM tests (18-19) had concentrations between 700-850 μg/m^3 (Table A.2). In general, the engine loading condition made only a slight difference in the EC to OC ratio during testing (i.e., high loading resulted in somewhat higher EC as expected), and no discernable difference was observed in the performance of any of the monitors based on the loading condition.

As mentioned earlier, the parameter of practical interest for the continuous monitors tested here is EC mass concentration and so all results below are presented on this basis. However, some results are discussed in the context of mass since monitor performance issues (e.g., due to filter loading effects) may be fundamentally related to mass.

As expected, the OCEC field monitor results matched the 5040 results very well in the laboratory tests. Indeed, considering that the OCEC field monitor effectively uses the same thermal-optical method as the 5040 Standard Method and is not subject to issues related to uniformity of particle deposition (i.e., since the entire filter area is analyzed), the monitor results in this study can generally be regarded as verification of the 5040 results. Figure 3.2 compares the EC concentration results from OCEC field monitor and the standard 5040 samples (all data tabulated in Table A.3). Only one of 19 tests produced a data point that did not fit the trend of the other data. This statistical outlier (determined as a variance greater than three σ away from the mean of the ratio between monitor and 5040 results) is shown as point "A" in the figure. Inaccurate 5040 data are probably responsible for point A, which was also found to be an outlier when comparing all other monitoring instruments to the 5040 results (Table A.4). Thus, the OCEC field monitor value was used for this data point instead of the 5040 value for evaluation of all other monitors.

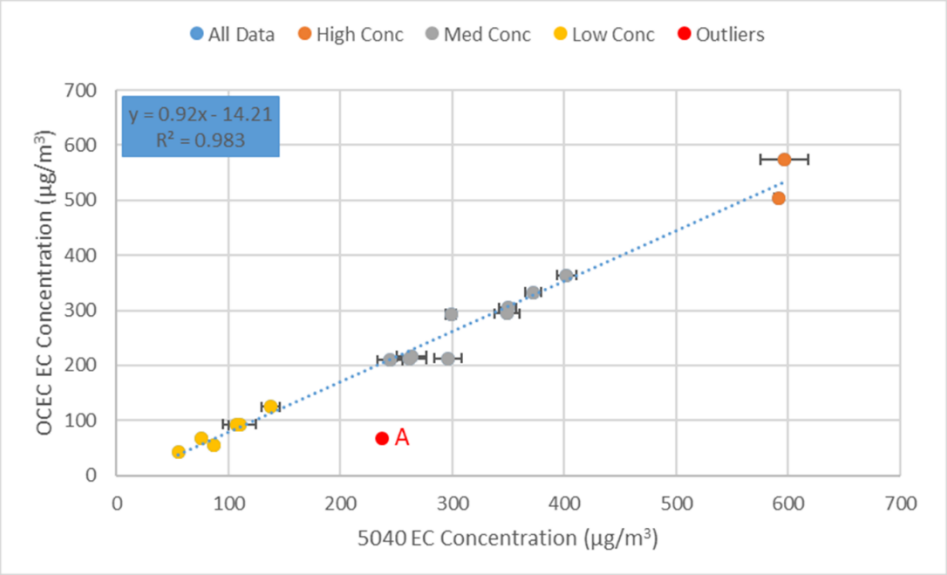

Figure 3.2: TWA EC concentration measured by OCEC field monitor versus 5040 Method for laboratory tests. Error bars represent 95% confidence intervals for replicate 5040 samples results; confidence intervals were not computed for OCEC field monitor data since individual samples collected within each test had variable collection times.

The Airtec-derived TWA values also correlated well with the 5040 data (Figure 3.3), which was expected since the Airtec is calibrated to the 5040 EC [5, 6]. A linear regression of data points from the low and medium DPM tests showed an R^2 of 0.83, a slope of 1.16, and an y-intercept of 18 µg/m^3. This fits well with field observations by Noll and Janisko (2013) in the same general EC ranges [5]. They found that the Airtec had a slight positive bias, which was more pronounced in the lowest EC concentrations. They also found that the bias diminished or even became slightly negative at higher EC concentrations, which is again consistent with the current study (Figure 3.3). This change in the Airtec's performance across EC concentrations undoubtedly happens due to the aforementioned filter loading effect, where particles eventually begin to load on top of one another. This effect is fundamentally an issue of mass accumulation rather than concentration in the sampling environment (i.e., it will happen once some total mass has been accumulated). For the tests conducted here, those with the highest sample masses (i.e., about 100 µg EC or more) did in fact fall below the trend line for the rest of the data – actually producing more accurate (though less precise) Airtec results.

As mentioned earlier, the AE33 uses a dual-spot method to correct data for the filter loading effect. Here, the instrument only reported corrected BC concentrations consistently (i.e., for every filter spot within a test) for the low DPM tests (1-8). For these, the correlation between TWA BC concentration and 5040 EC concentration values was good (Figure 3.4). The BC to EC ratio observed in these tests (i.e., indicated by the slope of the trend line in Figure 3.4) is generally consistent with several field observations (1.5-2.0) in similar EC concentrations [8,9], but it is much higher than the ratio (roughly 1.0) observed in another study where the EC concentrations were typically in the medium DPM range tested here [7]. In all of those studies, the AE33 was used to continuously monitor BC concentration, which was periodically compared to 5040 EC concentration.

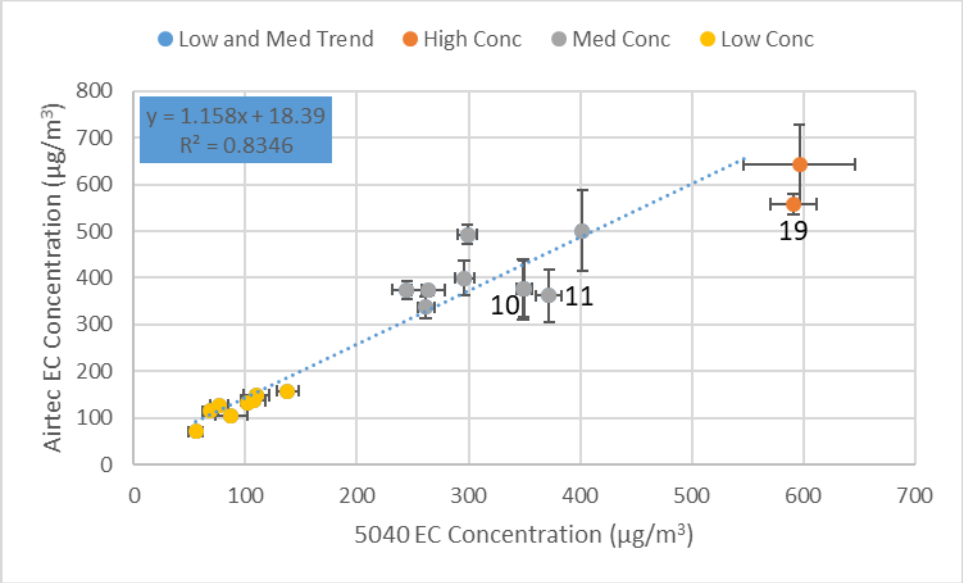

Figure 3.3: TWA EC concentration measured by Airtec monitors versus 5040 Method for laboratory tests. Error bars represent 95% confidence intervals for replicate 5040 samples and Airtec (5 monitors) results. Data points for tests 10, 11, and 19 are labeled, and these tests had relatively high sample masses of 98.71, 111.73, and 122.67 µg, respectively.

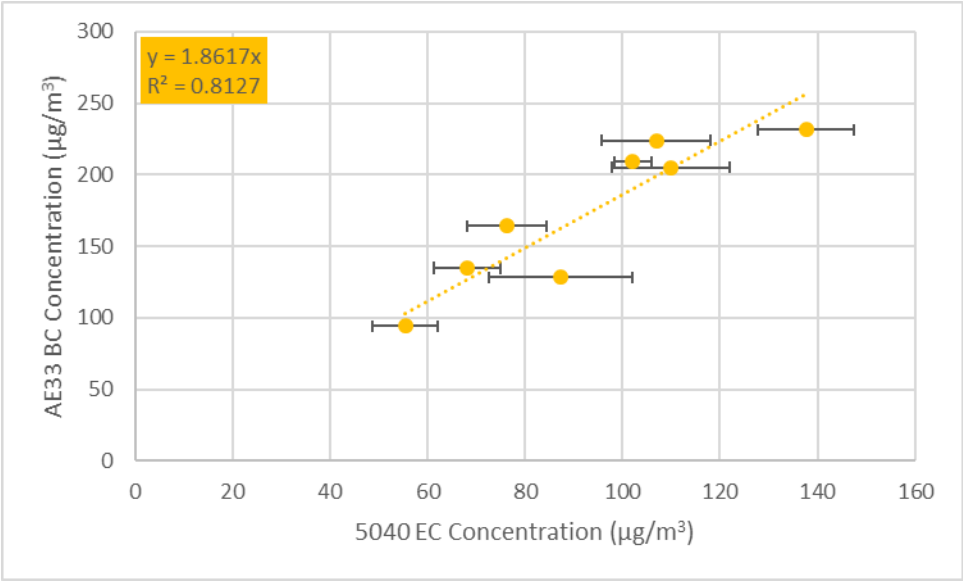

Figure 3.4: Corrected AE33 BC concentration versus 5040 EC concentration for low DPM laboratory tests. Error bars represent 95% confidence intervals for replicate 5040 samples; confidence intervals were not computed for AE33 data since individual filter spots within each test had variable collection times.

To examine the AE33 data across all 19 laboratory tests, the uncorrected BC concentration data was first used (Figure A.1). While the correlation to 5040 data over the entire EC concentration range was still fairly good (R^2 of 0.80), the apparent BC to EC ratio was quite low (slope of 0.88) – closer to the prior field study mentioned above in medium EC concentrations [7]. This is consistent with expectations for the uncorrected data, since the filter loading effect most severely impacts measurements in higher DPM concentrations (i.e., where the rate of mass accumulation on the filter is higher).

To further explore this, the AE33 data was also reduced to "first-minute" data, meaning that only the BC concentration measured during the first minute on each filter spot during a test was used to compute a TWA concentration for the test. This effectively focuses analysis on what should be the best data (i.e., least impacted by the filter loading effect) under the test conditions here - but makes the AE33 more of a semi-continuous monitor. Figure 3.5 shows the first-minute BC concentration. There is a clear change in the relationship with 5040 EC as concentration increases, producing a BC to EC ratio near 2.0 at low concentrations and a ratio near 1.0 at higher concentrations. These results more fully explain the previous observations of apparent variability in BC to EC ratio in different EC concentrations. Moreover, they suggest that some effect of filter loading is present even within the first minute of sample mass accumulation – possibly due to the filter media itself. Nevertheless, the first-minute data demonstrates the potential of the AE33 to reliably predict EC from BC across a wide range of concentrations.

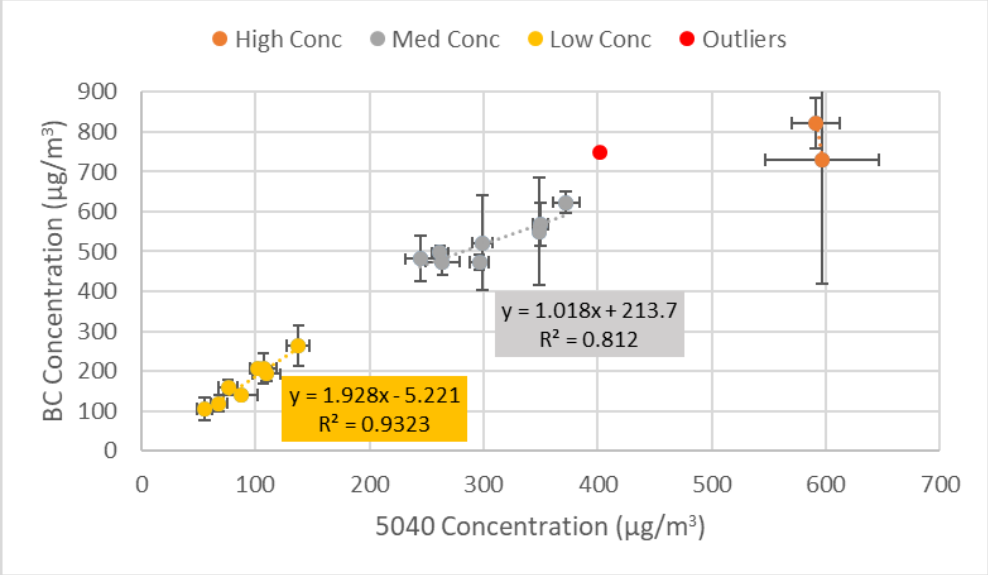

Figure 3.5: First-minute AE33 BC concentration versus 5040 EC concentration for laboratory tests. Error bars represent 95% confidence intervals for replicate 5040 samples and first-minute data from all AE33 filter spots in each test.

Since, in its current form, the Airwatch only yields laser absorbance values, one objective of including it in this study was to gather additional calibration data against 5040 EC. For this, it is important to measure a range of absorbance values that correspond to accumulated EC mass values on the Airwatch filter. Further, it is important that the range of mass values covered by the calibration curve includes the values of practical interest for field monitoring applications. Because the Airwatch is intended as a continuous monitor, it should have a relatively fast data collection rate. To match the AE33 and Airtec, a 1-minute time basis was chosen for this study and therefore 1-minute absorbance and accumulated mass values were used to construct the calibration curve (Figure 3.6).

To determine a 1-minute mass accumulation value for each test, the average 5040 EC value was divided by the total test time. This assumes that the EC concentration in the test chamber was constant during the test. To determine corresponding 1-minute absorbance values for each test, the initial and final voltage values for each minute of data collection were used to calculate a series of 1-minute absorbance values for the test, and then these were averaged. Since the aforementioned fibrous filter loading effect (see Figure 3.1) was observed in all Airwatch data in this study, the 1-minute absorbance values for each test were only determined from "complete" filter spots (i.e., spots that were loaded to the point where the instrument self-advanced to a clean spot). This is because the relative influence of the initial drop in absorbance due to mass loading between the filter fibers should be higher on spots that were only partially loaded. Here, partially loaded filter spots were considered to be the last filter spot in tests with multiple spots, or the only spot in tests with a single spot (i.e., the tape never advanced). Five out of the 19 laboratory tests in this study only had a single filter spot on the Airwatch and those tests were not included in the calibration curve.

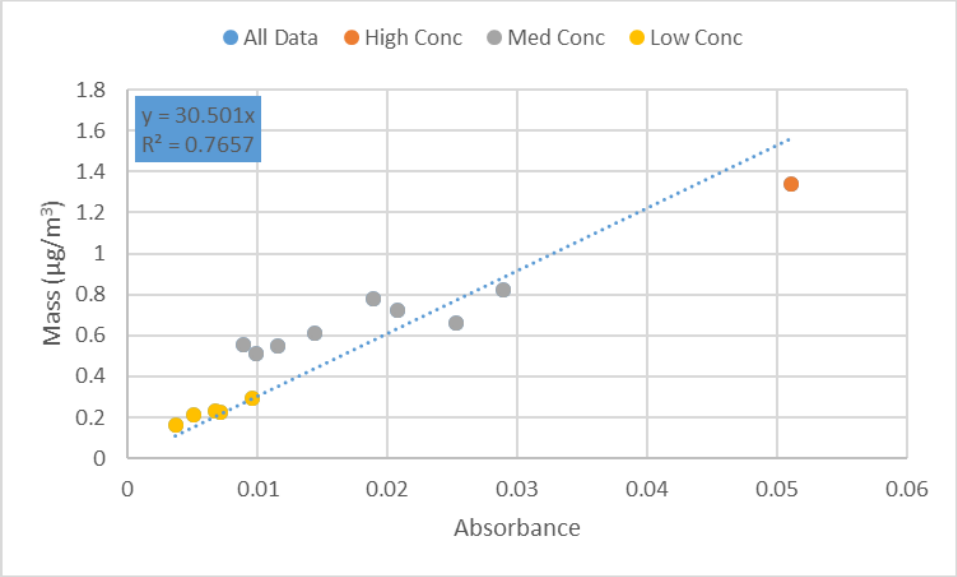

Figure 3.6: Airwatch calibration curve showing EC mass accumulated on filter versus laser absorbance.

The slope of the linear trend line in Figure 3.6 is higher than that produced in a previous calibration of the same Airwatch unit (i.e., slope of approximately 17) [7]. This difference is attributed to a change in the filter material between the two calibration efforts. Here, the material was clearly fibrous and previously it appeared to be non-fibrous (i.e., relatively constant absorbance values were produced in a series of tests in the same Marple chamber under near constant EC concentration). As mentioned above, the fibrous filter loading effect results in relatively high absorbance values at the beginning of data collection on each filter spot before the absorbance begins to stabilize and behave ideally; and these high initial values skew the average absorbance on the entire filter spot.

Also notable from Figure 3.6 is the fact that the Airwatch absorbance appears too low in some of the tests in the medium concentration category (i.e., data points fall relatively far above the trendline). This is indicative of the more common filter loading effect exhibited by laser-based monitors, which happens when particles begin to pile on top of one another to reduce laser absorbance response. It is unclear why this behavior was only exhibited in some of the medium concentration tests – and not in the one high concentration test – but several confounding factors are possible including non-uniformity of the filter tape material, which change the relative influence of the fibrous filter loading phase of mass accumulation.

Field Testing

EC concentrations in the stationary sampling location of the study mine were relatively low during the field testing. The 5040 samples gathered during 11 separate observation periods (5 hours each) indicated a range of about 18-125 µg/m^3 (Table A.5); and the OCEC field monitor, which captured data continually over most of the study period, indicated a range of 10-120 µg/m^3 (Fig A.2). These concentrations are comparable to those in the low DPM category of laboratory tests and represent field conditions that may be typical of many underground mines. The sort of area monitoring conducted in this study should not be construed as a way to estimate personal exposures (i.e., which are measured on an individual who may move to different locations, be protected by an enclosed cab or ventilated work room, etc.) However, it is worth noting for context that the EC range observed here is a practical range of interest for mine engineering, considering the guidance set by regulatory limits on personal exposures (i.e., 160 µg/m^3 TC, which is about 123 µg/m^3 EC using the typical assumption of a TC/EC ratio of 1.3).

Figure 3.7 provides a comparison of instrument biases for all monitors versus the average TWA 5040 EC values measured for the 11 observation periods; data in the figure is tabulated in Table A.6. The absolute maximum bias for EC on any monitor was less than 60%. The OCEC field monitor consistently exhibited a negative bias (Figure 3.7a),

which may seem surprising based on its near perfect correlation with 5040 data in the laboratory. This can be explained at least in part by the semi-continuous sampling mode of the instrument and the general trends in DPM levels in the monitoring location. For the field testing, the OCEC monitor was programmed to collect 30-minute samples on the hour (i.e., 30-minute sample, followed by 20-minute analysis time and 10 minutes of downtime before the next sample collection began), so each data point in Figure 3.7 represents a TWA of five samples. In the particular sampling location for this study, there are two general DPM sources. DPM moves through this area as a sort of background concentration that slowly travels with air coming from the primary production zone and other areas in the mine with significant DPM emissions. It is also emitted directly adjacent to the monitoring location by haul trucks dumping material into the crusher and other vehicles coming to and from the location for specific work activities. While a semi-continuous monitor may be well-suited to track the gradual trends associated with the background DPM, it may not consistently capture trends associated with DPM pulses. Indeed, the conditions in the monitoring location for this study should only ever result in an underestimation of EC by a semi-continuous monitor since there may be periodic spikes in DPM to temporarily increase the concentration, but overall reductions in DPM only happen gradually as the background concentration decreases.

For the Airtec, the bias plot in Figure 3.7b is based on a comparison of the average Airtec TWA EC concentration (i.e., determined using two or three monitors in each observation period) versus that TWA 5040 EC concentration. The absolute bias of the Airtec was generally within about 30%. The one exception was during the observation period with the lowest 5040 EC concentration (i.e., 18 μg/m3), where the Airtec bias was 55%. These results are consistent with expectations based on other studies (e.g., [5]), and given that the Airtec was designed for sampling in higher concentrations and for longer sampling periods than used in this study, its performance here can be considered quite good.

For the AE33, Figure 3.7c shows the bias versus 5040 EC for both BC and EC concentrations. The BC concentration was determined as a TWA value for each observation period. During the field testing, the AE33 tended to collect on a single filter spot for 30-90 minutes, which yielded about 3-10 spots for each 5-hour observation; and in the relatively low concentrations present during testing, the instrument consistently reported corrected BC concentrations. These were simply averaged (following interpolation between data breaks for filter advances) to arrive at a TWA value for each observation period. To determine a TWA EC concentration for each period, the relationship between BC and 5040 EC shown in Figure 3.4 was used. As seen in Figure 3.7, there was a consistent positive bias for AE33 BC versus 5040 EC, which was expected based on the laboratory testing here and prior field testing in relatively low concentrations [cite JV's papers here]. However, the calculated AE33 EC consistently tended to underestimate the 5040 EC. This suggests that the BC to EC ratio in the field testing was actually lower than that shown in Figure 3.4. Since the AE33 works as a continuous monitor, the primary cause for underestimation of EC is probably not the same as discussed for the OCEC field monitor. Rather, it is possible the monitor behaves differently (in terms of the apparent BC to EC ratio) in the DPM concentration range covered by these field observations. Another possibility is that very fine mineral dust (i.e., smaller than the cut size of the sampling cyclone) may have interfered with measurements. Nevertheless, the range of the bias for the calculated AE33 EC values was relatively small (i.e., about -15% to -40%), which suggests a primary problem with the BC to EC ratio accuracy rather than precision of measurements.

For the Airwatch, data was only collected for seven of the 11 observation periods where 5040 samples were also collected. Near the end of week 6 of the field study, the clamping mechanism for the filter tape failed and this caused the instrument to not auto-advance the tape. For the periods where the Airwatch was functioning properly, EC concentration values were determined using the relationship between absorbance and 5040 EC mass shown in Figure 3.6. Like for the laboratory tests, absorbances were determined on a 1-minute basis and then the corresponding EC mass was used to calculate EC concentration (i.e., using the Airwatch flow rate). The concentration values for all complete filter spots in a given observation period were then averaged and used to produce a TWA EC concentration value for the entire observation period. (Similar to the AE33, filter spots on the Airwatch tended to represent about 30-90 minutes of data collection during the field testing.) Figure 3.7d shows that the Airwatch EC generally underestimated 5040 EC. Interestingly, the two largest bias values (i.e., -28% and -52%) were observed for the last two observation periods that the Airwatch was used. This may suggest that the instrument was beginning to experience problems even before the clamping mechanism completely failed. If the filter tape advances late, the Airwatch data should indeed underestimate EC because an overloaded filter spot will exhibit the filter loading effect noted earlier (i.e., where particles begin to pile on top of each other with a reduced response in

laser absorbance). The Airwatch bias in the first five observation periods ranged between 14% and -15%, which is encouraging albeit based on relatively few observations.

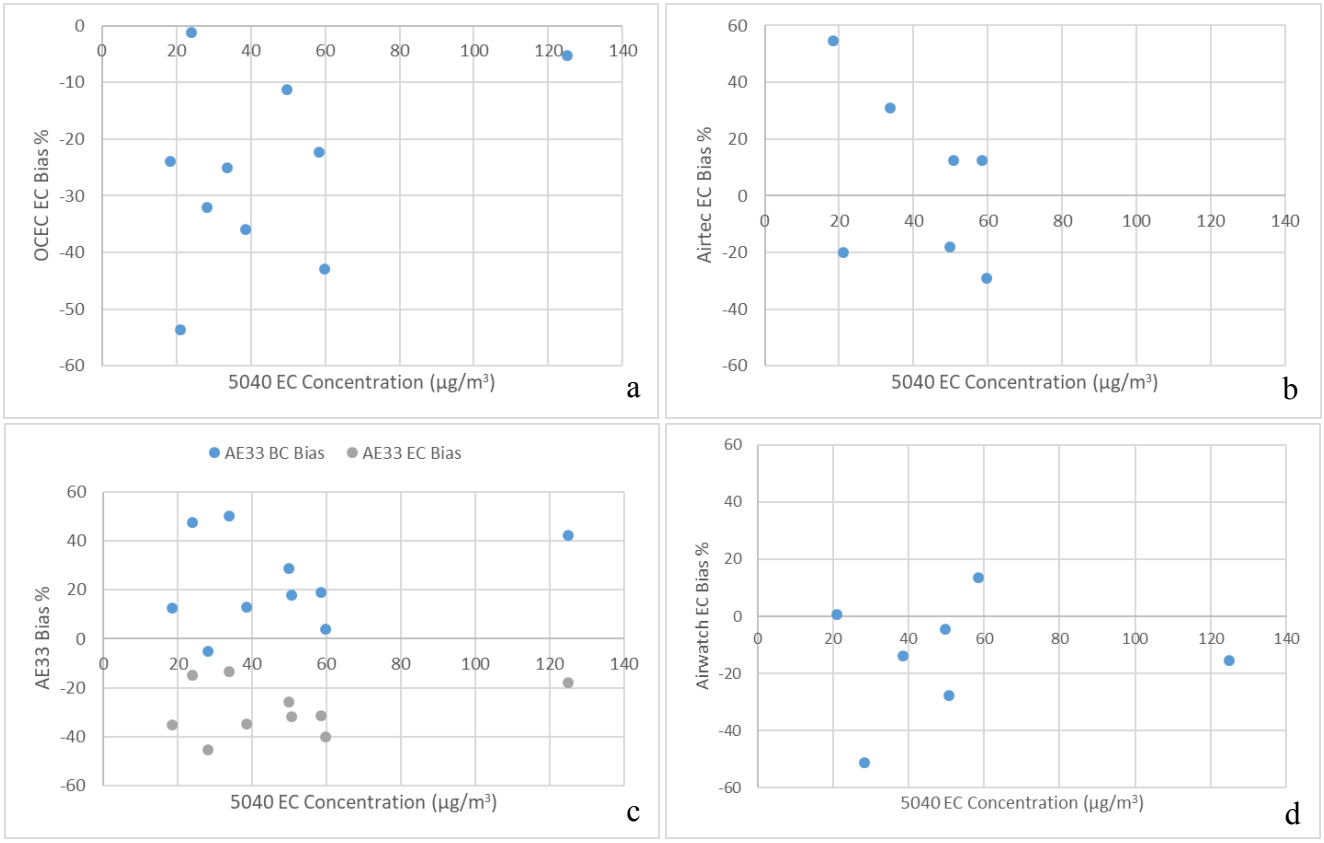

Figure 3.7: Bias plots for OCEC field monitor, Airtec, AE33, and Airwatch monitors (a-d respectively) as compared to 5040 EC concentrations.

In order to further evaluate the performance of the monitors in this study, even when 5040 samples could not be collected, time-series data was analyzed. Figure 3.8 shows an example of data collected by the OCEC field monitor, AE33 and Airwatch over six consecutive days. The data from all three monitors tends to track well together, and exhibits a pattern consistent with expectations based on activities in the mine. The concentration in the monitoring location appears to peak on mid-Saturday morning, which is about 8 hours after the final production shift concluded late on Friday night. The concentration then continues to decline until mid-Monday. Maintenance and support activities resumed during first shift on Monday, and production activities resumed during second shift. About 8 hours after production began on Monday, the concentration began to gradually increase. The periodic spikes in concentration are attributed to activity directly adjacent to the monitoring location (e.g., haul trucks dumping into the crusher). In some cases, the OCEC field monitor appears to catch these DPM pulses, but they are more pronounced in the continuous data. The oscillations in the AE33 and Airwatch data are generally attributed to effects of filter loading discussed earlier.

To further evaluate the correlation between the monitors tested here, Figure 3.9 shows a comparison of the AE33 and Airwatch data against the OCEC field monitor across the entire field study. To construct this plot, TWA values for BC or EC concentration were determined for each AE33 or Airwatch filter spot that collected data during the study. A corresponding EC data point from the OCEC field monitor was calculated by determining a TWA value based on the EC values measured or interpolated during the time period of the AE33 or Airwatch filter spot. Because the OCEC field monitor does tend to underestimate 5040 EC, at least during time where DPM emissions may occur relatively close to the monitoring locations, the correlation coefficients in Figure 3.9 are probably more important than the slope of the trendlines shown. Based on the R^2 value for the AE33 (i.e., about 0.93), it and OCEC

field monitor appear to have tracked very well together during the field study. For the Airwatch, the correlation is not as strong, and it is particularly weak for data collected during the final days of Airwatch field testing before the clamping mechanism failed (around November 6, 2017). Figure 3.9 shows data from these final days in grey. The R^2 value including these data is 0.76, but it improves to 0.85 if they are excluded.

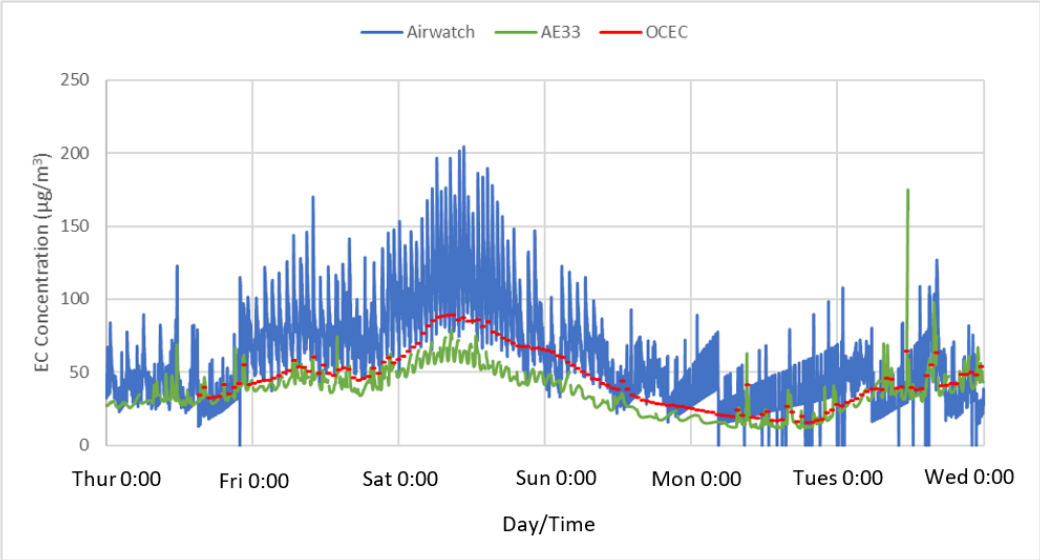

Figure 3.8: EC concentration measured by the OCEC field monitor, AE33, and Airwatch over six consecutive days (Thursday to Wednesday) in an underground stone mine. Airwatch concentrations were determined on a 5-minute rolling average for this plot.

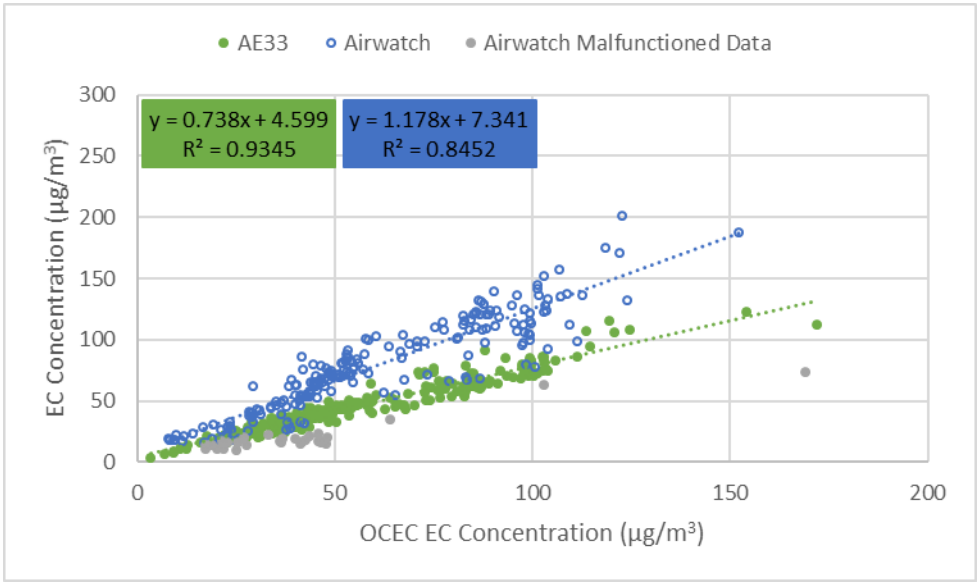

Figure 3.9: Comparison of AE33 and Airwatch EC concentrations to OCEC EC concentration for duration of 8-week field study.

Discussion

Overall, the laboratory and field testing here indicate that the OCEC field monitor, AE33 and Airwatch all have potential for long-term and autonomous DPM monitoring in underground mines. While the EC concentrations in the monitoring location of the study mine were relatively low during the field demonstration, the values observed here are certainly within the range of interest for many mines. Moreover, the laboratory tests in this study covered a very

wide range of EC concentrations such that important insights about the practical operating limits for each monitor were gained. Considering all of the results, some remarks can be made regarding the general data quality, usability and readiness of each instrument for mine monitoring applications.

The OCEC field monitor produced reliable EC data – similar to the traditional 5040 EC – across a wide range of concentrations in the laboratory. However, in the field it consistently underestimated 5040 EC. While this is largely attributed to the semi-continuous nature of this monitor and the fact that DPM pulses were likely in the field monitoring location, further testing is needed to confirm that explanation and demonstrate the instrument in a wider range of mine settings. Regarding readiness and practicality for mine applications, the OCEC monitor does represent an off-the-shelf option, with capabilities for the user to define many sample collection and analysis parameters if desired. Although not a focus of the current study, this monitor's ability to measure OC in addition to EC may also be of real interest in some particular mine applications. The monitor does require consumables (i.e., gases and filters), and the frequency for replacing these and conducting instrument maintenance would be highly dependent on the environmental circumstances. Further, while the field testing here demonstrated the OCEC field monitor can be operated in a working mine, selection of the installation location must be carefully considered – both to protect the instrument and to ensure that monitoring data can be accurately interpreted.

The AE33 is another option that is already commercially available. In this study, at lower EC concentrations (i.e., about 200 $\mu g/m^3$ or less), the AE33 produced BC data that correlated fairly well to the standard 5040 EC. It also tracked well with other monitors in the field, indicating it can provide reliable monitoring data over extended periods of time. The lower EC range might be important for many mine monitoring applications, where the objective is to catch an impending exceedance of a particular threshold value. Moreover, it seems reasonable that the filter loading issue that affects the AE33 at higher concentrations could be resolved via some fairly simple modifications (e.g., a lower sample flowrate, sample dilution, or an alternate filter media). The filter tape is the only consumable for the AE33 and replacement frequency would be dependent on conditions in the monitoring location. The instrument is housed within an environmental enclosure to protect it from dust and humidity but, again, selection of an appropriate installation location should be carefully considered.

The Airwatch prototype tested in this study performed well in that its raw output data (i.e., optical sensor voltage) could be transformed into absorbance values and correlated to 5040 EC, and it successfully collected data for extended periods of time in the field. Considering that the filter tape material tested in this study was not ideal, the correlation between the Airwatch EC and 5040 EC was generally quite good. For further testing and development, a non-fibrous filter material may yield even better results. The failure of the clamping mechanism that occurred toward the end of the field testing represents a relatively minor design problem, but this and other mechanical components should undergo long-term testing in a variety of mine conditions to ensure the Airwatch perform reliably in its intended applications. If fully developed, the Airwatch might represent a sort of rugged, mobile option for continuous DPM monitoring for mines looking to answer basic engineering questions.

Importantly, none of the continuous DPM monitors tested here were evaluated for specific analytical interferences from other aerosols. DPM was the only particulate in the sampling environment during the laboratory tests, and sharp cut cyclones were used to limit mineral dust interference during the field testing. Application-specific consideration should be given to possible interferences in the intended monitoring environment.

Conclusions

Capabilities for continuous DPM monitoring in underground mines would be valuable for both protection of worker health and engineering purposes. This study tested three continuous monitors in the laboratory and in the field, all of which appear to have potential for mine applications. The OCEC field monitor may be best suited for applications where long-term and high-level data is needed, but the semi-continuous nature of the instrument does not prevent observation of important trends. The AE33 Aethalometer represents another off-the-shelf option, which can reliably measure BC concentration across a primary range of interest for mines. The Airwatch monitor is still in development, but could eventually be a continuous version of the handheld Airtec monitor – specifically designed for high DPM and physically challenging mine environments.

Acknowledgements

The authors thank NIOSH/CDC for funding this work (contract number 200-2014-59646). Views expressed here represent those of the authors and not NIOSH or any other entity. We thank all personnel at the study mine for their cooperation, guidance, and continual support of this work. At Virginia Tech, we also thank Forest Wright for help with data collection and analysis, and Chreston Miller for his support with Airwatch data processing. Finally, we thank Tony Hansen at Magee Scientific for his continued technical support and guidance with the AE33.

References

[1] D. B. Kittelson, "Engines and Nanoparticles: A Review", J. Aerosol Sci. Vol. 29, 1997.

[2] R.H. Grau III, S.B. Robertson, T.P. Mucho, F. Garcia, A.C. Smith, "NIOSH Ventilation Research Addressing Diesel Emissions and Other Air Quality Issues in Nonmetal Mines", SME Annual Meeting, Phoenix, AZ, 2002.

[3] J. Noll, Timko, R., McWilliams, L., Hall, P., and R. Haney, "Sampling results of the improved SKC diesel particulate matter cassette", Journal of Occupational and Environmental Hygiene 29-37, 2010.

[4] OSHA – MSHA, "Diesel Exhaust/Diesel Particulate Matter", November 2012.

[5] J. D. Noll, S. Janisko, "Evaluation of a Wearable Monitor for Measuring Real-Time Diesel Particulate Matter Concentrations in Several Underground Mines", Journal of Occupational and Environmental Hygiene, 10: 716-722, 2013.

[6] Janisko, S., and Noll, J.D., "Near real time monitoring of diesel particulate matter in underground mines," Proceedings of the 12th U.S./North American Mine Ventilation Symposium, pp. 509-513, 2008.

[7] C. Barrett, S. Gaillard, E. Sarver, "Demonstration of Continuous Monitors for Tracking DPM Trends over Prolonged Periods in an Underground Mine", 16th North American Mine Ventilation Symposium,2017.

[8] Volkwein, J. C., C. Barrett, E. Sarver, and A.D.A Hansen, "Application of an Environmental 'Black Carbon' Particulate Sensor for Continuous Measurement of DPM in Three Underground Mines", The Australian Mine Ventilation Conference, 2017.

[9] Volkwein, J C, Robertson, K and Hansen, A D A, "Long-term continuous measurement of diesel particulate matter patterns in a large underground metal mine", Proceedings 16th North American Mine Ventilation Symposium (ed: J Brune), pp 5–19, (Society for Mining, Metallurgy, and Exploration: Littleton, CO), 2017.

[10] Nomadics, Inc., "Autonomous Networked EC Monitor Final Report", Contract: 200-2010-36901.

[11] Sunset Laboratory Inc., "Organic Carbon and Elemental Carbon Field Instrument, Model 4 User's Manual".

[12] Yu, Chang Ho, Patton, Allison P., Zhang, Andrew, Fanac, Zhi-Hua (Tina), Weisel, Clifford P., and Lioy, Paul J. "Evaluation of Diesel Exhaust Continuous Monitors in Controlled Environmental Conditions", Journal of Occupational and Environmental Hygiene, 2015.

[13] Cauda, Emanuele, Sheehan, Maura, Gussman, Robert, Kenny, Lee and Volkwein, Jon. "An Evaluation of Sharp Cut Cyclones for Sampling Diesel Particulate Matter Aerosol in the Presence of Respirable Dust". Annals of Occupational Hygiene, Vol 58., No. 8, 995- 1005, 2017.

[14] NIOSH, "Elemental Carbon (Diesel Particulate): Method 5040, Issue 3, March 15, 2003.

[15] S. Gaillard, E. McCullough, E. Sarver, "Area Monitoring and Spot-Checking for DPM in an Underground Mine" Mining Engineering, Vol. 68, No. 12 pg. 57-63, 2016.

[16] J. Jimenez, C. Claiborn, T. Larson, T. Gould, T.W. Kirchstetter, L. Gundel "Loading Effect Correction for Real-Time Aethalometer Measurements of Fresh Diesel Soot", Journal of the Air and Waste Management Association, 57:7, 868-873, 2007.

[17] Weingartner, E., Saathoff, H., Schnaiter, M., Streit, N., Bitnar, B., and Baltensperger, U.,"Absorption of light by soot particles: determination of the absorption coefficient by means of aethalometers", J. Aerosol Sci., 34, 1445–1463, doi:10.1016/S0021- 8502(03)00359-8, 2003.

[18] L. Drinovec, G. Mocnik, P. Zotter, A. S. H. Prévôt, C. Ruckstuhl, E. Coz, M. Rupakheti, J. Sciare, T. Müller, A. Wiedensohler, and A. D. A. Hansen, "The "dual-spot" Aethalometer: an improved measurement of aerosol black carbon with real-time loading compensation" Atmos. Meas. Tech. Discuss.: 30 September 2014.

Summary and Conclusions

All three of the monitors tested here demonstrated the ability to autonomously monitor and track DPM trends over prolonged time periods in an underground mine environment. However, a number of practical limitations and challenges were discovered in these studies, which are relevant for further considerations surrounding future applications.

The Airwatch, which was prototyped with the specific intent to be used as a continuous monitor for mine environments, has now been demonstrated several times underground and calibrated twice to the 5040 Standard Method measure of elemental carbon (EC). Based on these studies, the Airwatch shows clear potential for mine monitoring applications. However, it still needs major modifications if it is to be fully developed toward commercialization. These modifications must include improved data output in terms of selecting an appropriate time-basis for measurements that will cover the range of expected DPM concentrations of interest for mines, and the actual data display and transfer capabilities. Further, some mechanical issues must also be addressed, particularly with respect to the clamping mechanism around the active sample collection spot on the filter tape and the tape advance mechanism. It is also critical to identify a uniform filter tape product that can be obtained with consistent quality to reduce the overall impacts and variability of the filter loading effects observed to date.

The Magee Scientific AE33 black carbon (BC) Aethalometer is already commercially used as an environmental monitor, and had been previously undergone limited demonstration in underground mines. Based on the studies reported here, this instrument is currently suited to monitoring applications where maximum EC concentrations are 250-300 $\mu g/m^3$. Above this, the apparent BC to EC ratio begins to change significantly, making interpretation of data difficult. However, in that lower concentration range, the AE33 seems to represent an off-the-shelf option for mines wanting to continuously track DPM. It may offer near-term use in a variety of engineering applications, including ventilation-on-demand.

The OCEC semi-continuous field monitor, commercially available from Sunset Laboratory Inc., has only been used as an environmental monitor in the past. By using the same analysis technique as the laboratory OCEC aerosol analyzer, the field monitor can report both EC and OC as time weighted average mass concentration values – thus offering lab-grade results. Here, the OCEC field monitor was demonstrated in an underground mining environment. Initial efforts to select an appropriate monitoring location and set the instrument up provided key lessons on some practical limitations (e.g., space and environmental requirements, use of gas cylinders, etc.) Moreover, the semi-continuous nature of the monitor may represent another limitation in applications where the ability to track relatively rapid changes in DPM is needed. Aside from those limitations, the field monitor appears to have promise for providing high quality data as an area monitor where general trends (i.e., over hours or longer) are the primary interest.

Further evaluation and field demonstration of these monitors should be the next step in determining the efficacy and practicability for specific mine applications.

Appendix A. Chapter 3 Supplemental Data

Table A.1: Monitoring dates and equipment used for sample collection.

Week	Days	Equipment Used
1	9/29 (F) – 10/5 (Th)	AE33, Airwatch, OCEC, 5040 (F, M)
2	10/6 (F) – 10/12 (Th)	AE33, Airwatch, OCEC, 5040 (M), Airtecs (M)
3	10/13 (F) – 10/19 (Th)	AE33 (F, Sa, Su, Th)
4	10/20 (F) – 10/26 (Th)	AE33, Airwatch, OCEC
5	10/27 (F) - 11/2 (Th)	AE33, Airwatch, OCEC, 5040 (F, M, Th), Airtecs (F, M, Th)
6	11/3 (F) - 11/9 (Th)	AE33, Airwatch, OCEC, 5040 (M), Airtecs (M)
7	11/10 (F) - 11/16 (Th)	AE33, Airwatch, OCEC, 5040 (F, M), Airtecs (F, M)
8	11/17 (F) - 11/20 (M)	AE33, Airwatch, OCEC, 5040 (F, M), Airtecs (F, M)

Table A.2: Summary of all used 5040 samples raw EC data. Highlighted values were identified as outliers. NA indicates that no data was available because the sample filter was not seated properly in the cassette.

	EC 5040 results (µg/m^3)							Total samples used
Test	**A**	**B**	**C**	**D**	**E**	**Average**	**95% CI**	**A-E**
1	174.6525	164.6523	163.5751	99.76715	123.8741	167.6266	6.91214	3
2	97.19194	118.4406	97.18831	115.0909	61.37003	106.9779	11.15652	4
3	105.7464	116.6405	111.0941	126.324	89.52635	109.8663	11.9938	5
4	125.6315	144.9276	104.1496	146.8895	133.3714	137.705	9.817282	4
5	66.4444	49.45409	60.1563	50.83037	50.22357	55.4217	6.612222	5
6	99.16544	89.05093	213.0814	73.39449	171.8541	87.2038	14.6927	3
7	72.03912	82.45878	86.49316	62.71091	77.18334	76.1771	8.144518	5
8	98.4701	99.81177	107.211	NA	102.9564	102.112	3.806693	4
9	380.0915	294.3282	294.7977	307.6803	533.2243	298.9354	8.573957	3
10	349.2365	352.7846	406.7504	344.6924	264.056	348.9045	4.590015	3
11	302.2227	381.2478	376.7563	354.7806	375.7241	372.1272	11.57399	4
12	348.2049	306.3664	344.7027	295.4893	356.2877	349.7318	6.723306	3
13	265.6914	236.2439	253.3949	257.3525	270.3465	261.696	7.560836	4
14	242.4218	287.7462	268.1296	268.3057	252.4444	263.81	15.17198	5
15	246.5931	335.4013	255.2755	231.8381	NA	244.569	13.40831	3
16	297.1557	255.9378	303.2635	249.3706	288.0944	296.171	8.636637	3
17	396.8917	404.0217	403.7834	380.5021	403.3917	402.022	3.361462	4
18	550.5409	600.5387	638.7406	314.6163	746.7265	596.6067	50.05133	3
19	575.6147	524.9336	610.306	424.9262	589.2699	591.0635	20.83396	3

Table A.3: Summary of all calibration data results for various analysis methods. NA indicates 95% confidence interval could not be calculated due to test only having one sample.

Test	5040 Avg	5040 95% CI	OCEC Avg	Airtec Avg	Airtec 95% CI	AE33 First Minute Avg	AE33 First Minute 95% CI	AE33 Uncorrected Avg	AE33 Corrected Avg	Airwatch last minute absorbance
1	167.63	6.91	37.24	115.33	7.97	118.62	20.96	78.78	134.99	0.29
2	106.98	11.16	41.42	138.37	4.91	207.07	37.49	129.78	223.85	0.38
3	109.87	11.99	41.76	148.53	8.77	192.93	19.42	134.53	205.16	0.36
4	137.70	9.82	38.31	158.61	4.33	263.29	50.07	147.31	231.45	0.38
5	55.42	6.61	43.65	70.92	2.08	105.36	27.58	79.27	94.34	0.30
6	87.20	14.69	56.11	105.84	2.93	140.16	NA	103.76	128.42	0.21
7	76.18	8.14	70.34	128.25	4.04	159.18	17.58	131.51	164.09	0.18
8	102.11	3.81	28.62	133.87	4.29	205.67	10.53	156.44	208.93	0.27
9	298.94	8.57	47.71	493.10	39.03	521.89	117.80	376.92	440.28	0.27
10	348.90	4.59	39.82	375.78	54.37	550.36	135.24	379.13	379.52	0.04
11	372.13	11.57	53.71	361.75	20.12	622.98	26.37	388.41	573.31	0.34
12	349.73	6.72	58.64	376.91	8.73	568.39	54.16	300.86	655.67	0.14
13	261.70	7.56	162.67	337.38	17.26	496.83	17.81	390.41	779.62	0.21
14	263.81	15.17	164.99	373.67	33.74	474.32	31.63	382.53	764.93	0.27
15	244.57	13.41	163.75	374.61	24.86	481.32	57.44	407.16	506.35	0.22
16	296.17	8.64	168.18	399.42	19.64	472.71	19.22	379.71	753.89	0.35
17	402.02	3.36	260.93	501.16	57.22	748.70	26.96	603.14	603.14	0.31
18	596.61	50.05	254.86	642.62	73.92	729.95	309.39	498.27	498.27	0.31
19	591.06	20.83	71.01	557.45	19.44	822.05	62.61	500.88	661.66	0.30

Table A.4: Summary of outlier data points identified for each instrument. Outliers were determined as points over three σ away from the mean instrument to 5040 ratio.

Test	AE33	AW	OCEC
1	Outlier	Outlier	Outlier
15		Outlier	
16			Outlier
17	Outlier	Outlier	

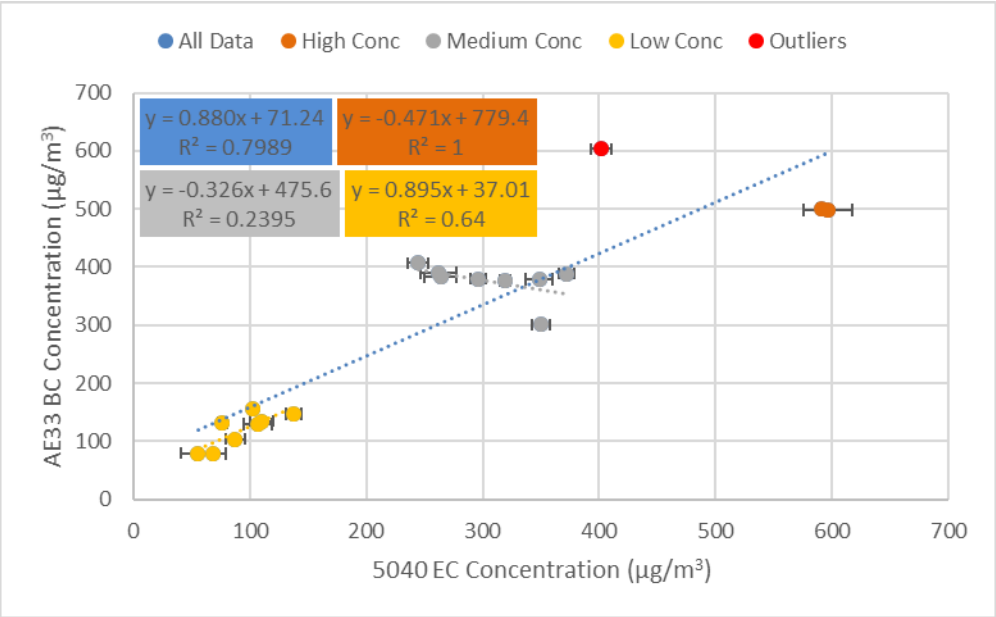

Figure A.1: AE33 BC uncorrected concentration as a function of 5040 EC concentration. Error bars represent 95% confidence in replicate 5040 values.

Table A.5: Summary of field 5040 EC concentrations and number of samples used in analysis. Highlighted values represent outliers.

	EC concentrations µg/m³					Total samples used
Date	**Unit 1**	**Unit 2**	**Unit 3**	**Average**	**95% CI**	**Units 1-3**
29-Sep	124.7346	125.3213	-	125.028	0.57488	2
2-Oct	33.75161	37.65076	39.33679	38.49377	1.652277	2
9-Oct	49.47409	50.11899	56.50907	49.79654	0.631981	2
27-Oct	67.56701	58.36188	58.57518	58.46853	0.209029	2
30-Oct	19.64384	29.58803	22.3624	21.00312	2.664138	2
2-Nov	48.11506	48.94915	52.43166	50.6904	2.786538	3
6-Nov	29.01781	22.10094	27.13139	28.0746	1.848649	2
10-Nov	24.97955	37.18405	22.89072	23.93513	2.047019	2
13-Nov	29.92836	20.64202	16.2423	18.44216	4.311643	2
17-Nov	60.90315	58.58463	37.88382	59.74389	2.272109	2
20-Nov	33.99728	38.09097	29.24563	33.77796	5.009246	3

Table A.6: Summary of all TWA values for each monitor during field testing.

Date	5040 TWA	OCEC TWA	AT TWA	AE33 TWA	Airwatch TWA
29-Sep	125.03	118.48	-	176.36	130.82
2-Oct	38.49	24.66	-	43.94	49.67
9-Oct	49.80	44.17	40.73	64.94	66.39
27-Oct	58.47	45.39	65.76	69.48	86.35
30-Oct	21.00	9.75	16.82		37.29
2-Nov	50.69	-	56.92	59.70	54.06
6-Nov	28.25	19.20	-	26.87	35.75
10-Nov	23.94	23.64	-	34.44	-
13-Nov	18.44	14.02	28.54	20.37	-
17-Nov	59.74	34.10	42.28	62.14	-
20-Nov	33.78	25.30	44.25	50.77	-

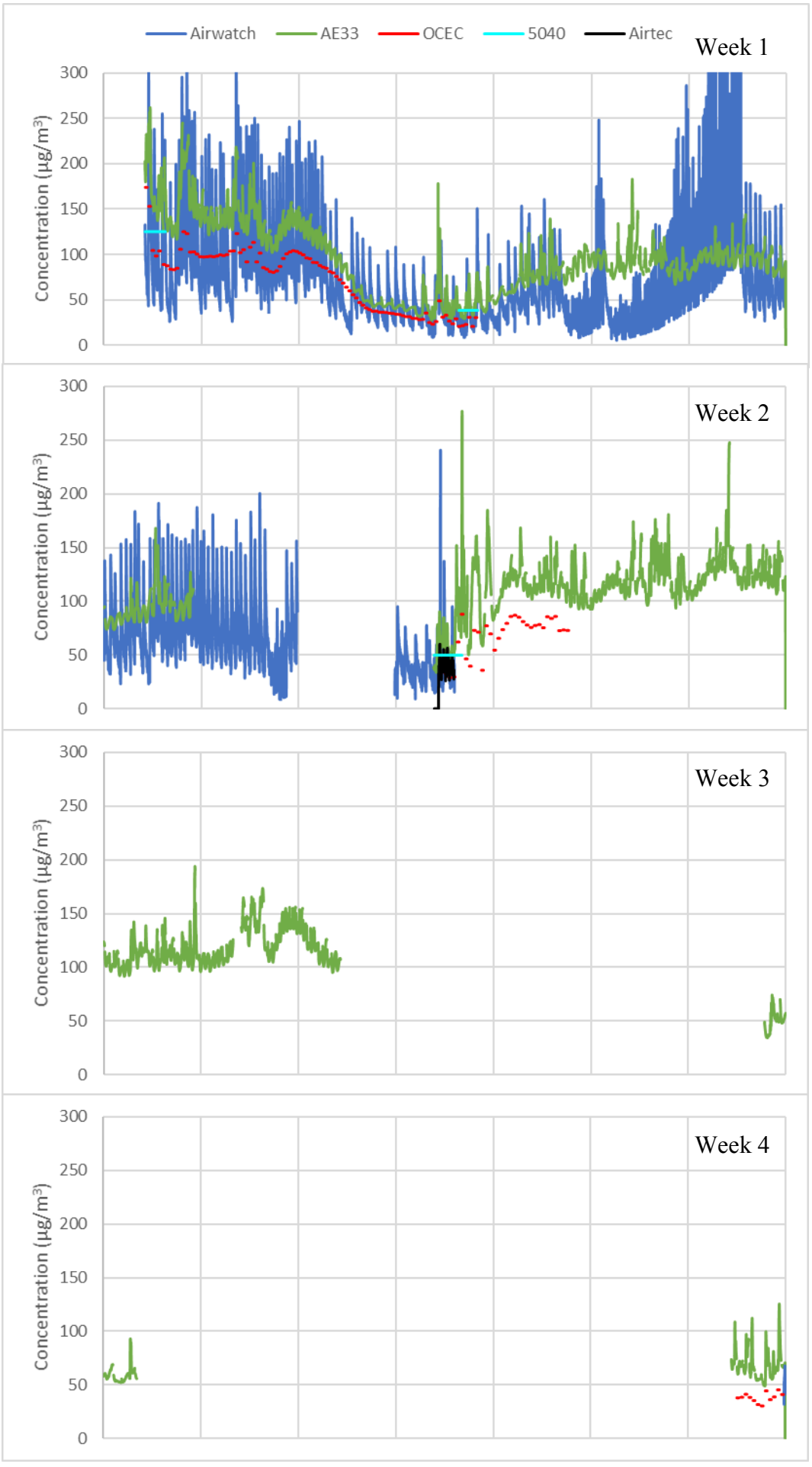
Airwatch
AE33
OCEC
5040
Airtec
Week 1
Week 2
Week 3
Week 4
Concentration (µg/m³)
0
50
100
150
200
250
300
Fri 0:00
Sun 0:00
Tues 0:00
Thur 0:00
Day/Time

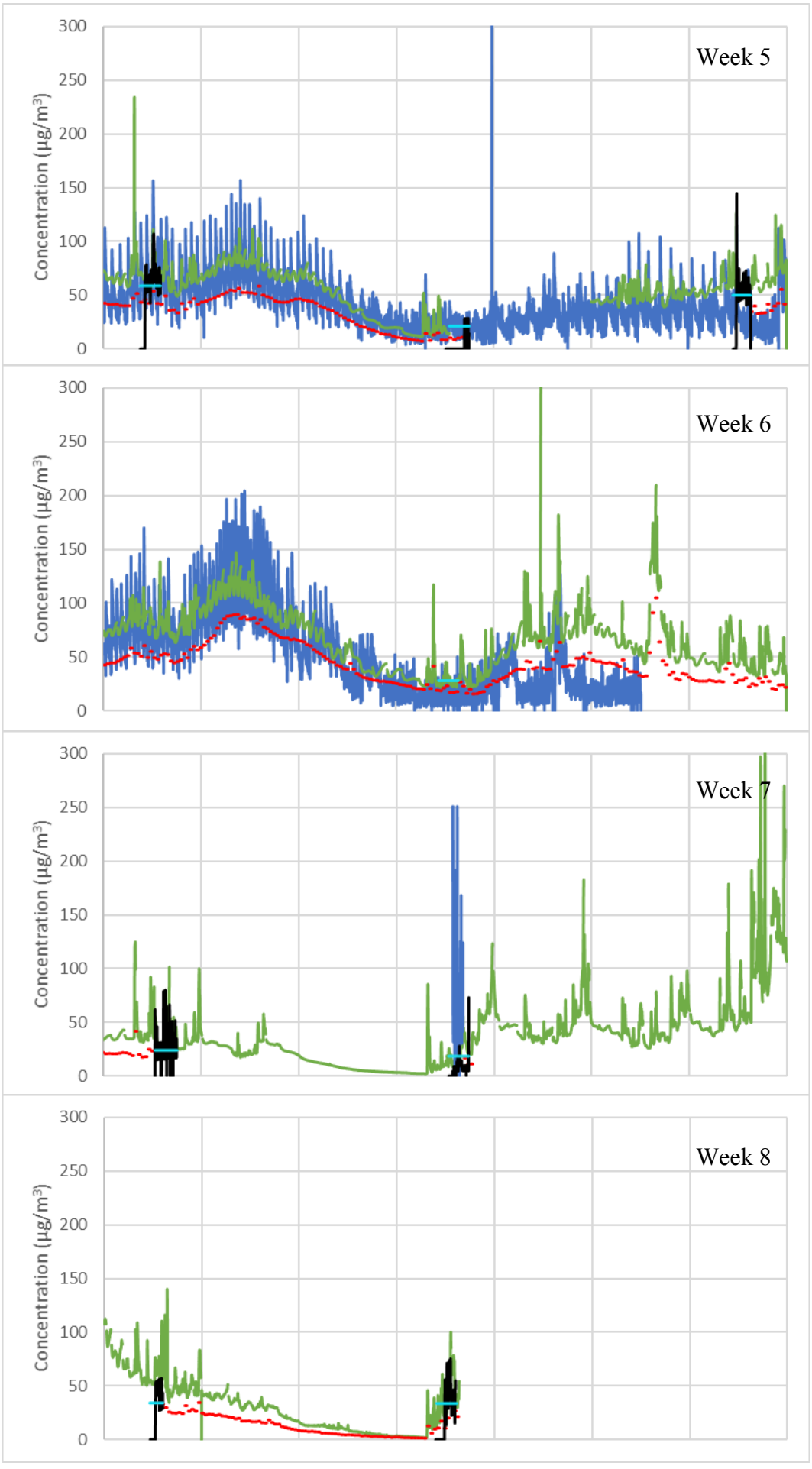

Figure A.2: Time series data for an 8-week field study divided into 8 separate weeks. Airwatch data was analyzed on a minute by minute basis for this plot. AE33 BC data was used.

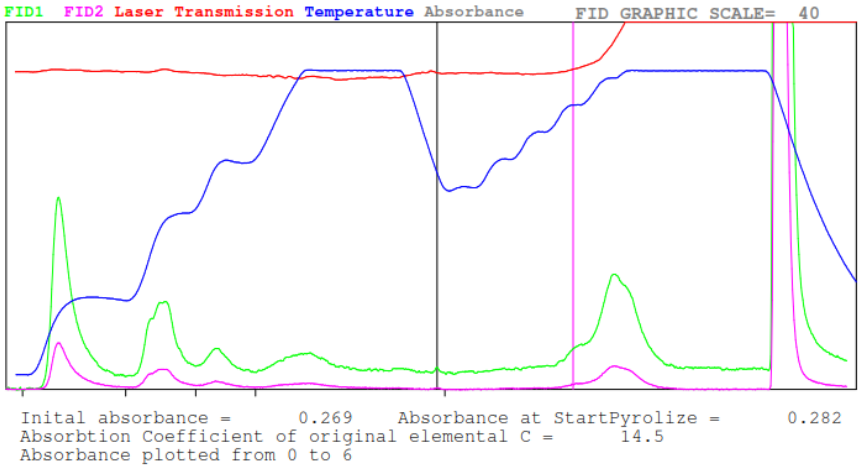

Figure A.3: Sample 1-A thermogram. Second punch analysis used.

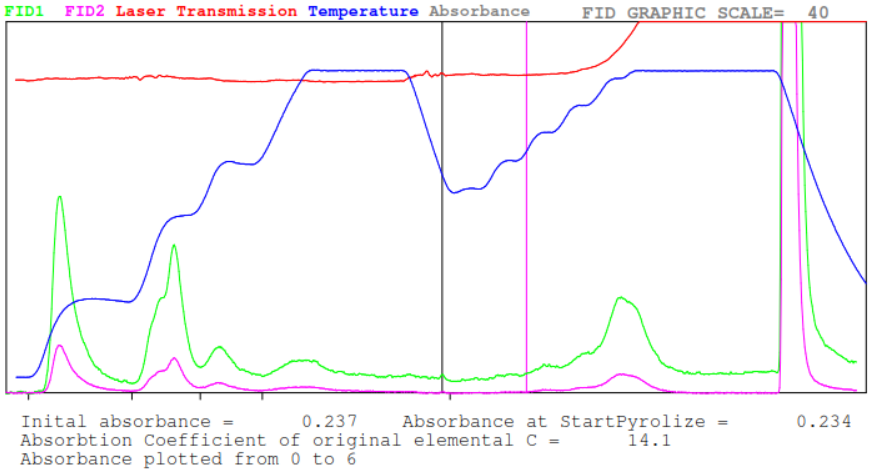

Figure A.4: Sample 1-B thermogram. Second punch analysis used.

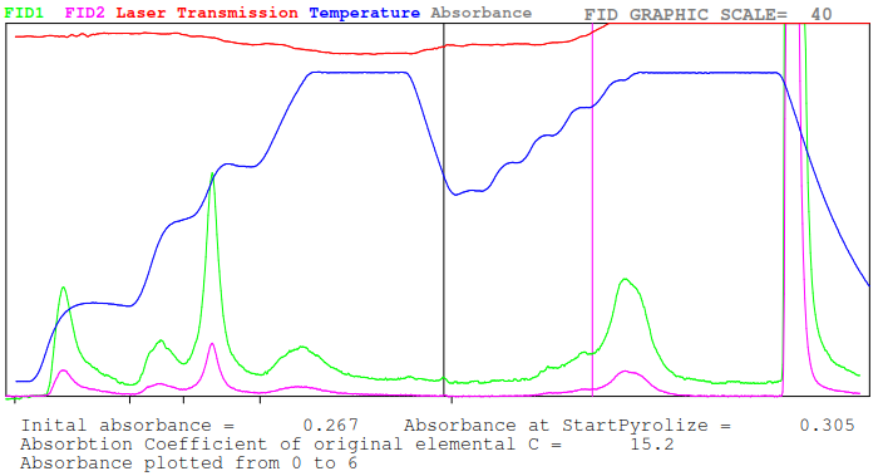

Figure A.5: Sample 1-C thermogram. Second punch analysis used.

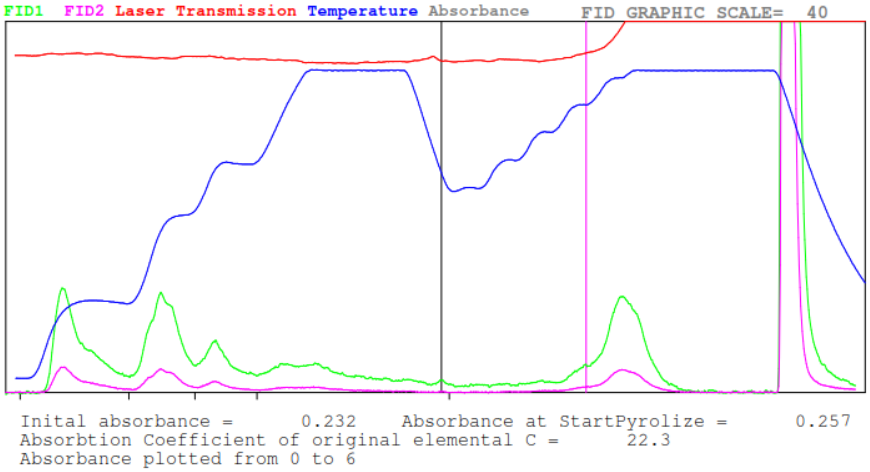

Figure A.6: Sample 1-D thermogram. Second punch analysis used.

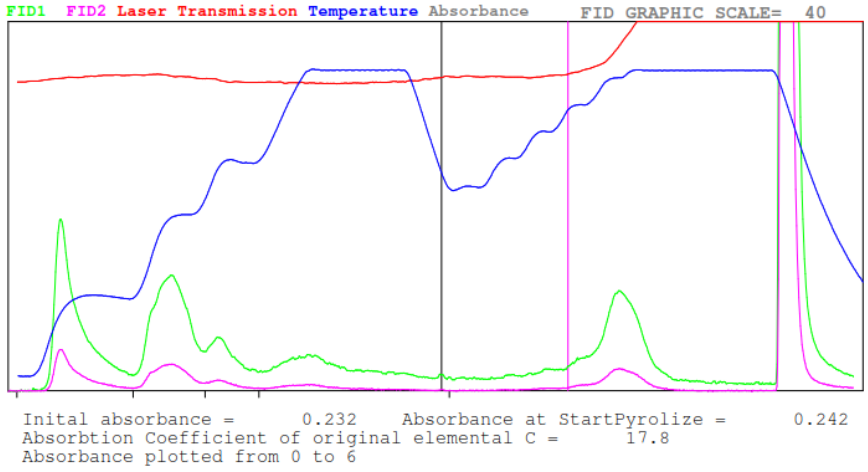

Figure A.7: Sample 1-E thermogram. Second punch analysis used.

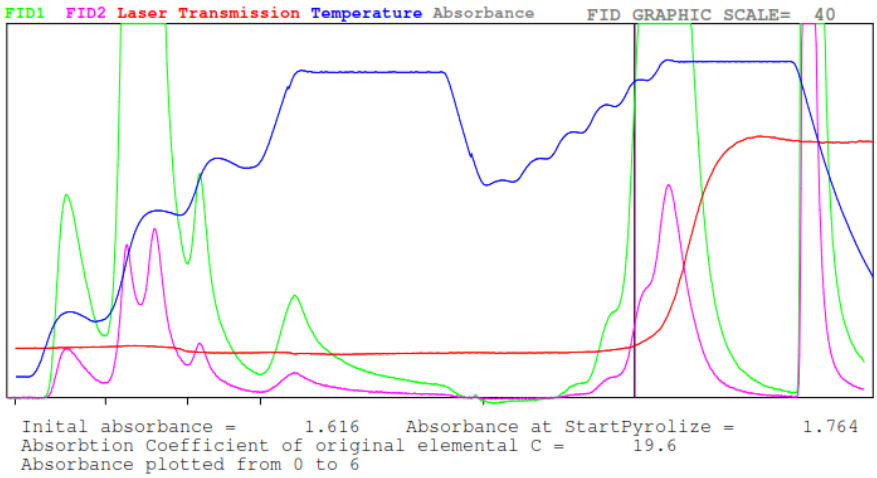

Figure A.8: Sample 2-A thermogram.

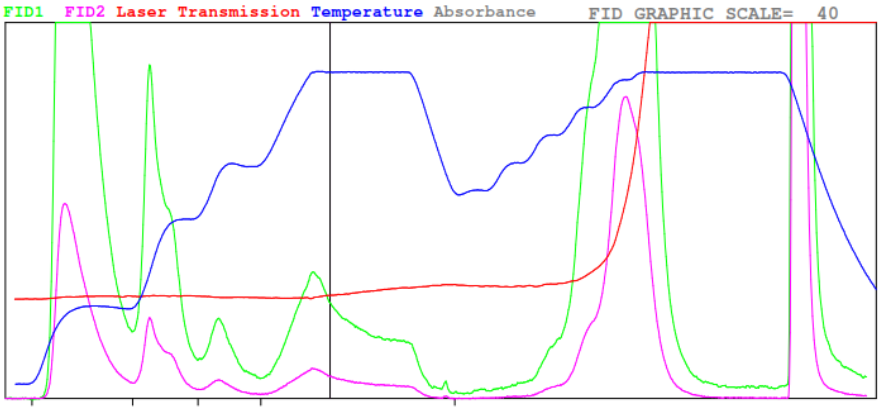

Figure A.9: Sample 2-B thermogram.

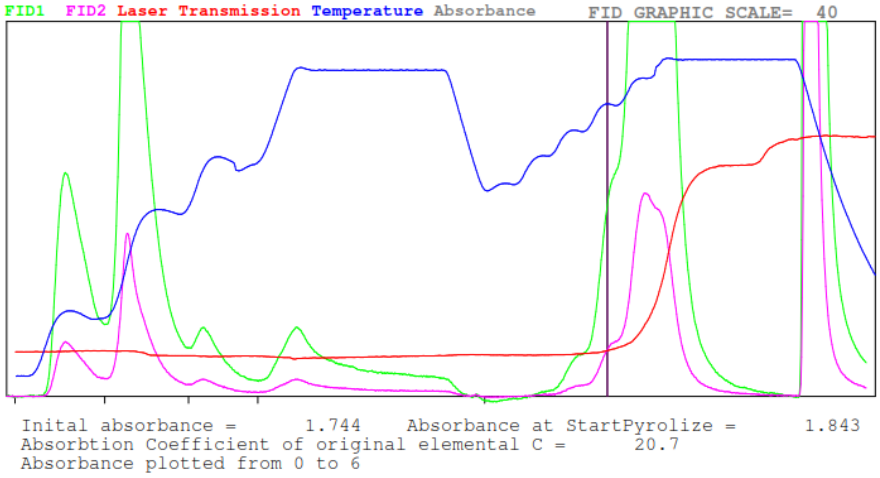

Figure A.10: Sample 2-C thermogram.

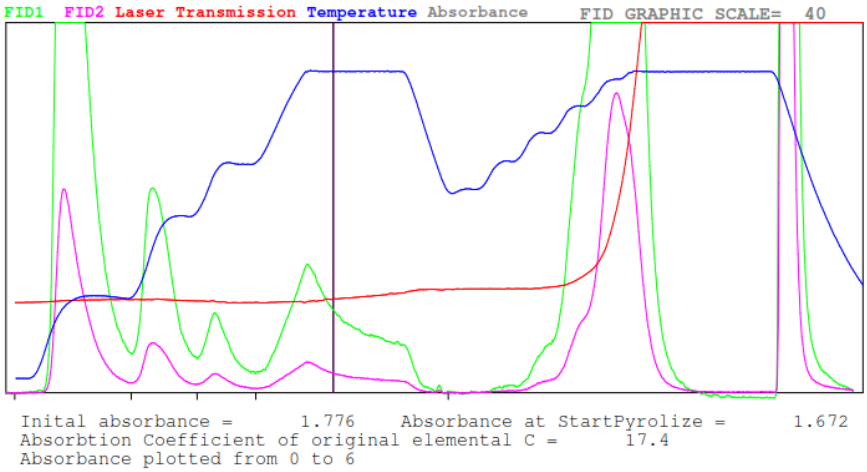

Figure A.11: Sample 2-D thermogram.

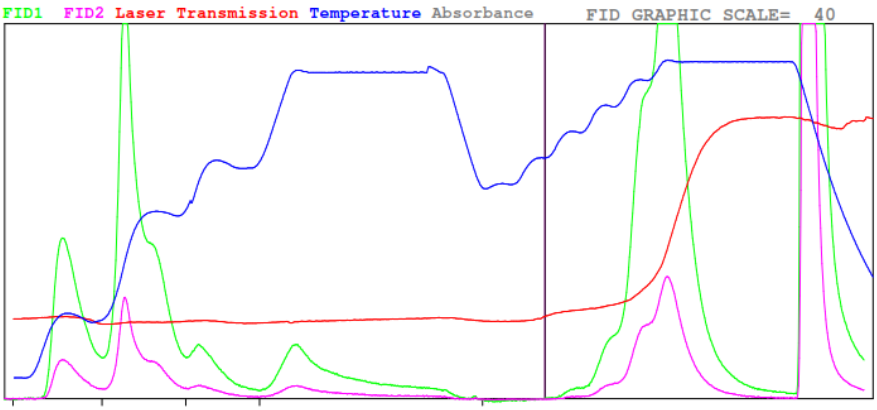

Figure A.12: Sample 2-E thermogram.

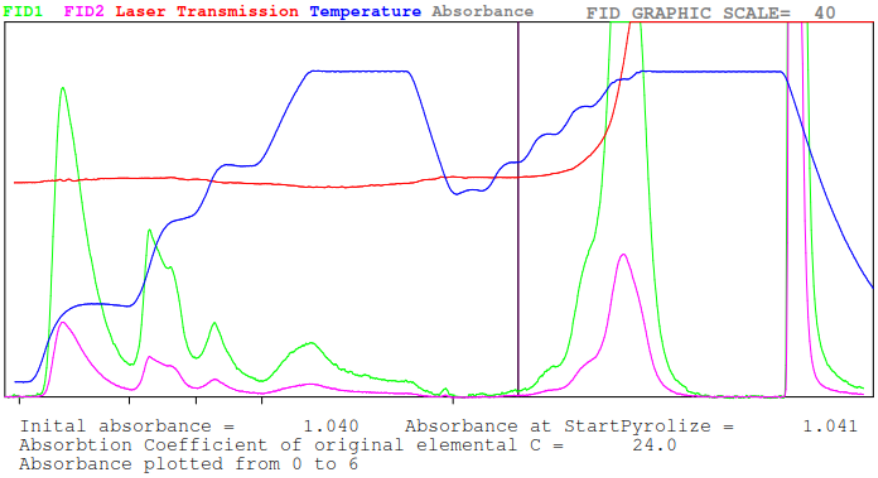

Figure A.13: Sample 3-A thermogram. Second punch analysis used.

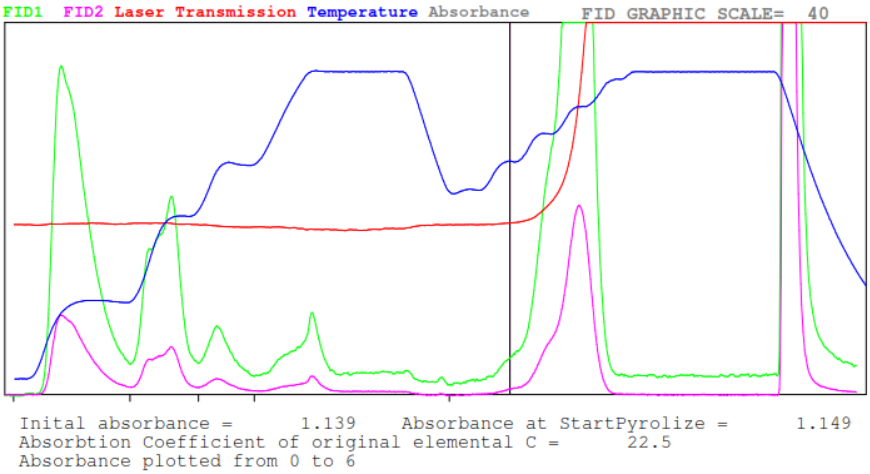

Figure A.14: Sample 3-B thermogram. Second punch analysis used.

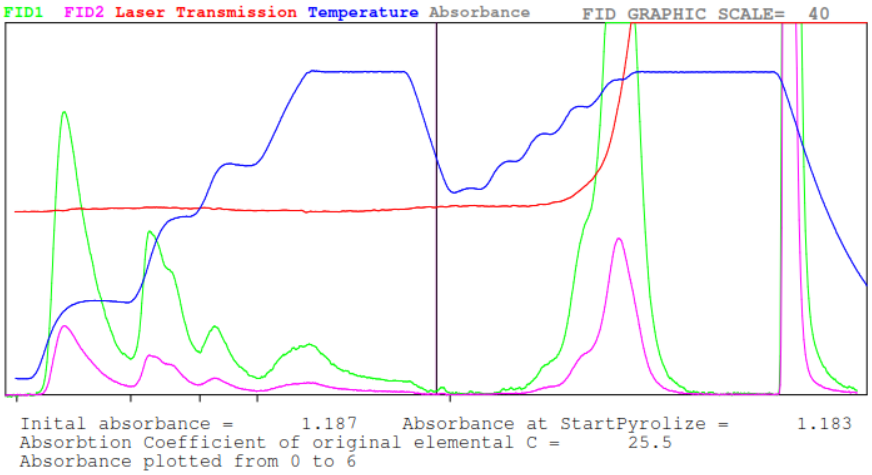

Figure A.15: Sample 3-C thermogram. Second punch analysis used.

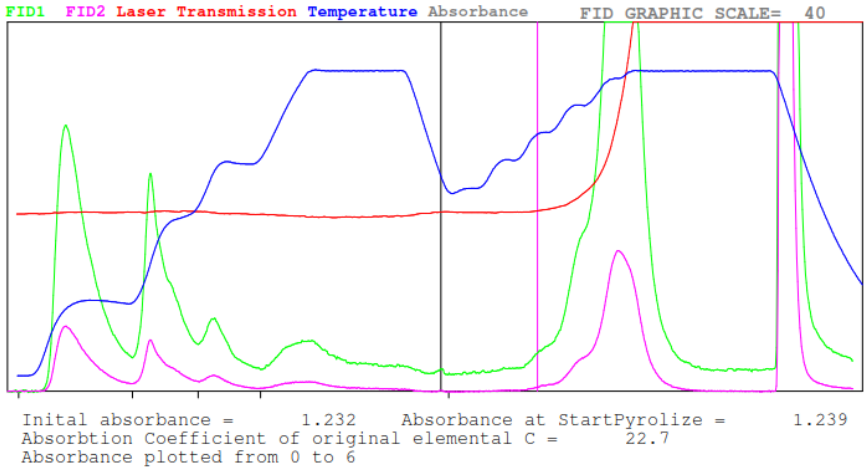

Figure A.16: Sample 3-D thermogram. Second punch analysis used.

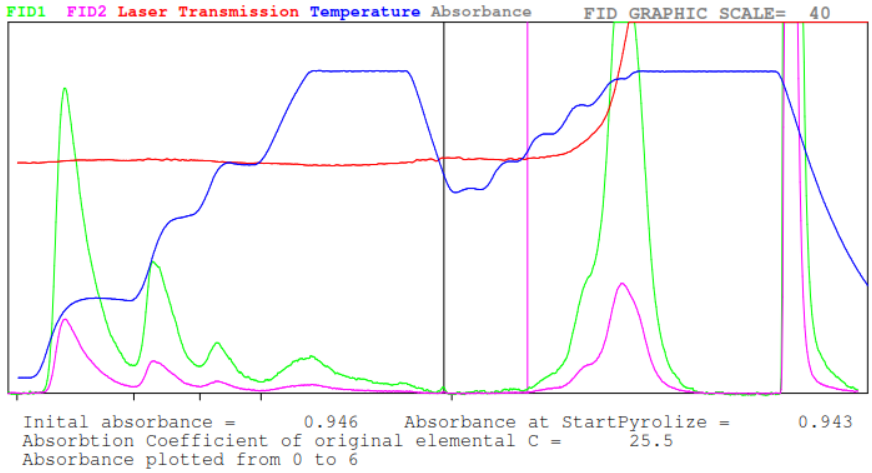

Figure A.17: Sample 3-E thermogram. Second punch analysis used.

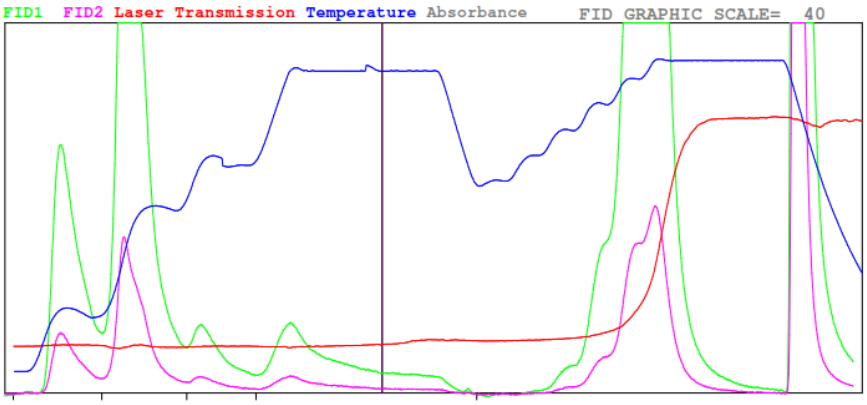

Figure A.18: Sample 4-A thermogram.

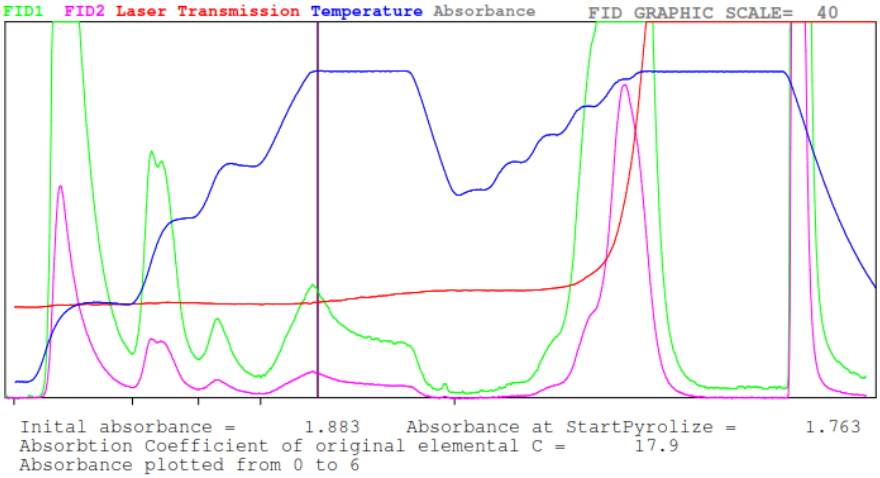

Figure A.19: Sample 4-B thermogram.

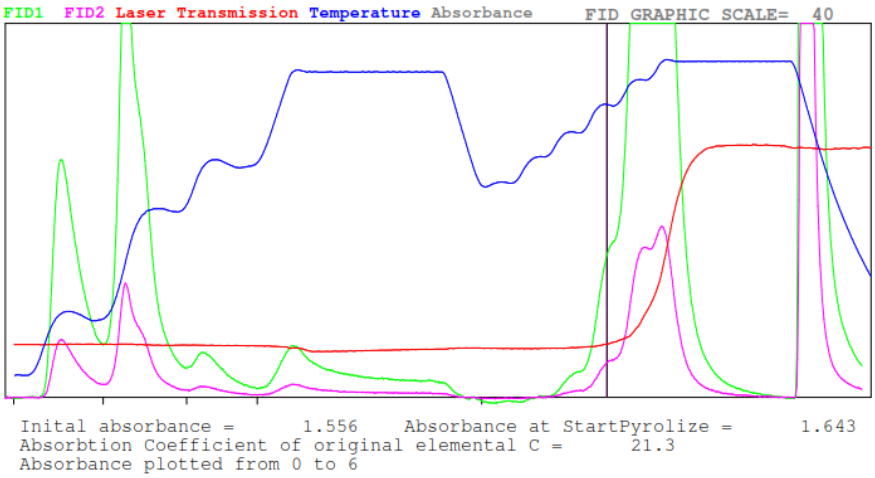

Figure A.20: Sample 4-C thermogram.

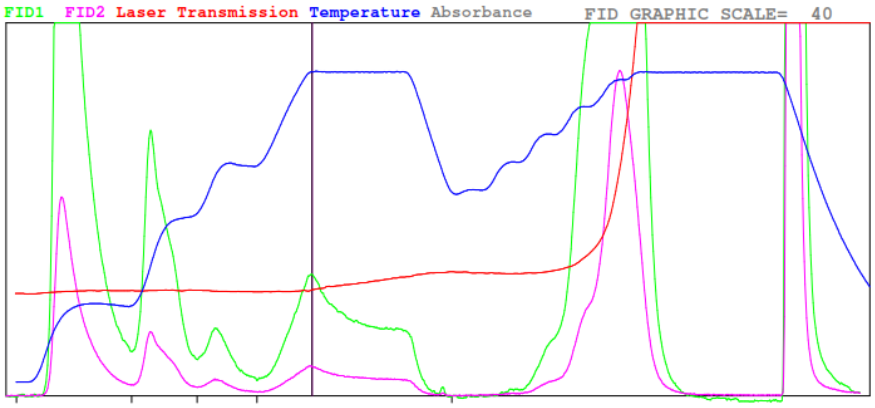

Figure A.21: Sample 4-D thermogram.

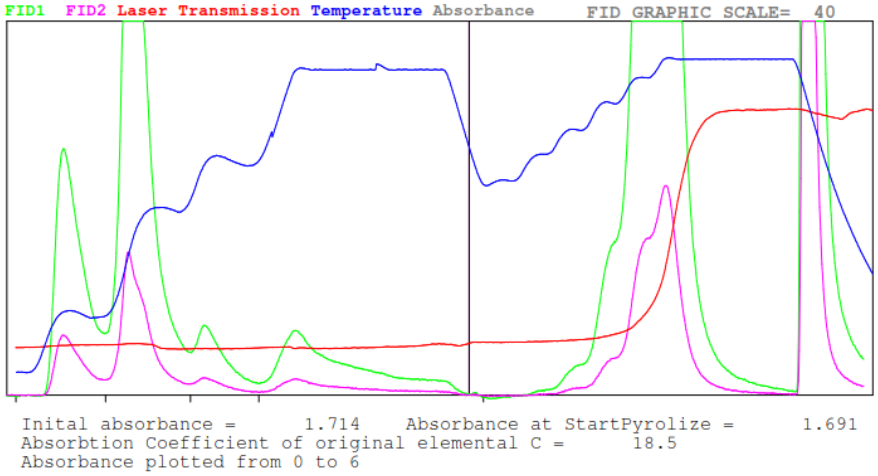

Figure A.22: Sample 4-E thermogram.

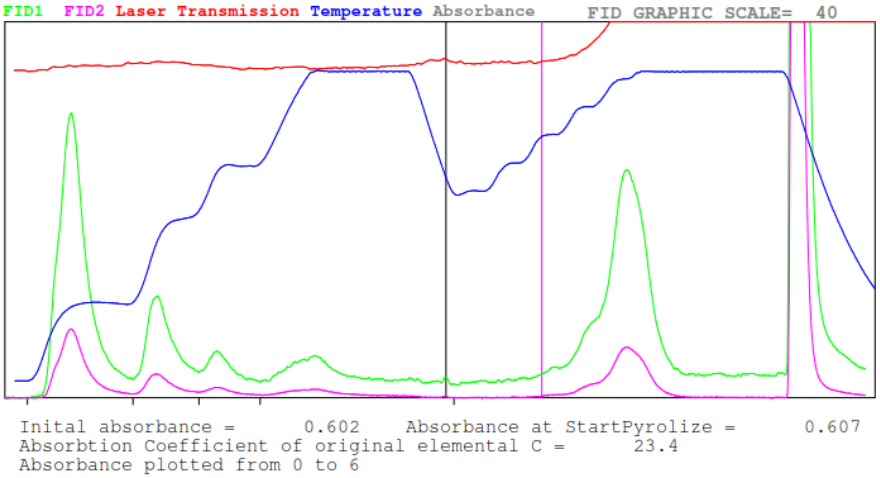

Figure A.23: Sample 5-A thermogram. Second punch analysis used.

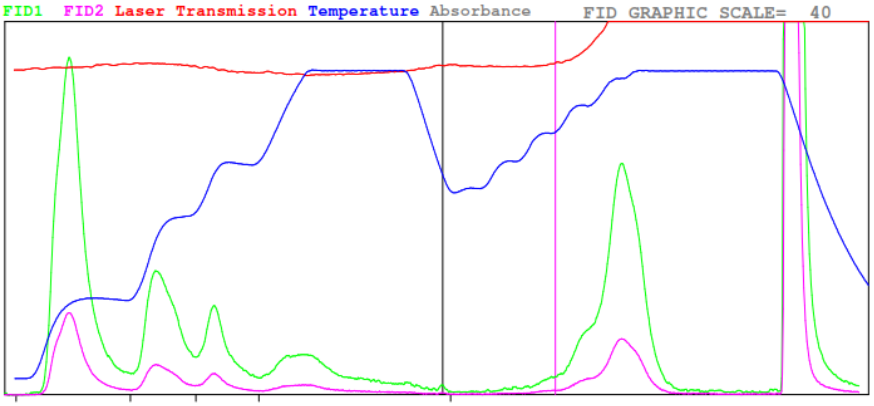

Inital absorbance = 0.601 Absorbance at StartPyrolize = 0.610
Absorbtion Coefficient of original elemental C = 31.3
Absorbance plotted from 0 to 6

Figure A.24: Sample 5-B thermogram. Second punch analysis used.

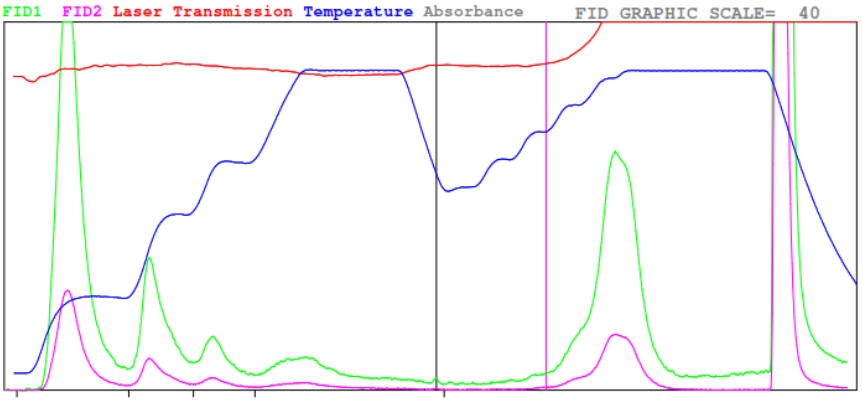

Inital absorbance = 0.676 Absorbance at StartPyrolize = 0.682
Absorbtion Coefficient of original elemental C = 28.5
Absorbance plotted from 0 to 6

Figure A.25: Sample 5-C thermogram. Second punch analysis used.

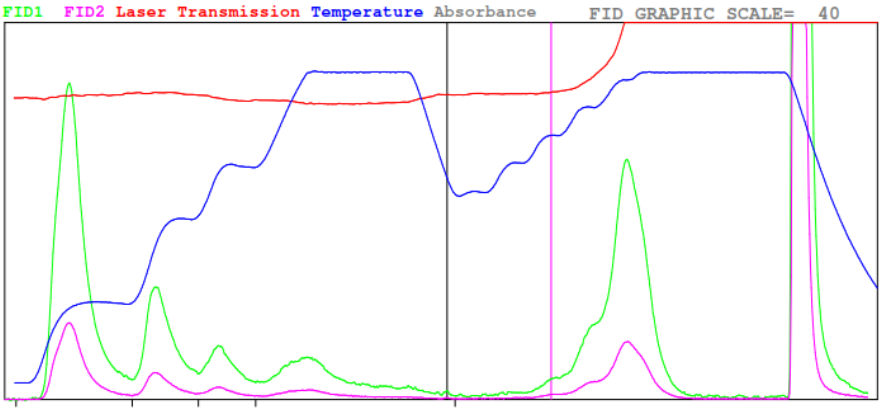

Inital absorbance = 0.616 Absorbance at StartPyrolize = 0.624
Absorbtion Coefficient of original elemental C = 30.3
Absorbance plotted from 0 to 6

Figure A.24: Sample 5-D thermogram. Second punch analysis used.

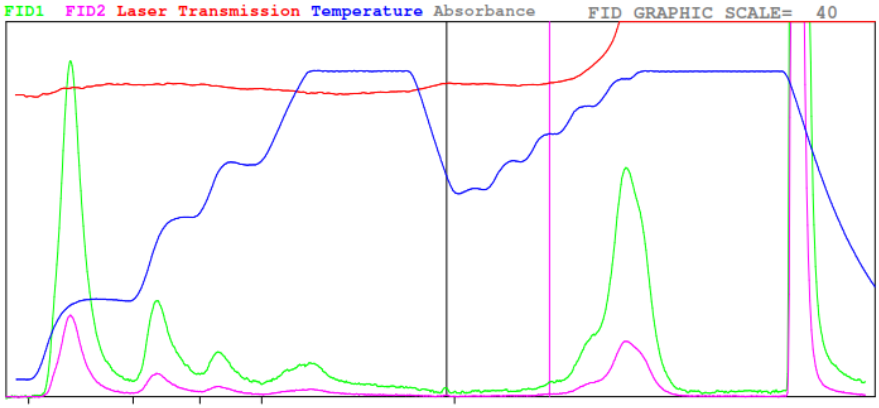

Figure A.27: Sample 5-E thermogram. Second punch analysis used.

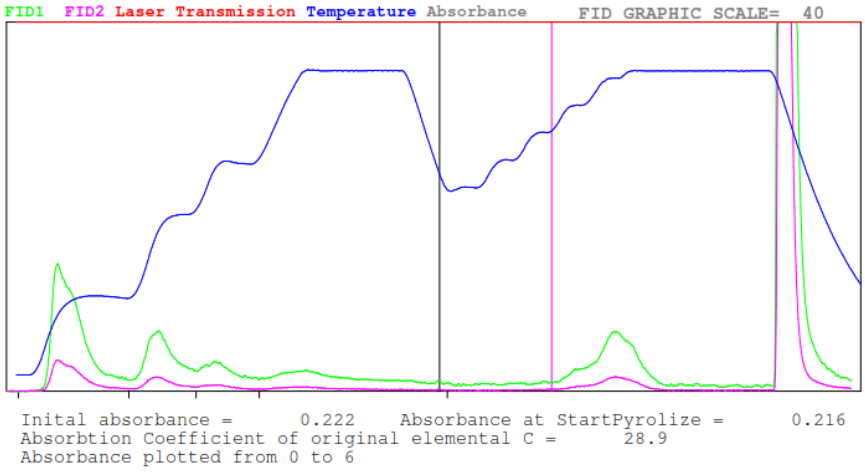

Figure A.28: Sample 6-A thermogram. Second punch analysis used.

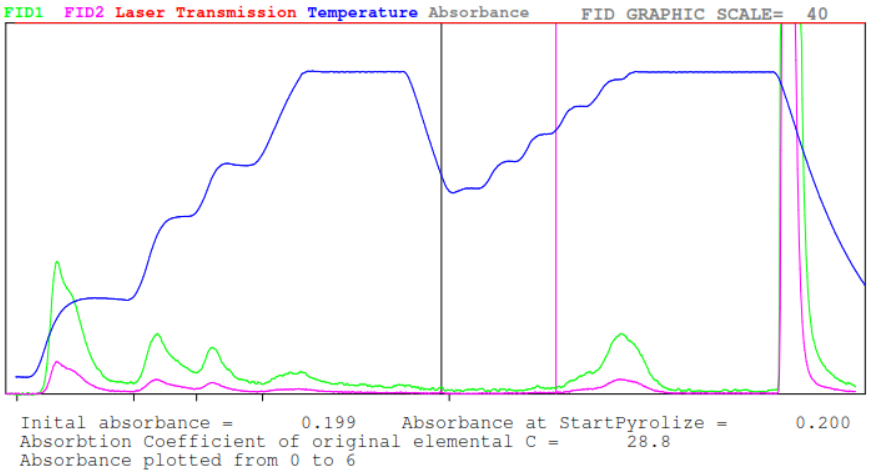

Figure A.29: Sample 6-B thermogram. Second punch analysis used.

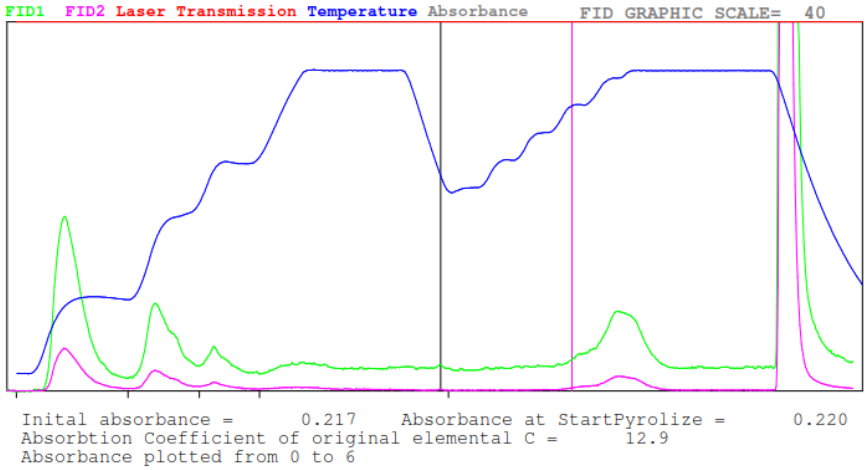

Figure A.30: Sample 6-C thermogram. Second punch analysis used.

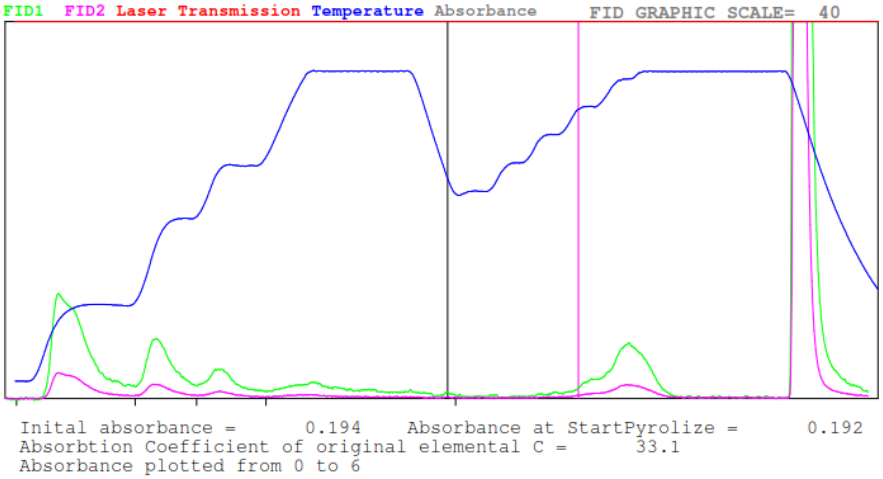

Figure A.31: Sample 6-D thermogram. Second punch analysis used.

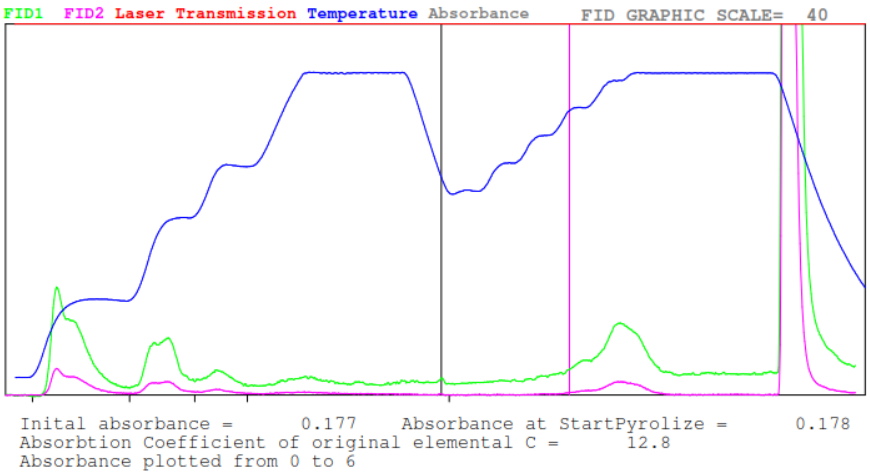

Figure A.32: Sample 6-E thermogram. Second punch analysis used.

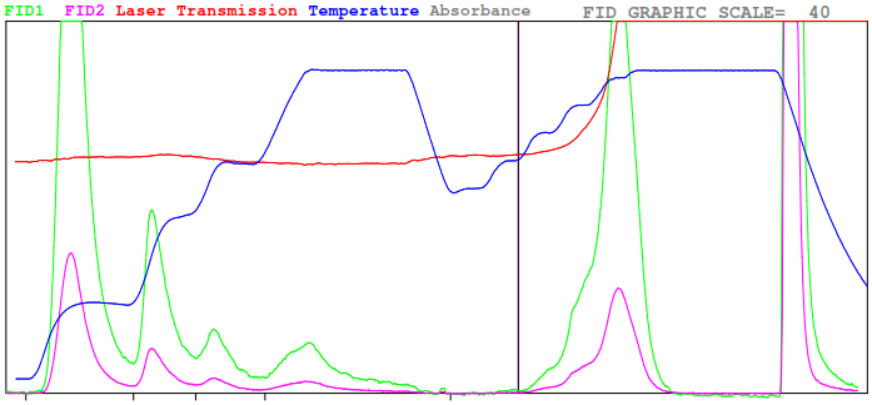

Figure 33: Sample 7-A thermogram. Second punch analysis used.

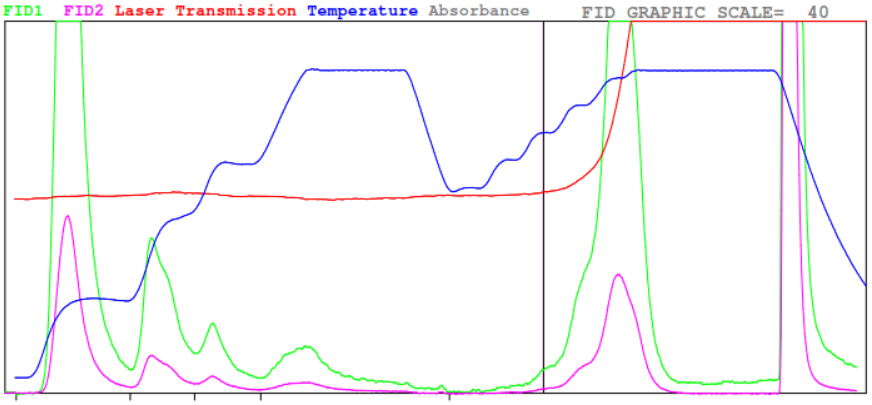

Figure A.34: Sample 7-B thermogram. Second punch analysis used.

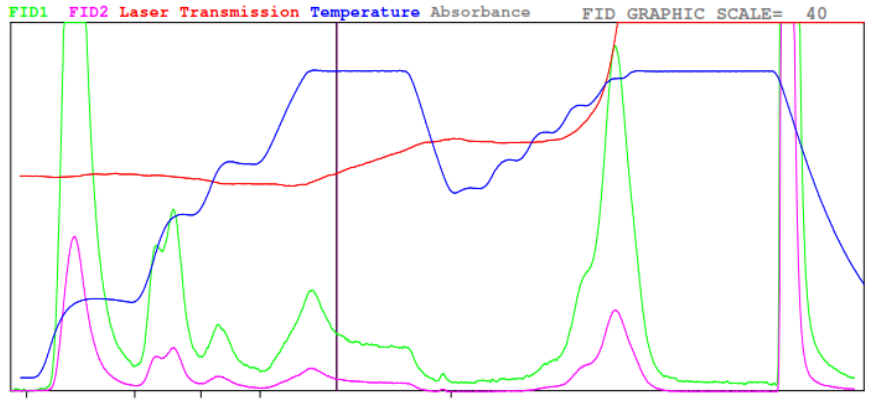

Figure A.35: Sample 7-C thermogram.

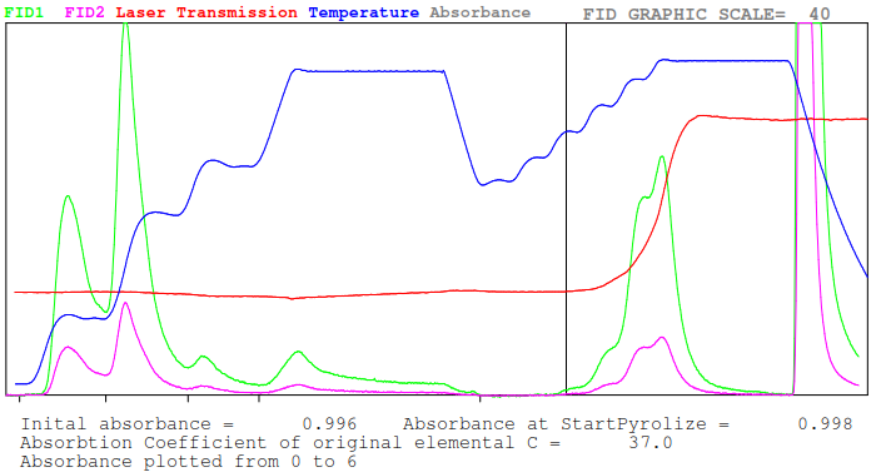

Figure A.36: Sample 7-D thermogram.

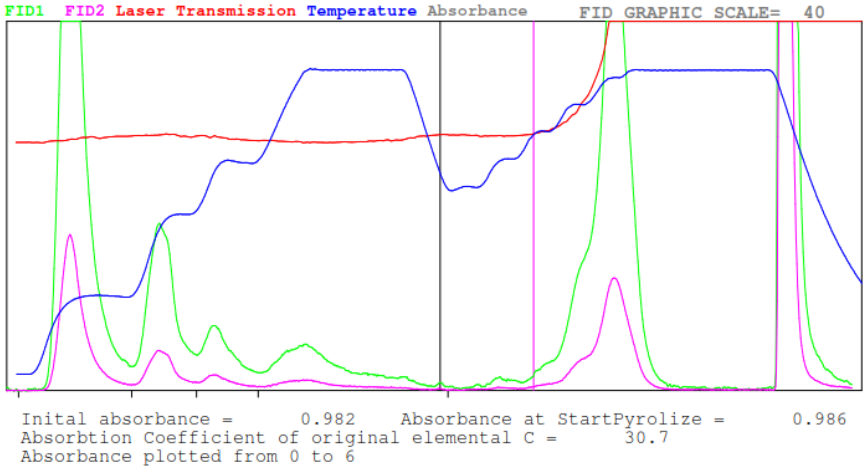

Figure A.37: Sample 7-E thermogram. Second punch analysis used.

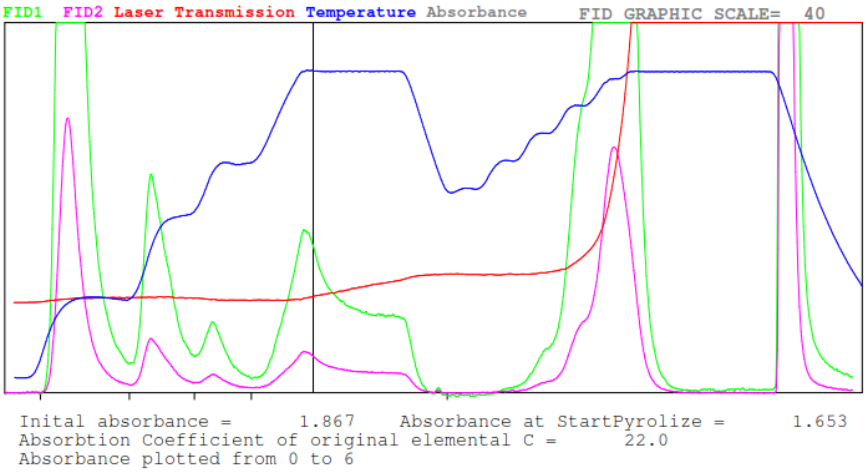

Figure A.38: Sample 8-A thermogram.

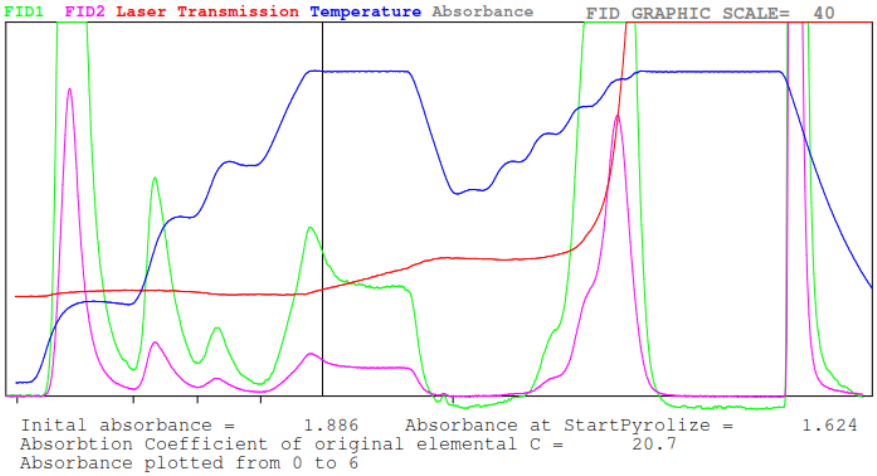

Figure A.39: Sample 8-B thermogram.

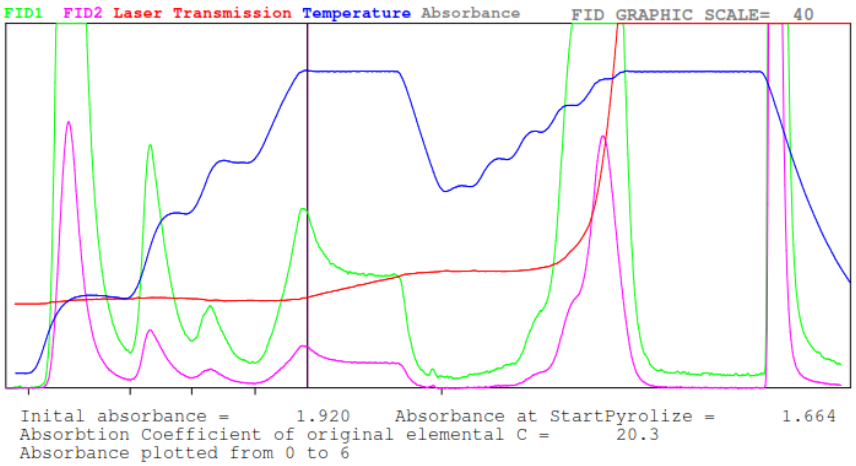

Figure A.40: Sample 8-C thermogram.

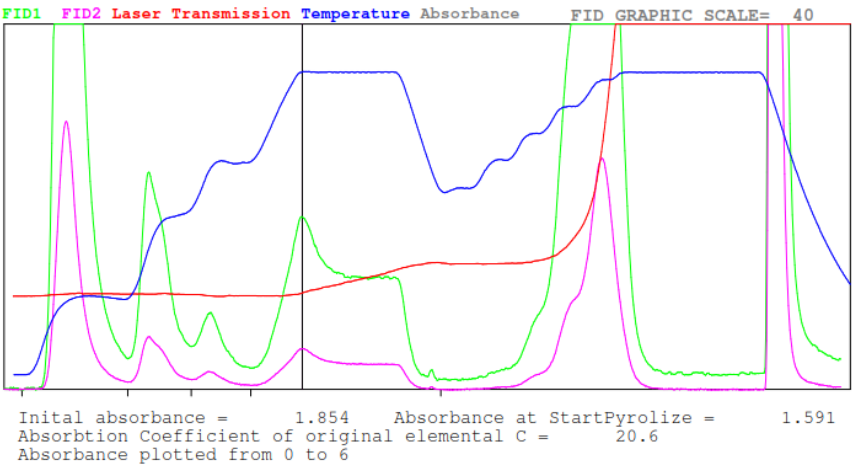

Figure A.41: Sample 8-E thermogram.

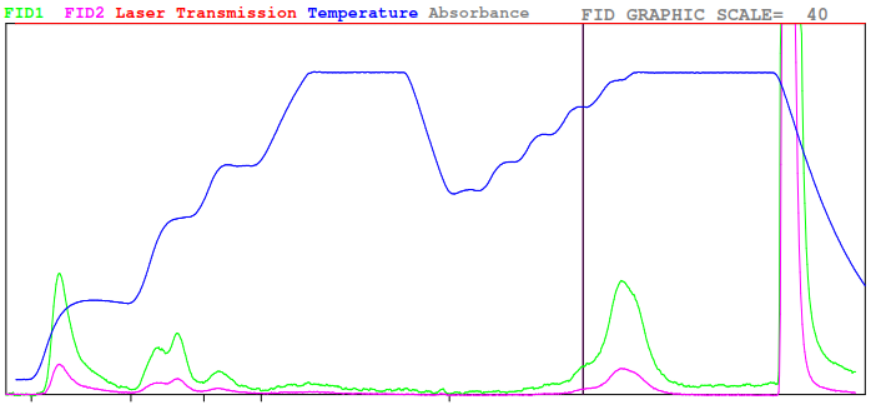

Figure A.42: Sample 9-A thermogram. Second punch analysis used.

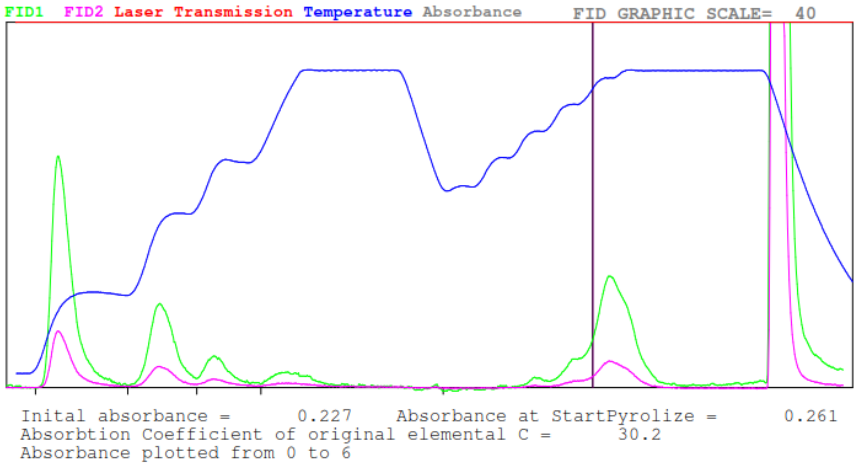

Figure A.43: Sample 9-B thermogram. Second punch analysis used.

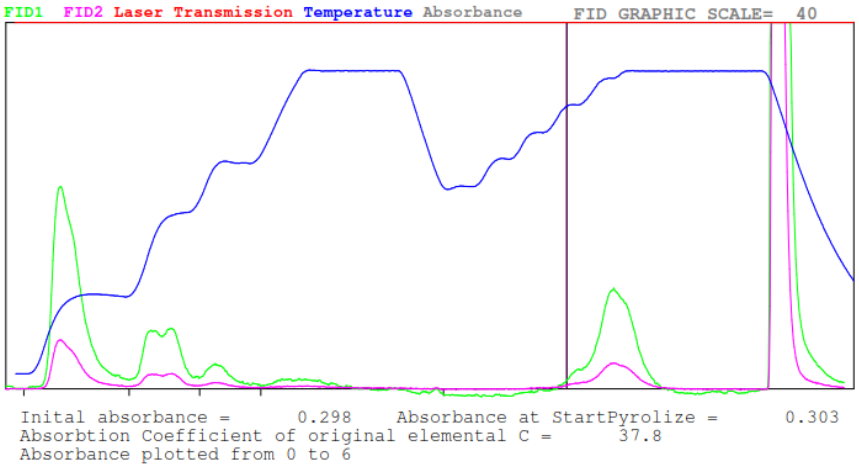

Figure A.44: Sample 9-C thermogram. Second punch analysis used.

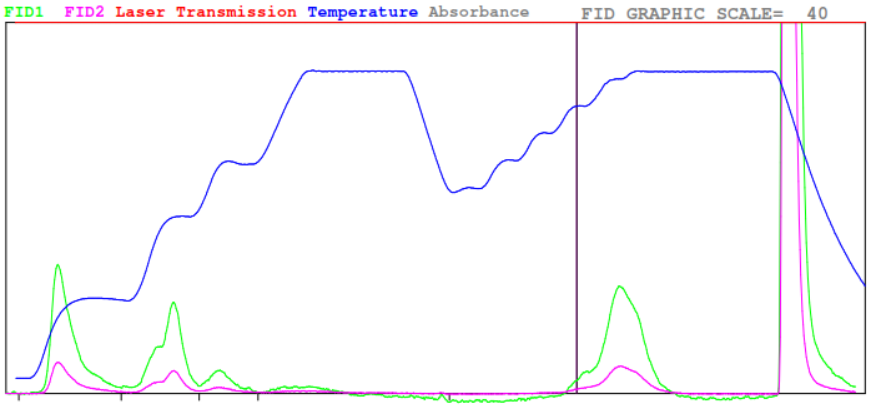

Figure A.45: Sample 9-D thermogram. Second punch analysis used.

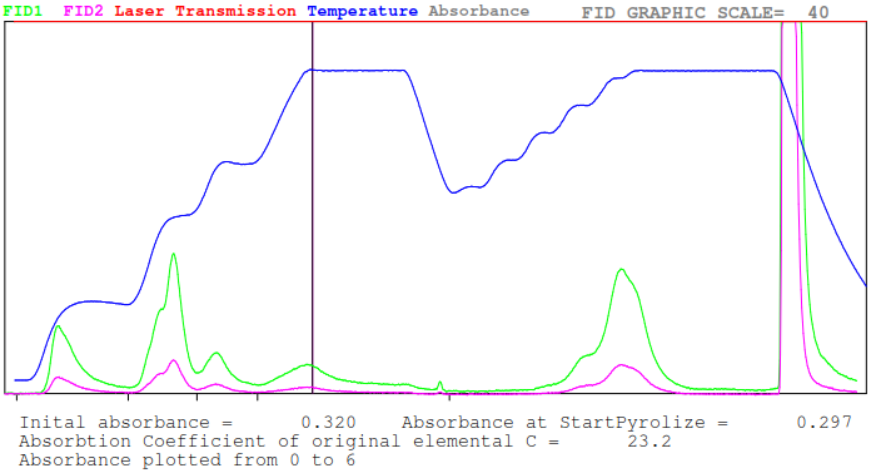

Figure A.46: Sample 9-E thermogram.

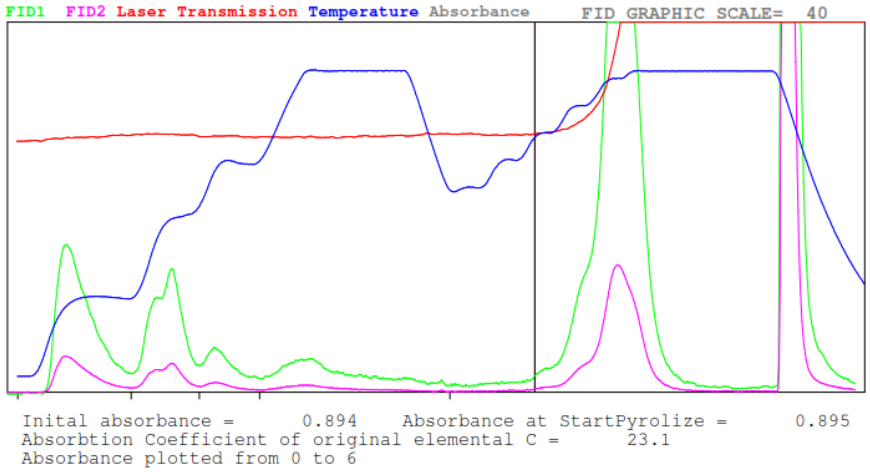

Figure A.47: Sample 10-A thermogram. Second punch analysis used.

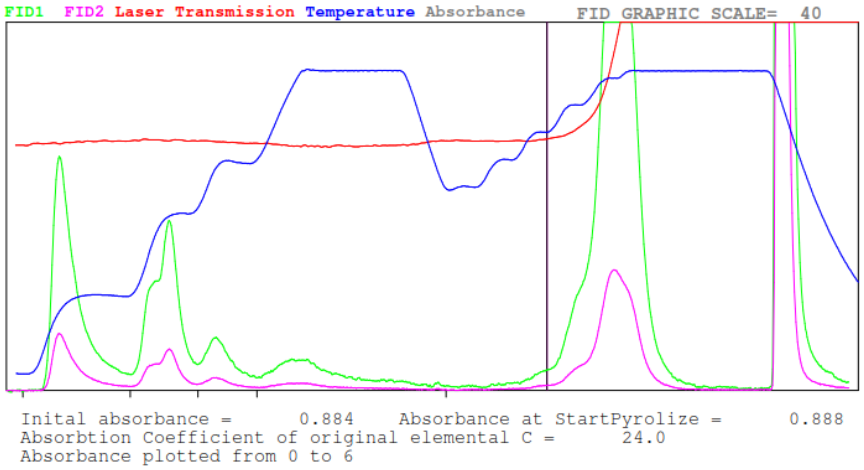

Figure A.48: Sample 10-B thermogram. Second punch analysis used.

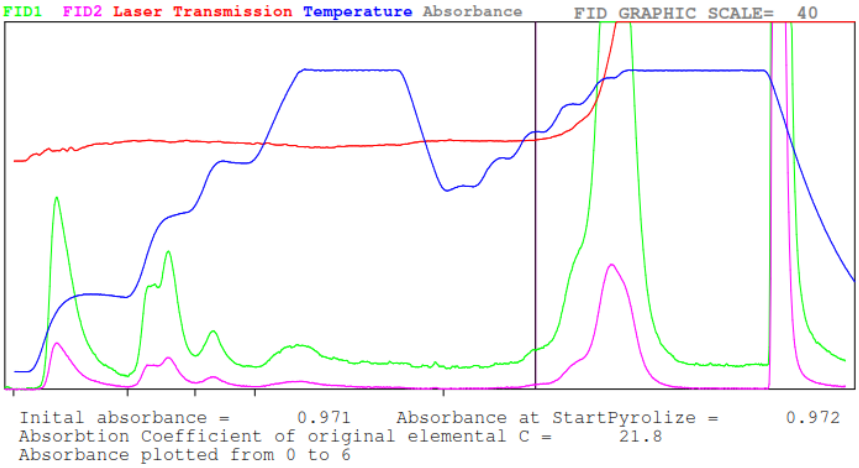

Figure A.49: Sample 10-C thermogram. Second punch analysis used.

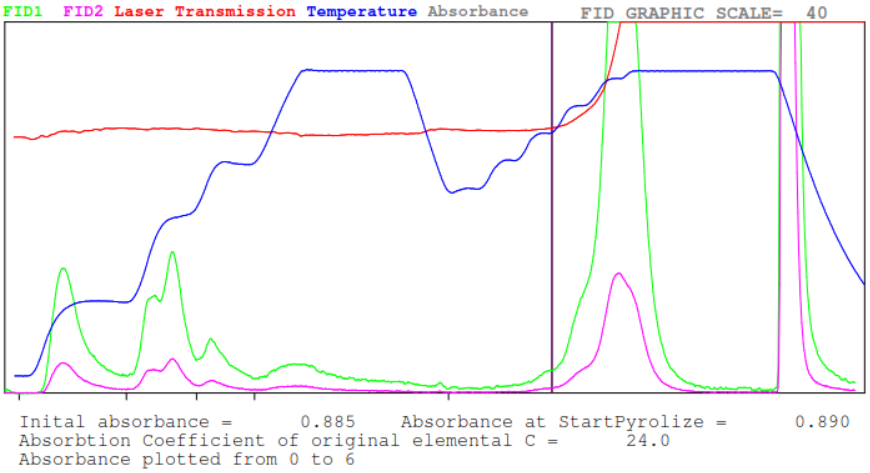

Figure A.50: Sample 10-D thermogram. Second punch analysis used.

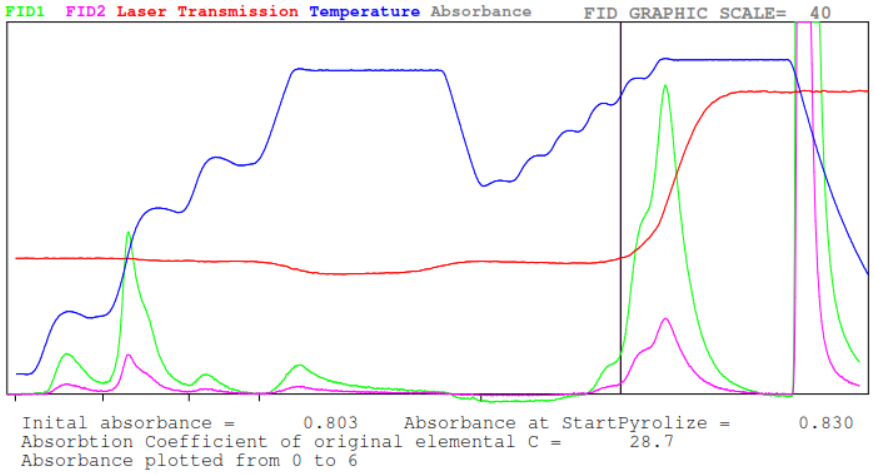

Figure A.51: Sample 10-E thermogram.

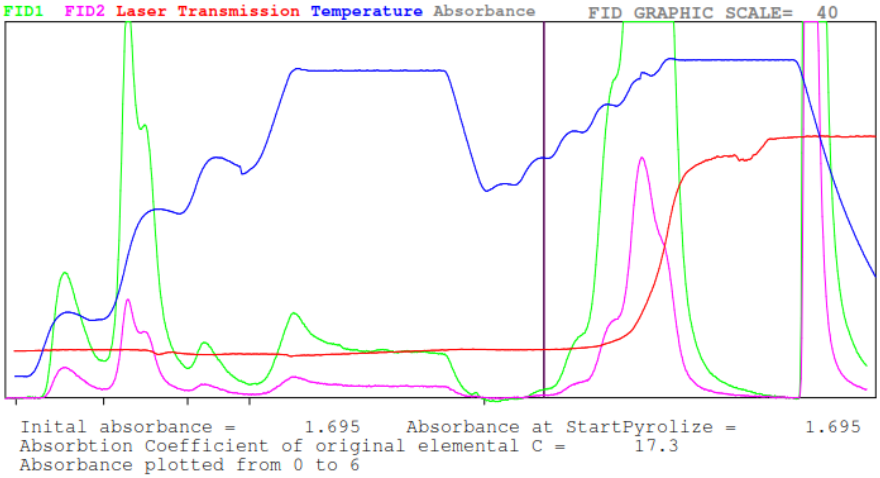

Figure A.52: Sample 11-A thermogram.

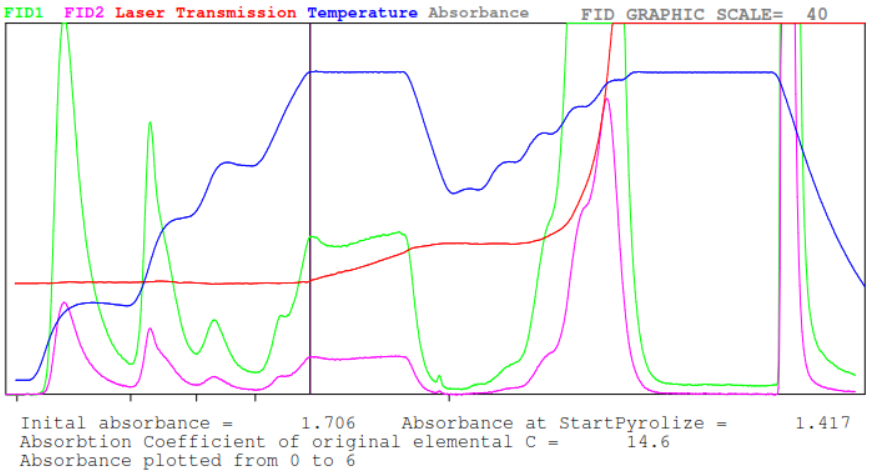

Figure A.53: Sample 11-B thermogram.

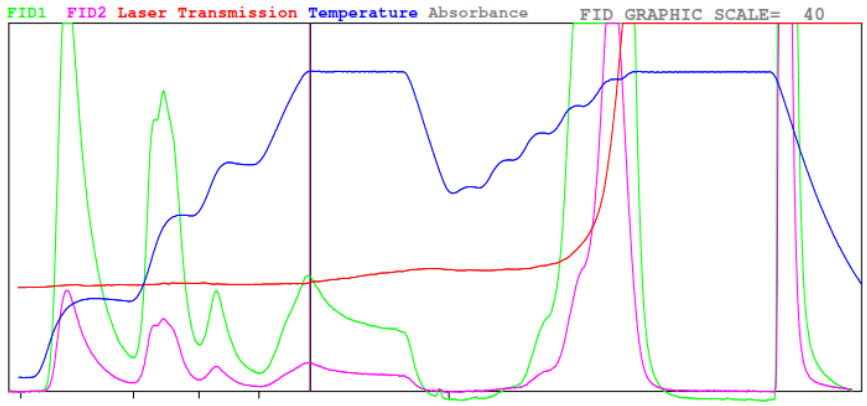

Figure A.54: Sample 11-C thermogram.

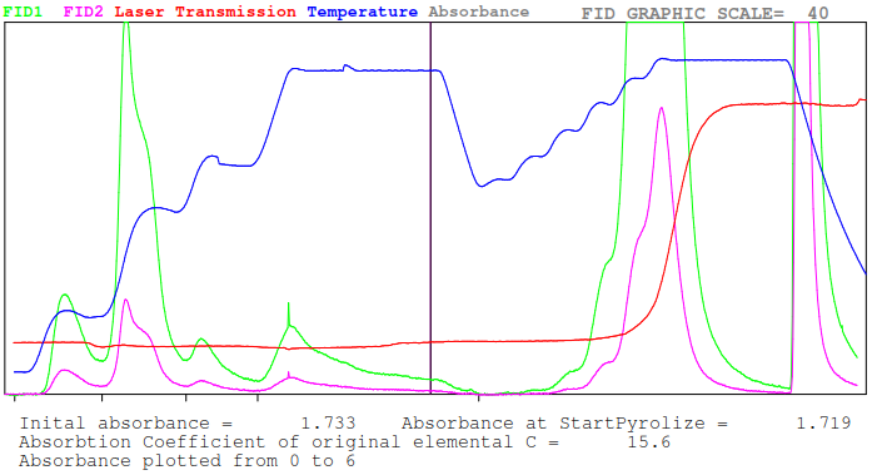

Figure A.55: Sample 11-D thermogram.

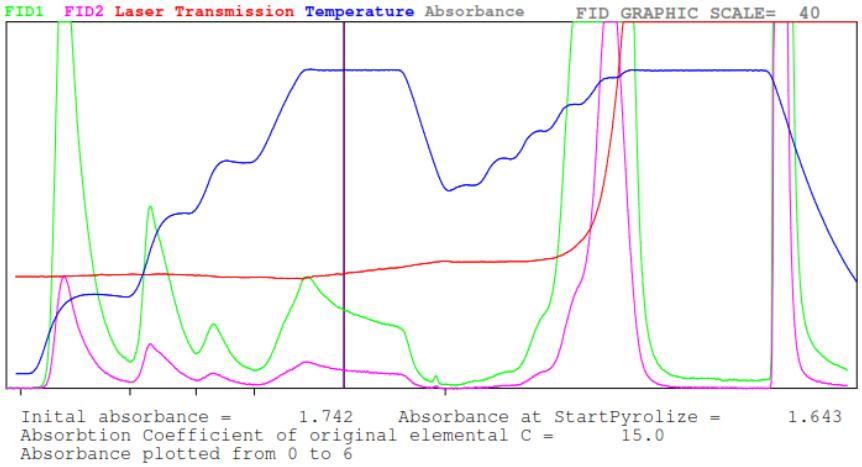

Figure A.56: Sample 11-E thermogram.

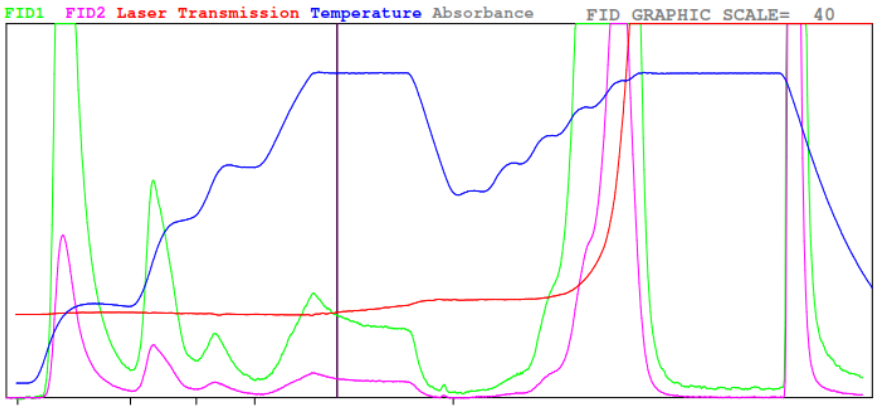

Inital absorbance = 2.118 Absorbance at StartPyrolize = 1.985
Absorbtion Coefficient of original elemental C = 16.4
Absorbance plotted from 0 to 6

Figure A.57: Sample 12-A thermogram.

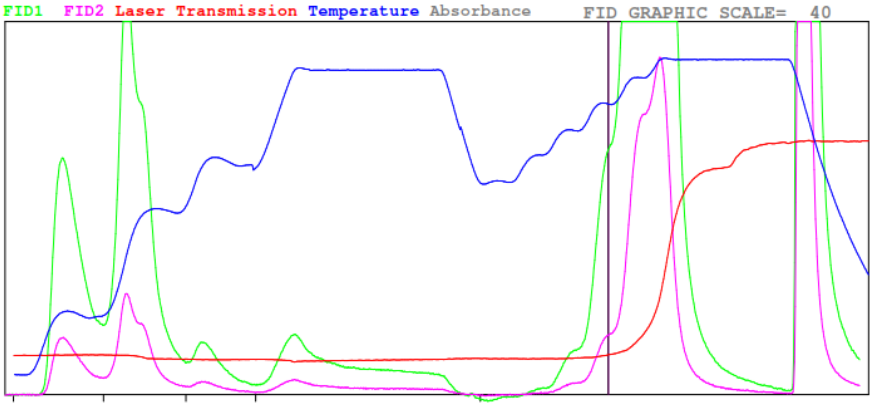

Inital absorbance = 1.863 Absorbance at StartPyrolize = 1.970
Absorbtion Coefficient of original elemental C = 15.5
Absorbance plotted from 0 to 6

Figure A.58: Sample 12-B thermogram.

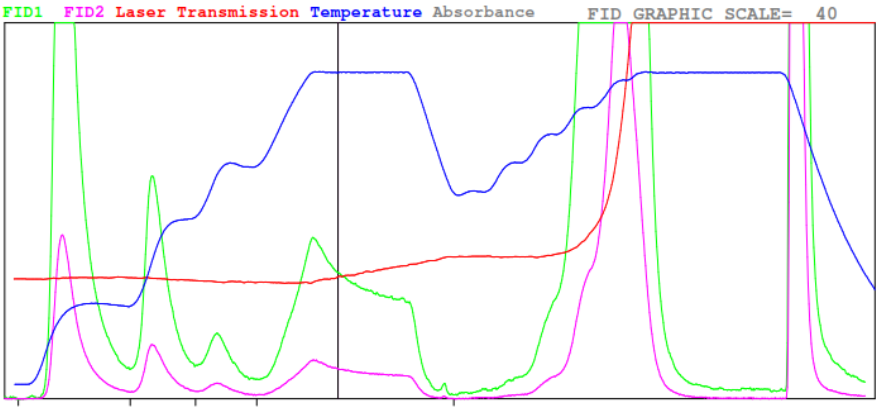

Inital absorbance = 1.953 Absorbance at StartPyrolize = 1.799
Absorbtion Coefficient of original elemental C = 14.9
Absorbance plotted from 0 to 6

Figure A.59: Sample 12-C thermogram.

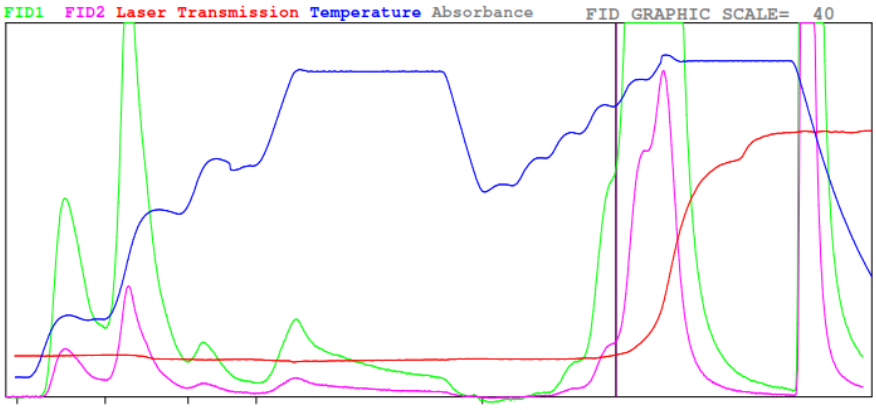

Figure A.60: Sample 12-D thermogram.

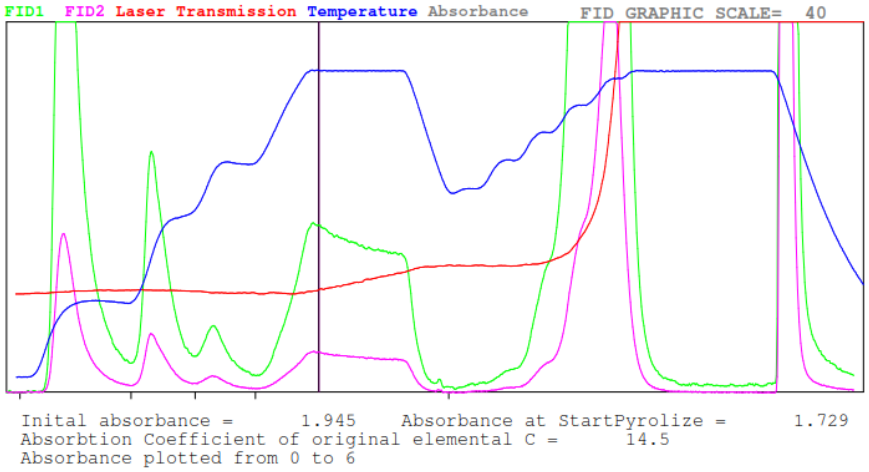

Figure A.61: Sample 12-E thermogram.

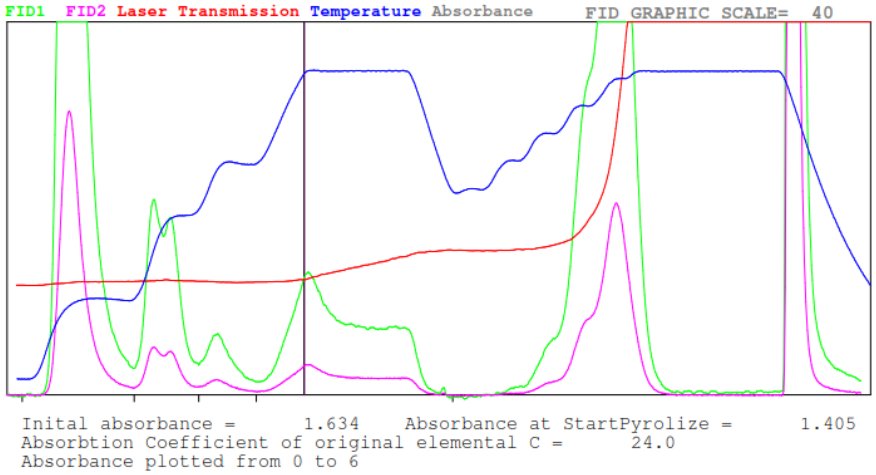

Figure A.62: Sample 13-A thermogram.

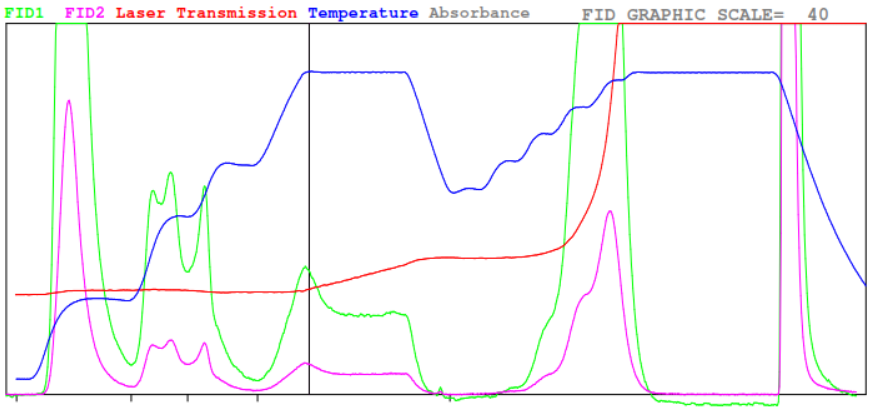

Figure A.63: Sample 13-B thermogram.

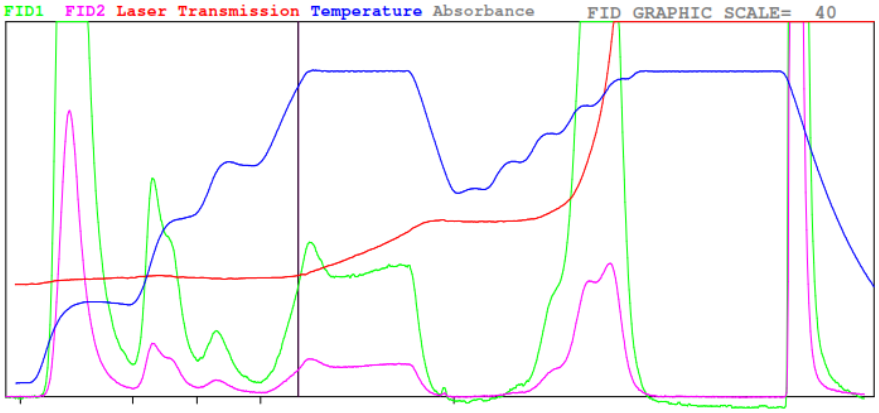

Figure A.645: Sample 13-C thermogram.

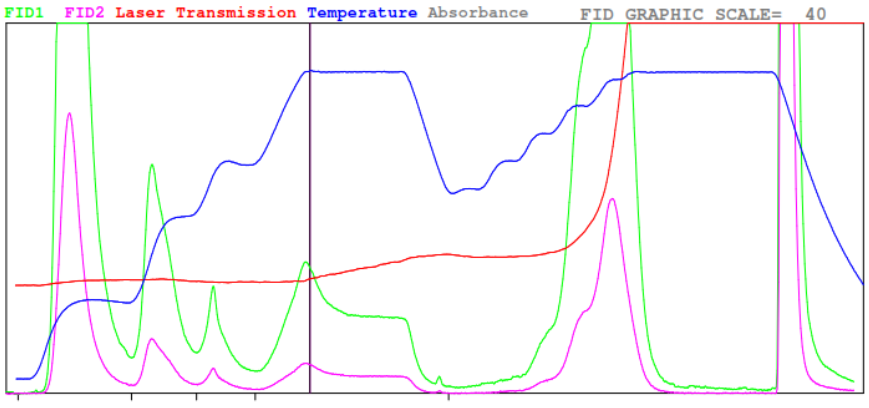

Figure A.65: Sample 13-D thermogram.

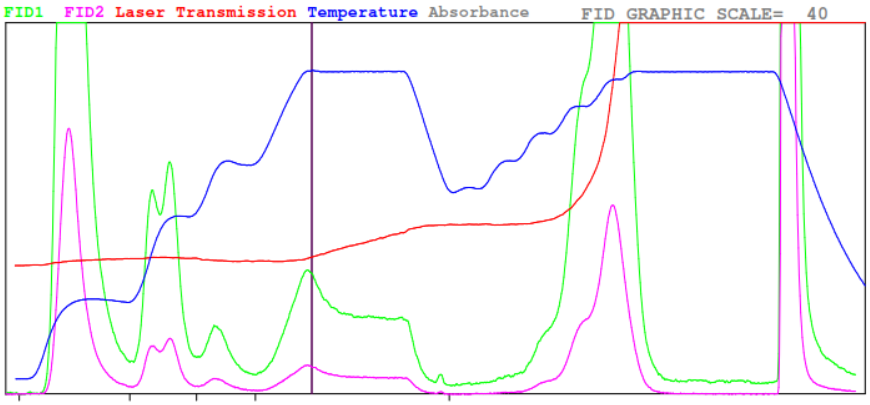

Figure A.666: Sample 13-E thermogram.

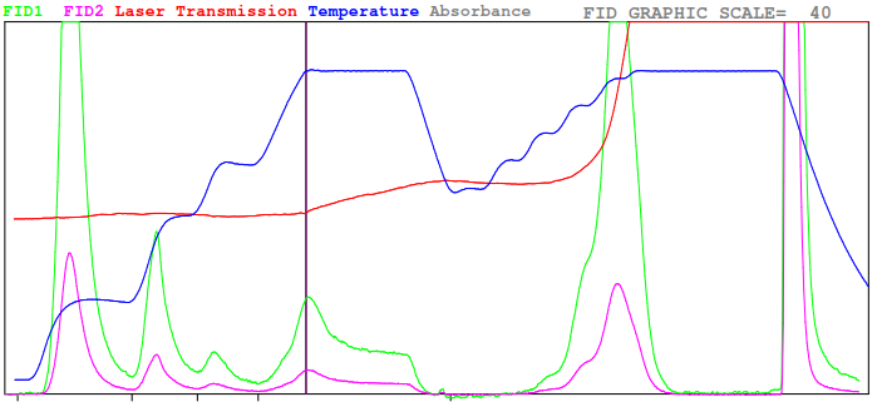

Figure A.67: Sample 14-A thermogram.

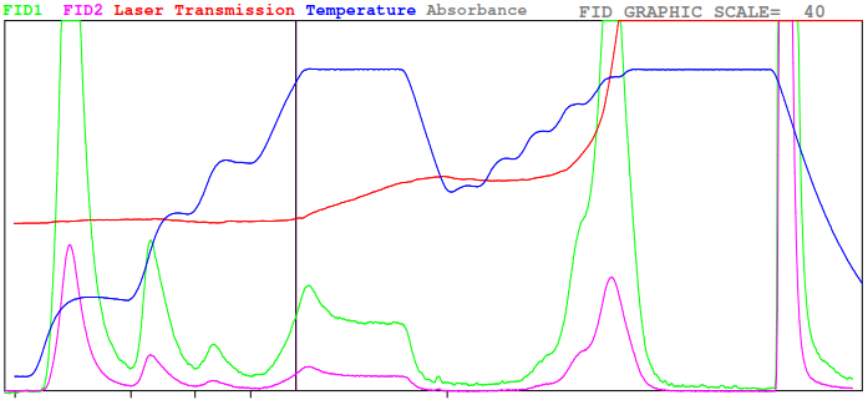

Figure A.68: Sample 14-B thermogram.

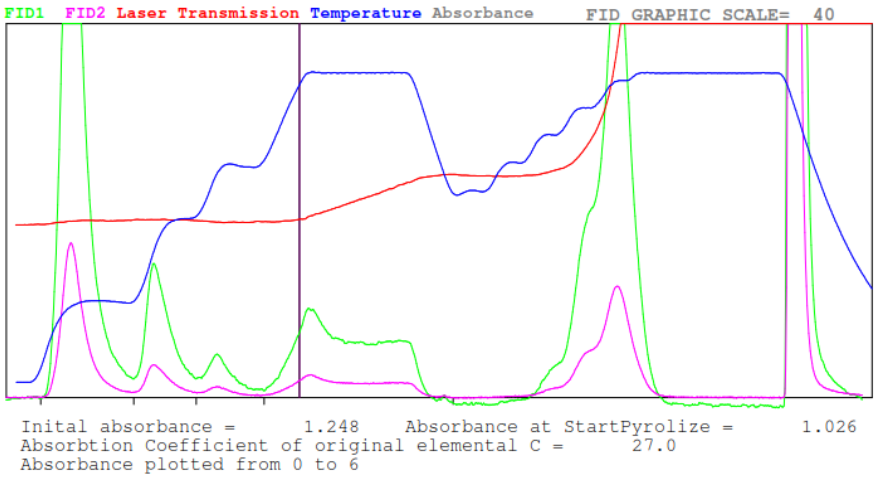

Figure A.69: Sample 14-C thermogram.

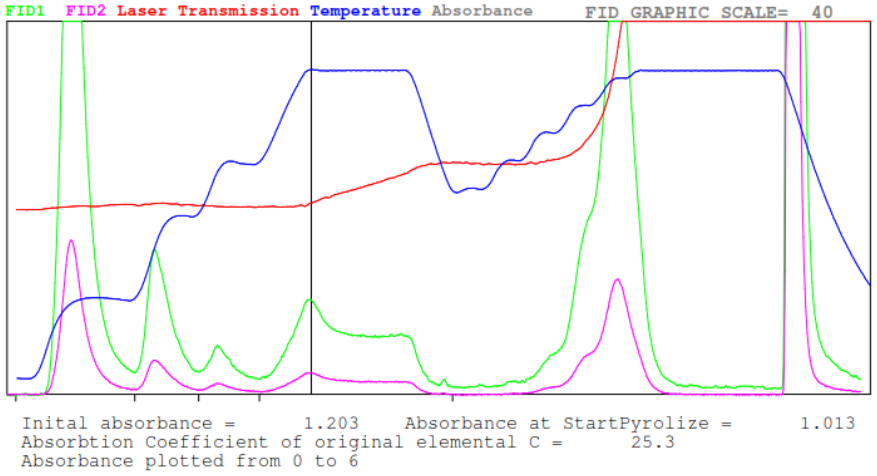

Figure A.70: Sample 14-D thermogram.

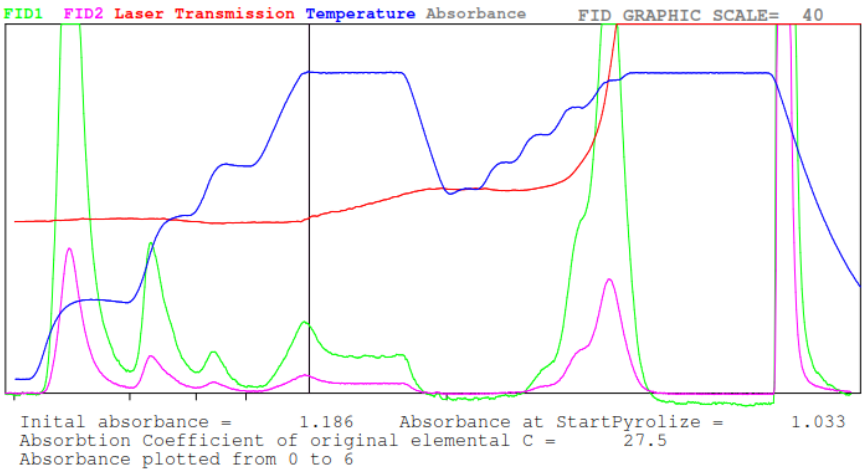

Figure A.71: Sample 14-E thermogram.

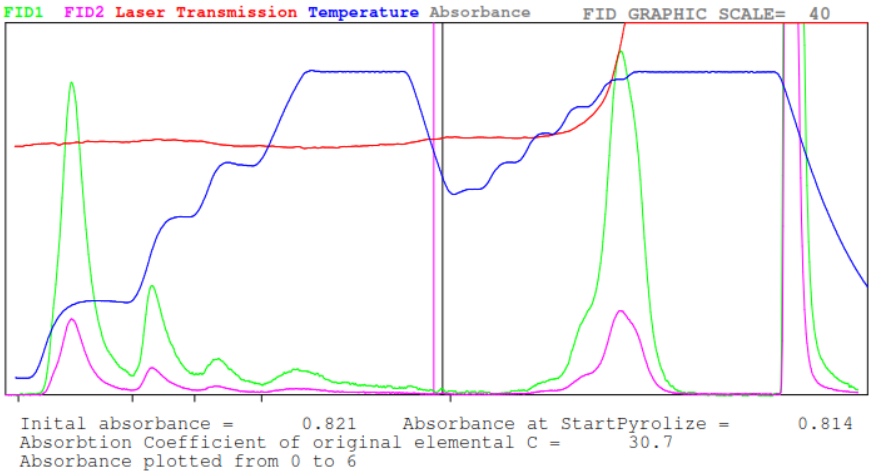

Figure A.72: Sample 15-A thermogram. Second punch analysis used.

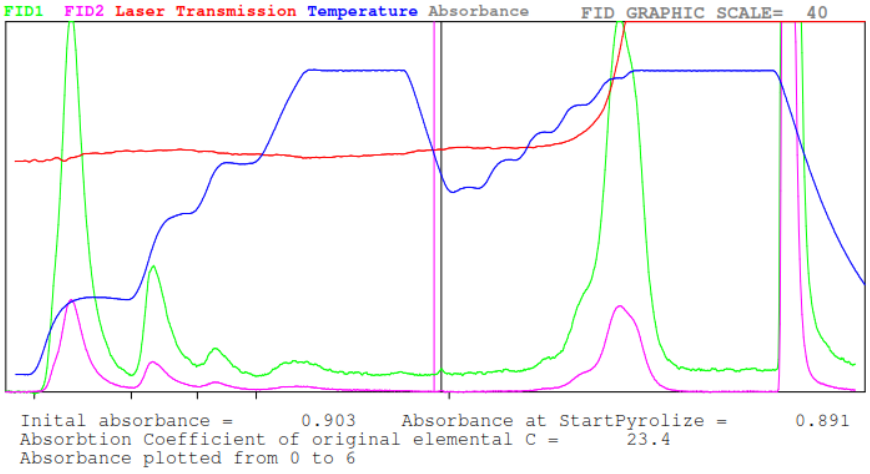

Figure A.73: Sample 15-B thermogram. Second punch analysis used.

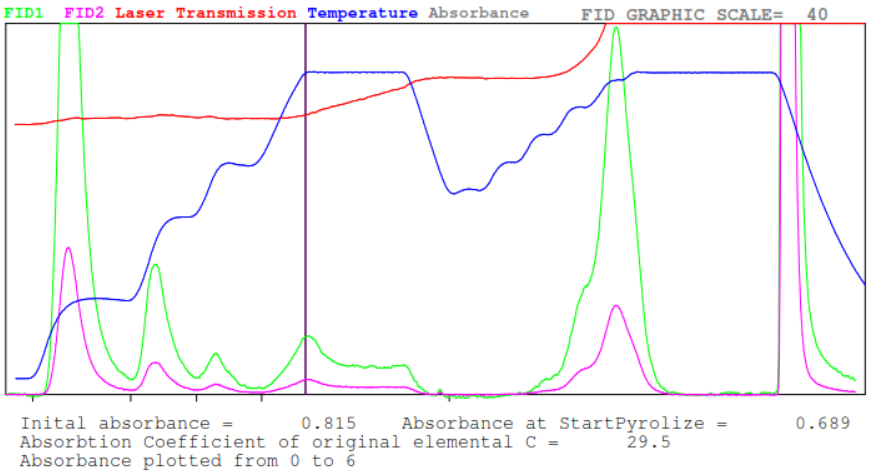

Figure A.74: Sample 15-C thermogram.

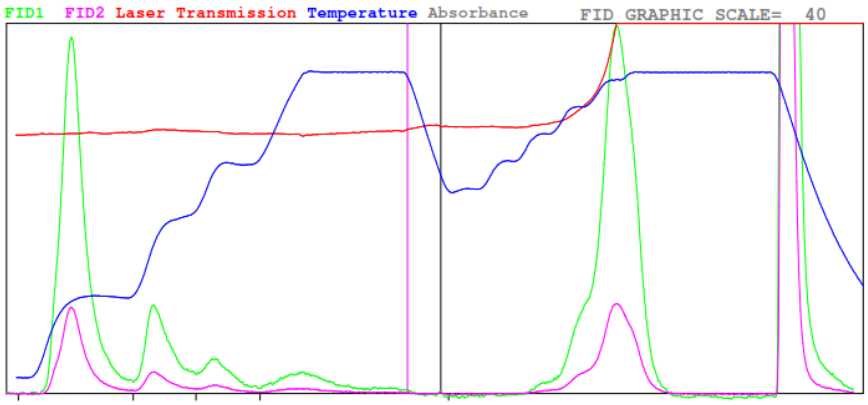

Inital absorbance = 0.831 Absorbance at StartPyrolize = 0.820
Absorbtion Coefficient of original elemental C = 31.5
Absorbance plotted from 0 to 6

Figure A.75: Sample 15-D thermogram. Second punch analysis used.

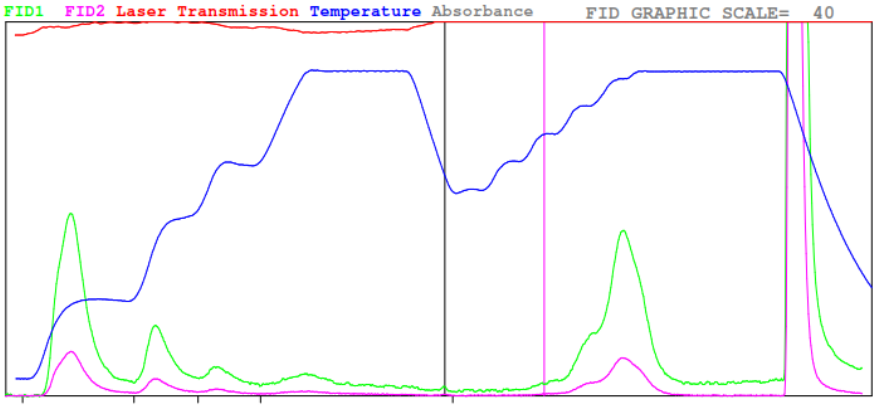

Inital absorbance = 0.447 Absorbance at StartPyrolize = 0.444
Absorbtion Coefficient of original elemental C = 28.3
Absorbance plotted from 0 to 6

Figure A.76: Sample 16-A thermogram. Second punch analysis used.

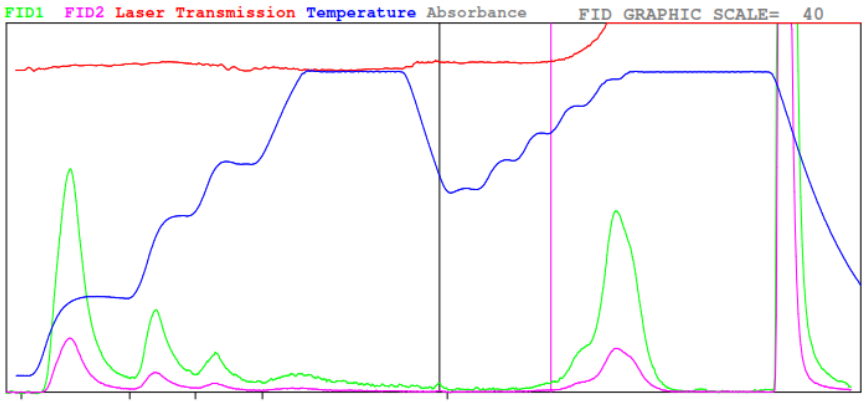

Inital absorbance = 0.529 Absorbance at StartPyrolize = 0.531
Absorbtion Coefficient of original elemental C = 36.8
Absorbance plotted from 0 to 6

Figure A.77: Sample 16-B thermogram. Second punch analysis used.

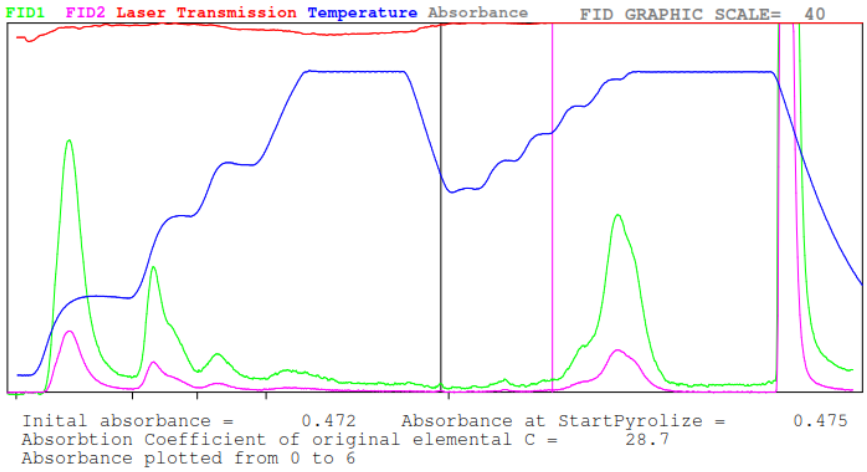

Figure A.78: Sample 16-C thermogram. Second punch analysis used.

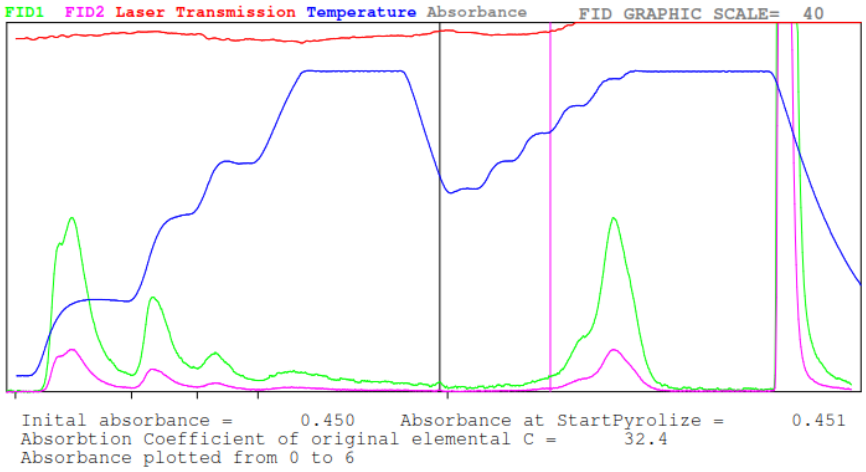

Figure A.79: Sample 16-D thermogram. Second punch analysis used.

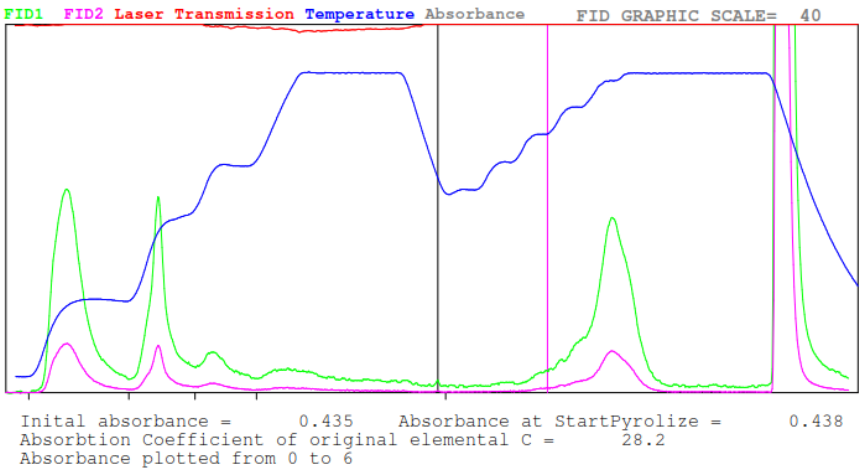

Figure A.80: Sample 16-E thermogram. Second punch analysis used.

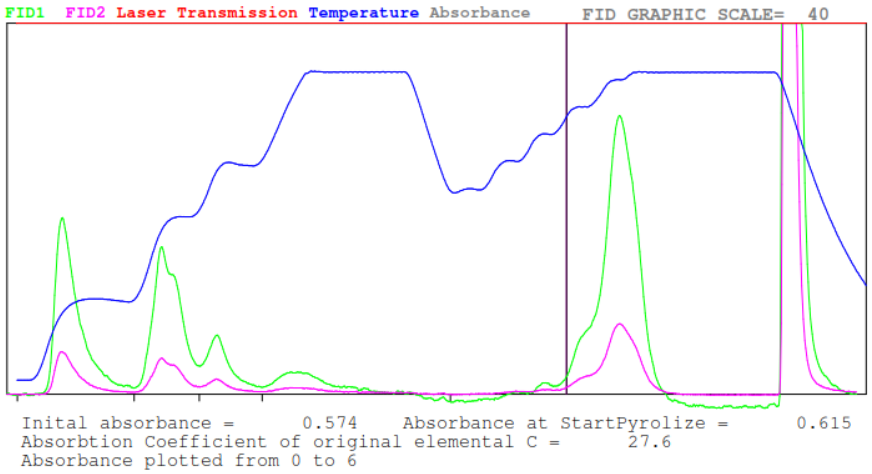

Figure A.81: Sample 17-A thermogram. Second punch analysis used.

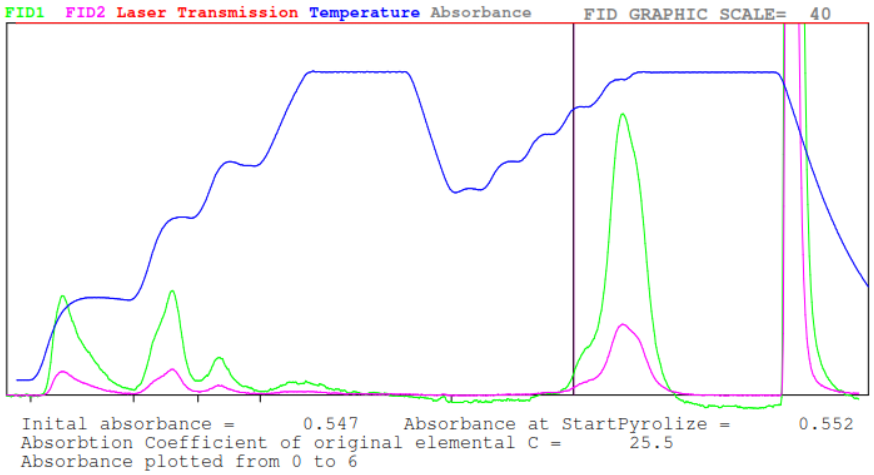

Figure A.82: Sample 17-B thermogram. Second punch analysis used.

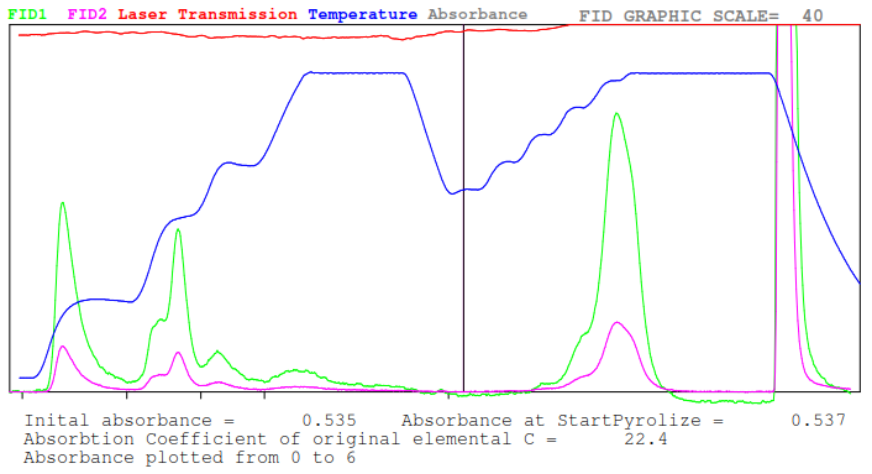

Figure A.83: Sample 17-C thermogram. Second punch analysis used.

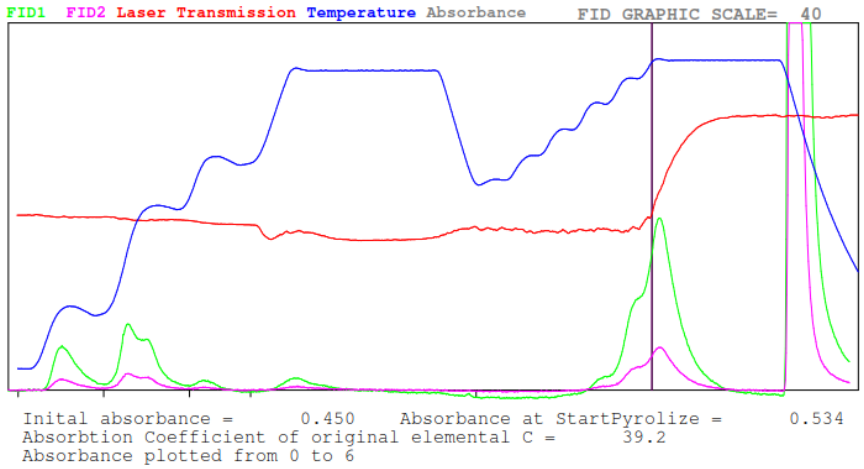

Figure A.84: Sample 17-D thermogram.

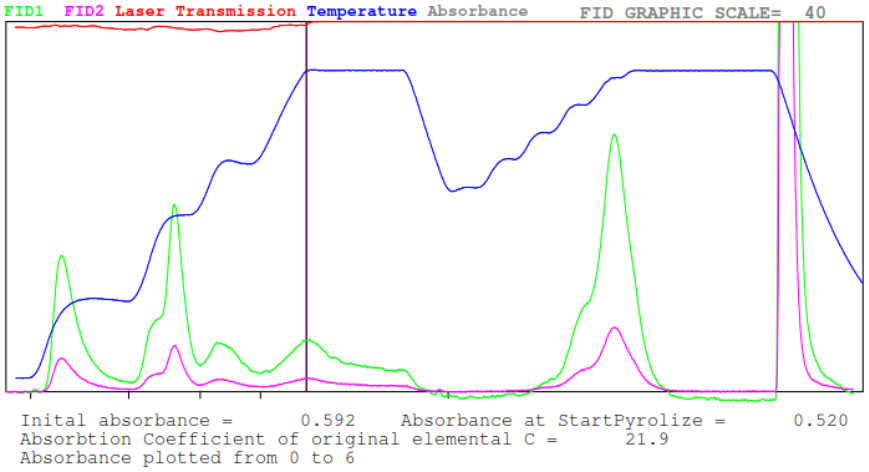

Figure A.85: Sample 17-E thermogram.

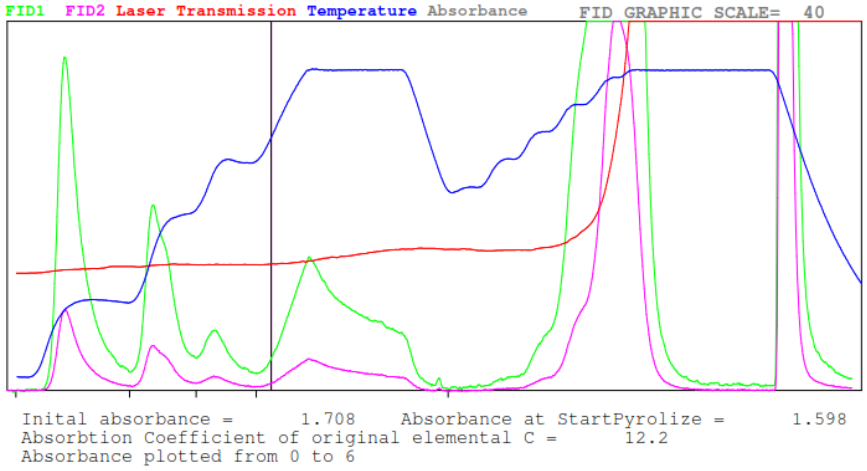

Figure A.86: Sample 18-A thermogram.

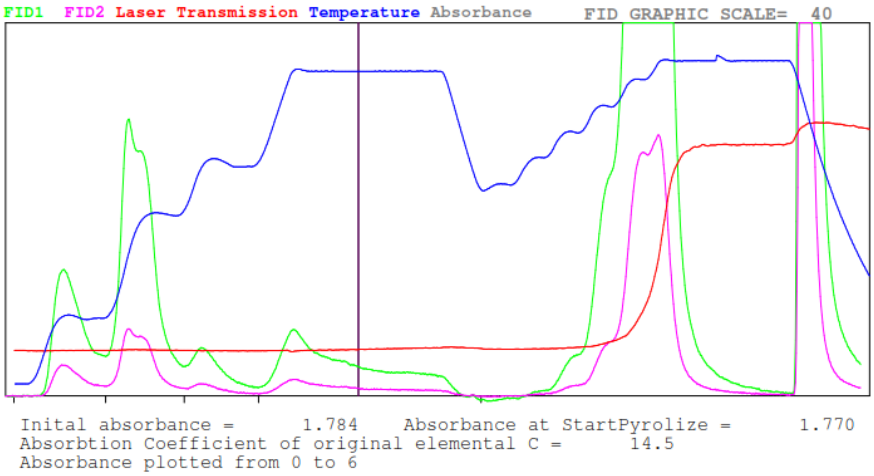

Figure A.87: Sample 18-B thermogram.

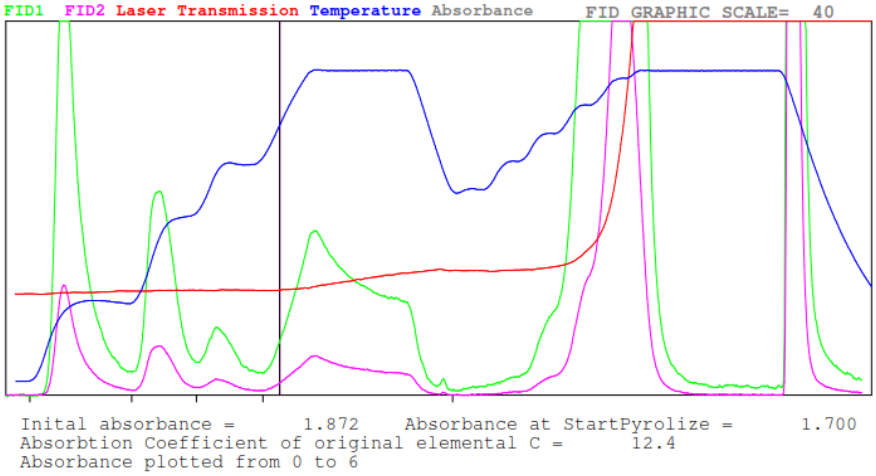

Figure A.88: Sample 18-C thermogram.

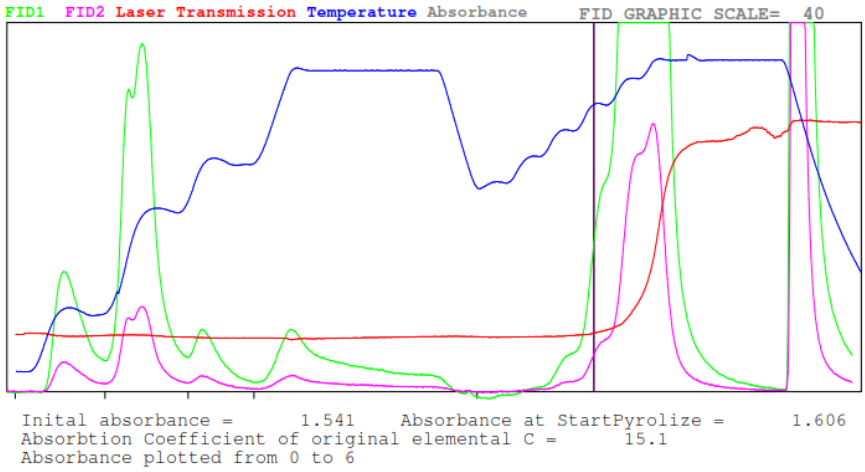

Figure A.89: Sample 18-D thermogram.

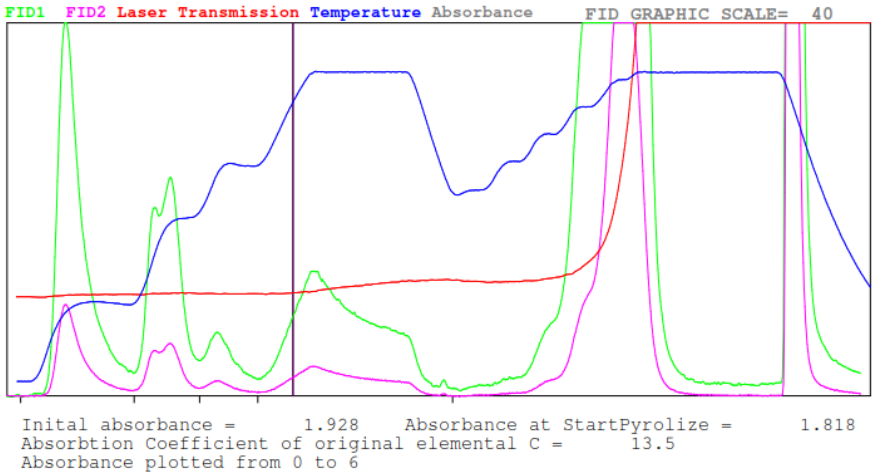

Figure A.90: Sample 18-E thermogram.

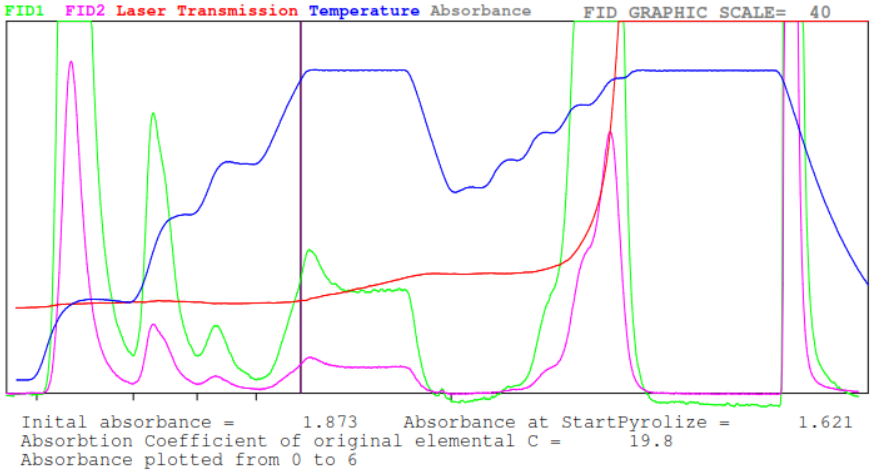

Figure A.91: Sample 19-A thermogram.

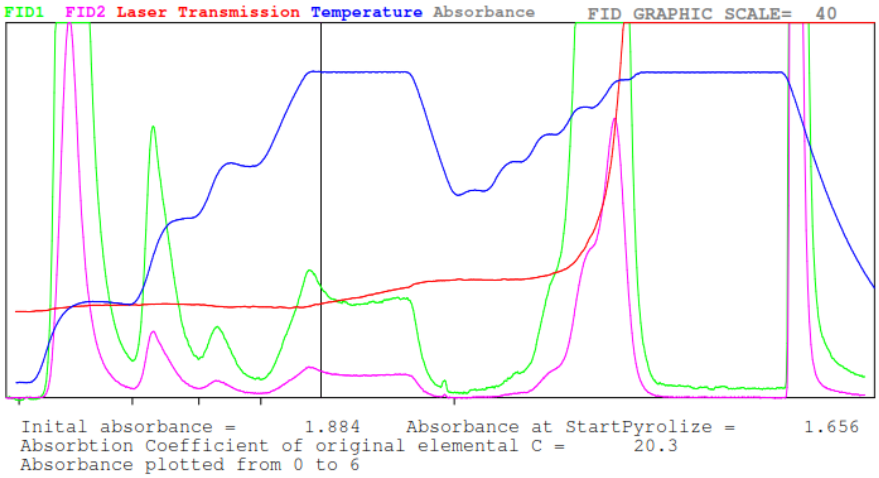

Figure A.92: Sample 19-B thermogram.

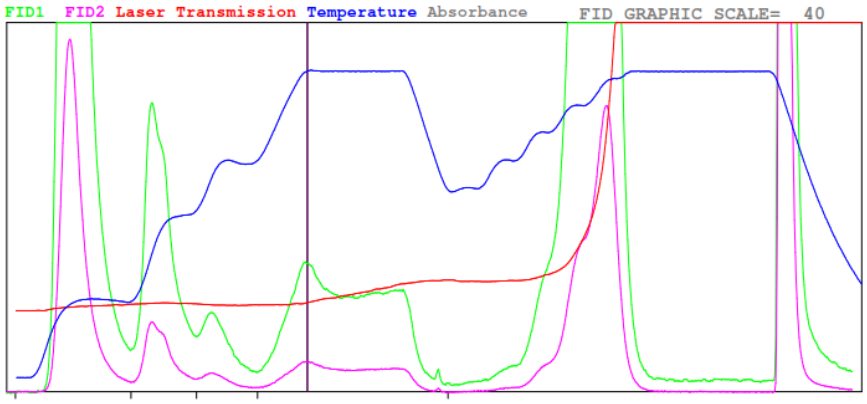

Figure A.93: Sample 19-C thermogram.

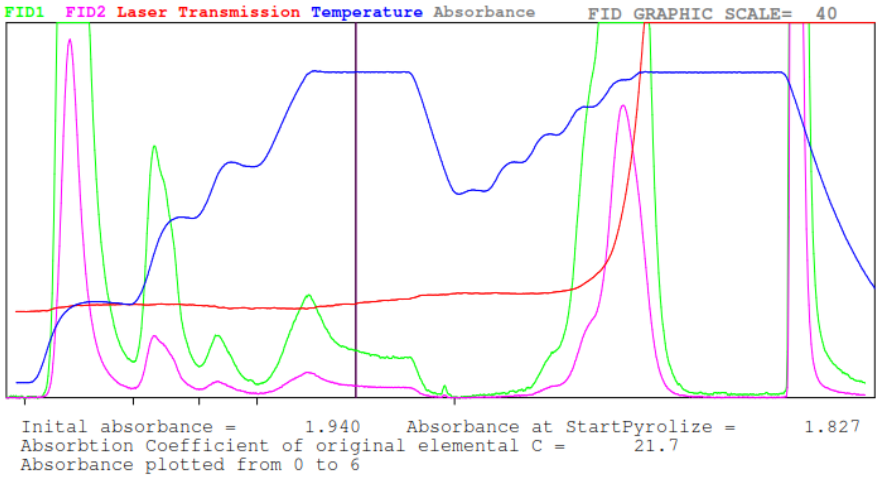

Figure A.94: Sample 19-D thermogram.

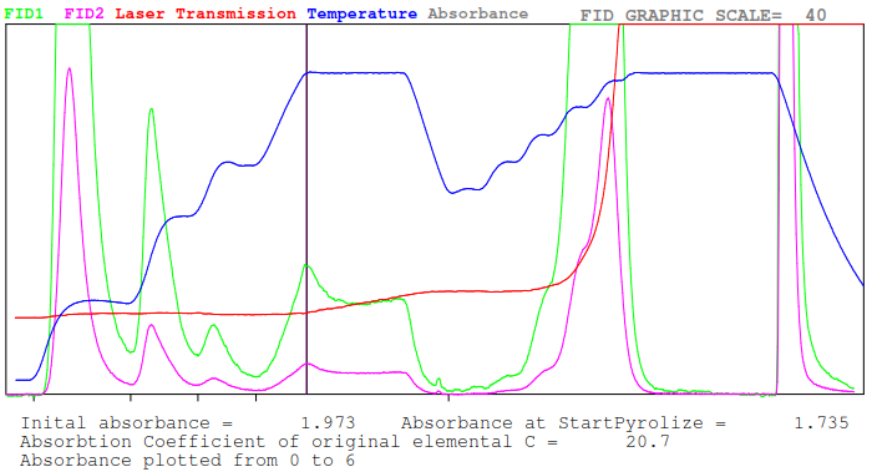

Figure A.95: Sample 19-E thermogram.

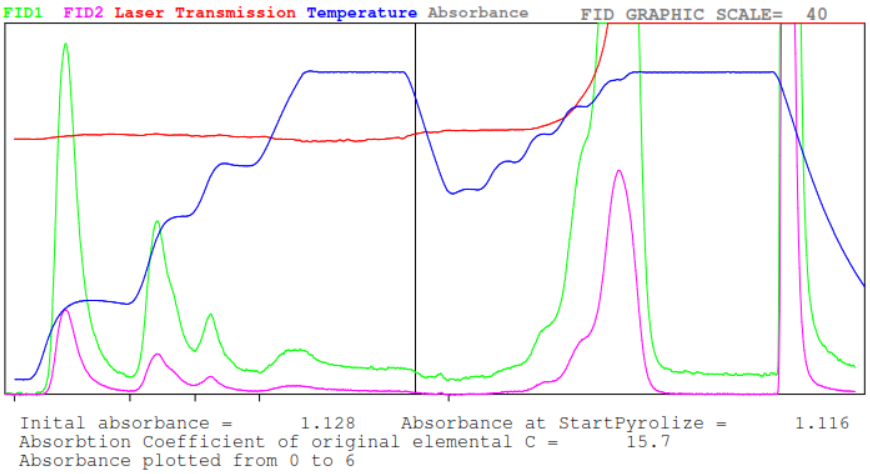

Figure A.96: 9.29.2017 unit 1 field sample thermogram.

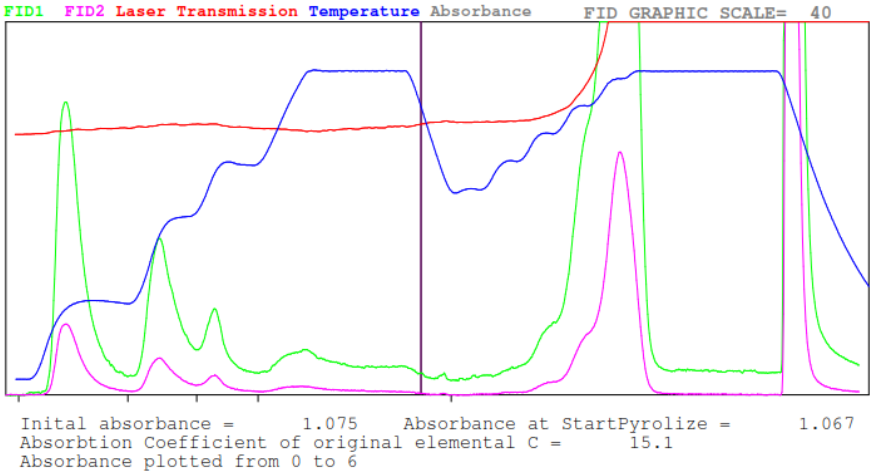

Figure A.97: 9.29.2017 unit 2 field sample thermogram.

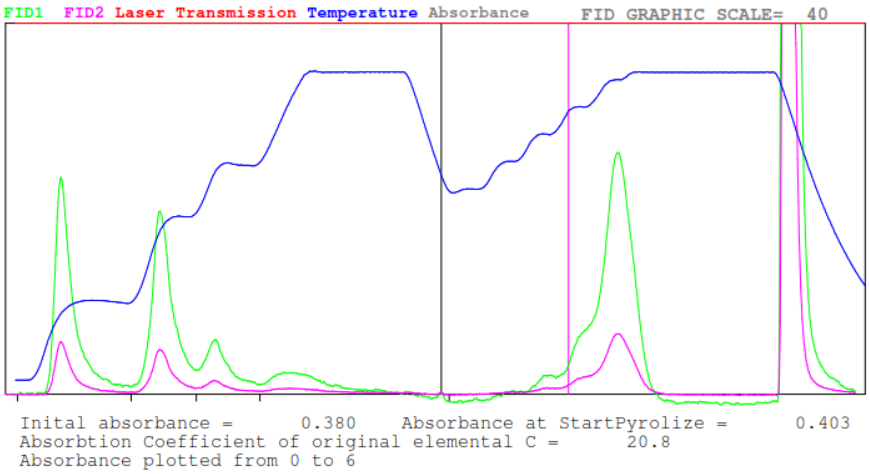

Figure A.98: 10.02.2017 unit 1 field sample thermogram.

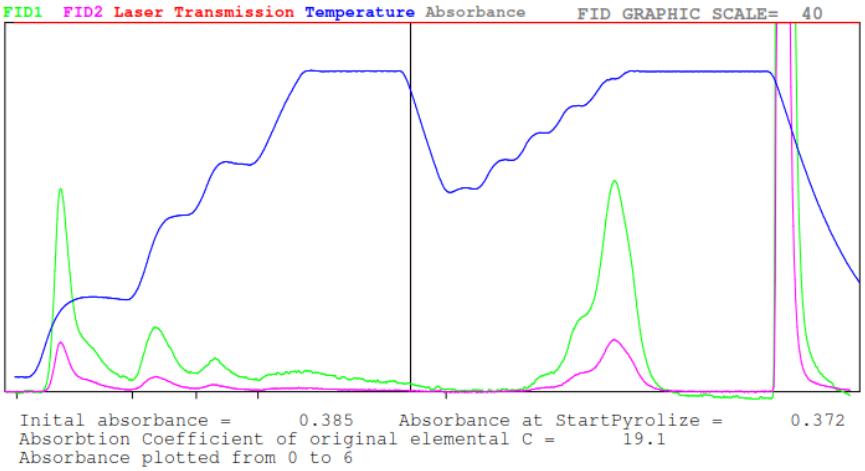

Figure A.99: 10.02.2017 unit 2 field sample thermogram.

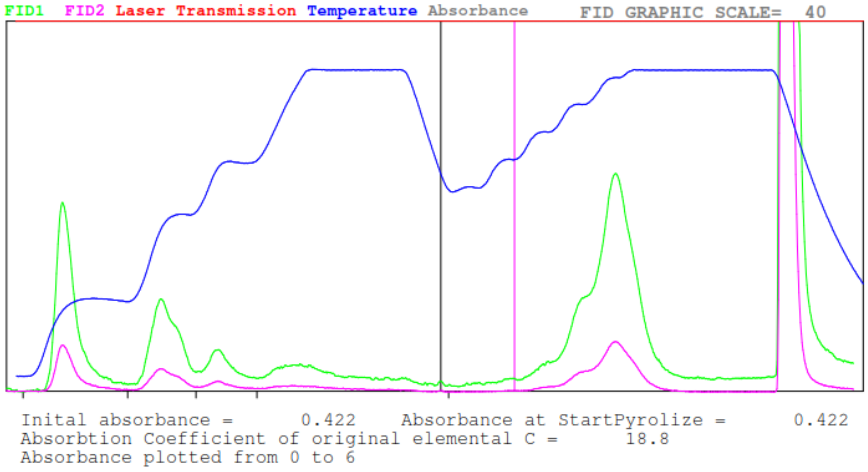

Figure A.100: 10.02.2017 unit 3 field sample thermogram.

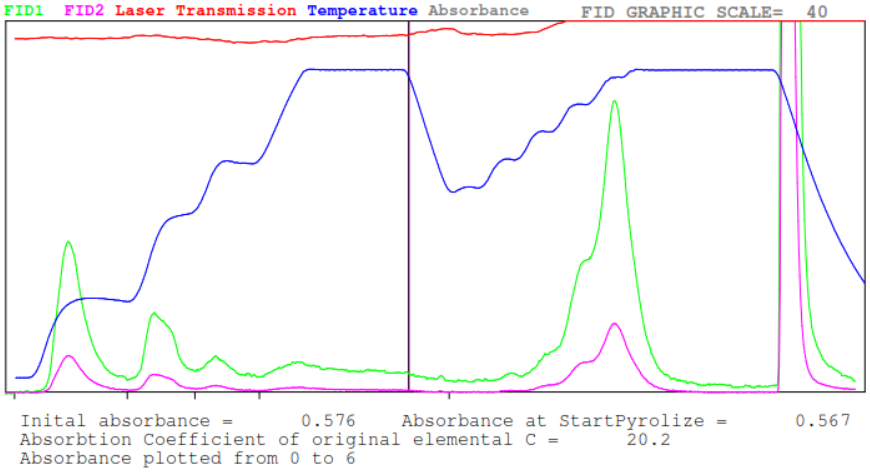

Figure A.101: 10.09.2017 unit 1 field sample thermogram.

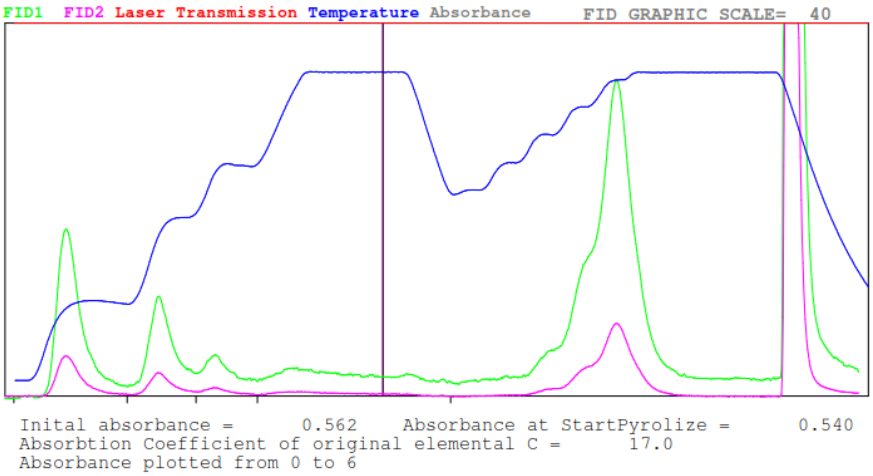

Figure A.102: 10.09.2017 unit 2 field sample thermogram.

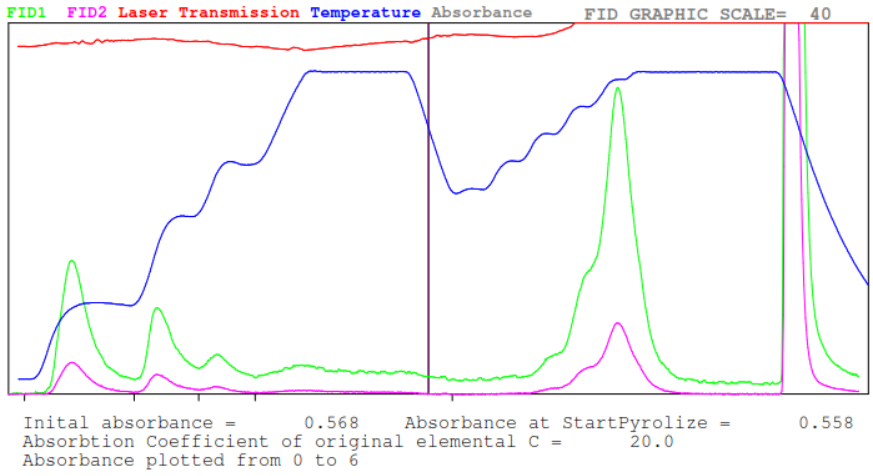

Figure A.103: 10.09.2017 unit 3 field sample thermogram.

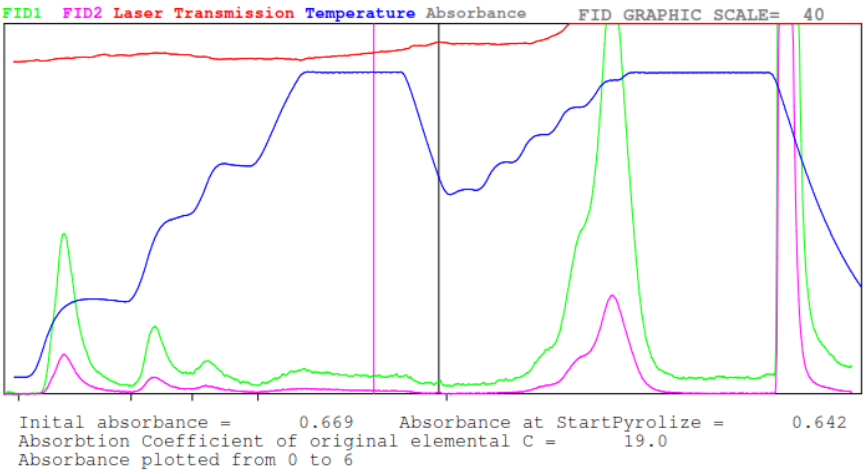

Figure A.104: 10.27.2017 unit 1 field sample thermogram.

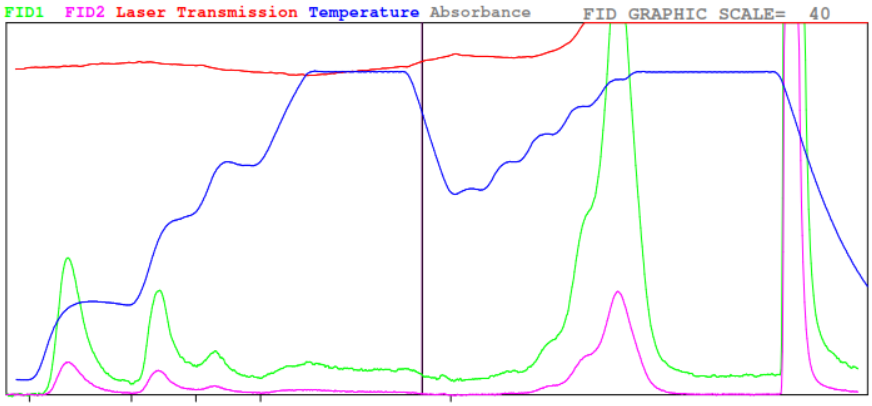

Figure A.105: 10.27.2017 unit 2 field sample thermogram.

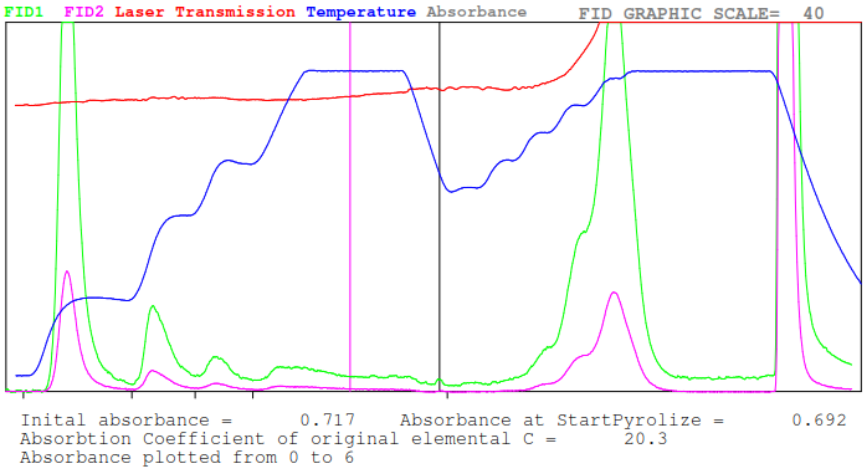

Figure A.106: 10.27.2017 unit 3 field sample thermogram.

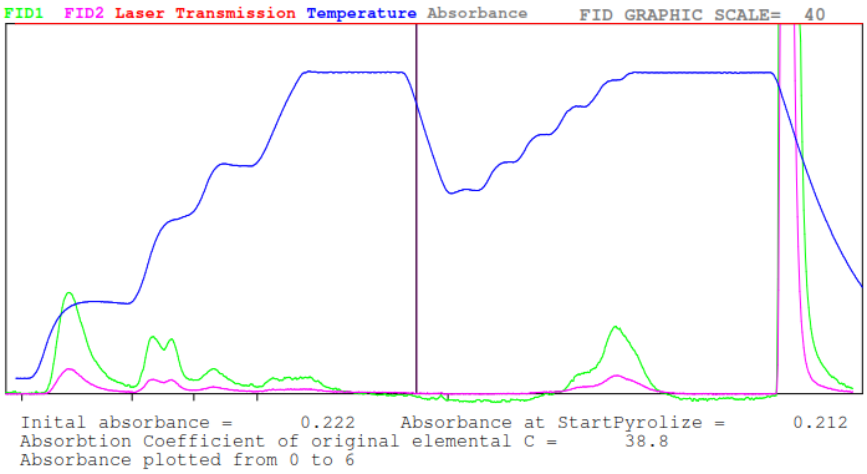

Figure A.107: 10.30.2017 unit 1 field sample thermogram.

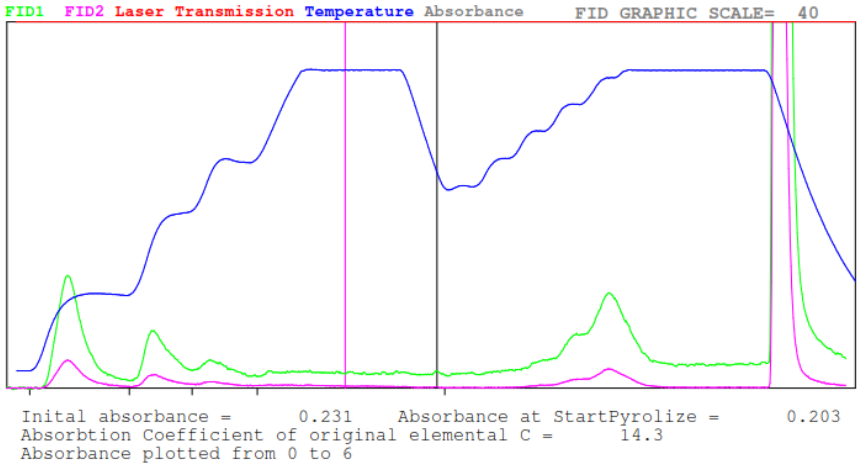

Figure A.108: 10.30.2017 unit 2 field sample thermogram. Second punch analysis used.

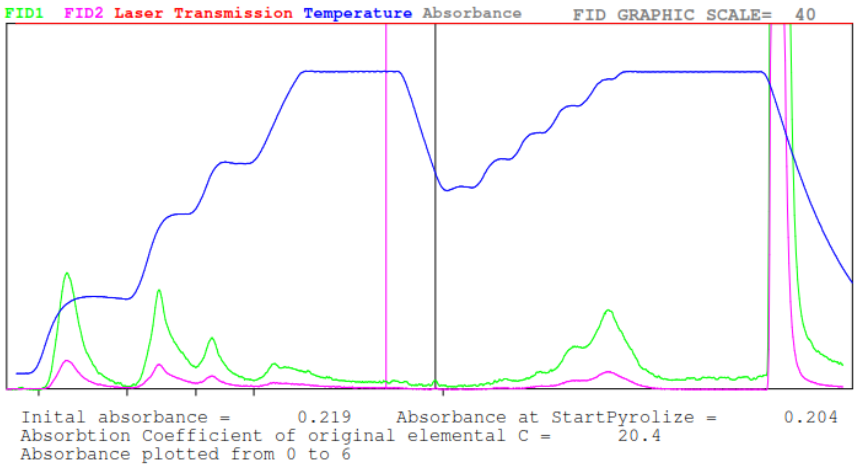

Figure A.109: 10.30.2017 unit 3 field sample thermogram.

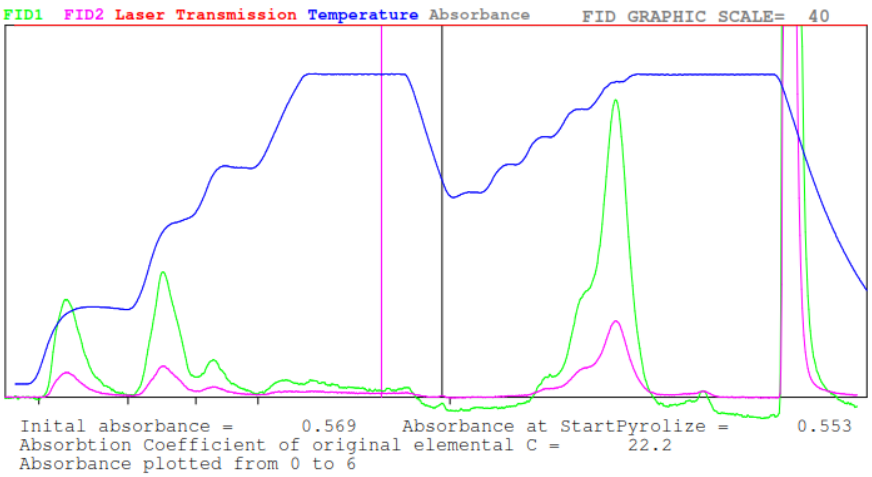

Figure A.110: 11.02.2017 unit 1 field sample thermogram.

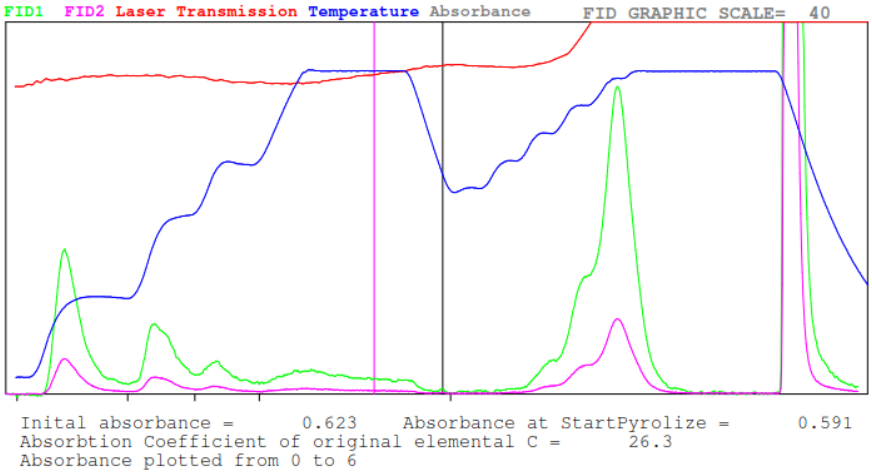

Figure A.111: 11.02.2017 unit 2 field sample thermogram. Second punch analysis used.

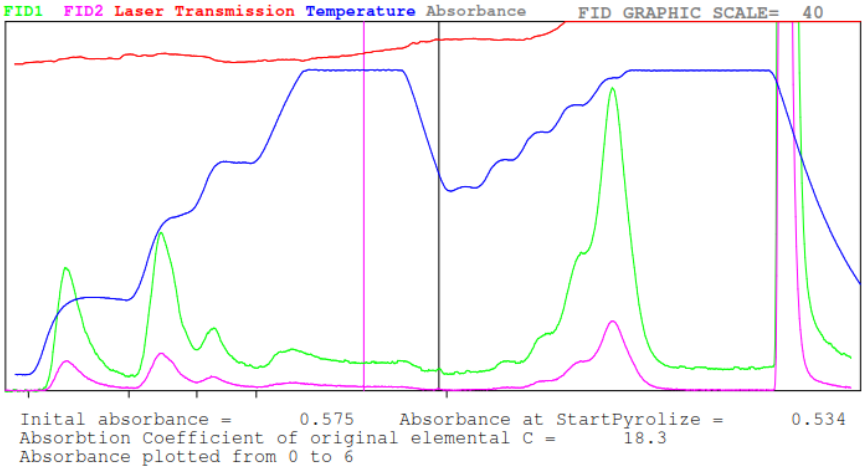

Figure A.112: 11.02.2017 unit 3 field sample thermogram.

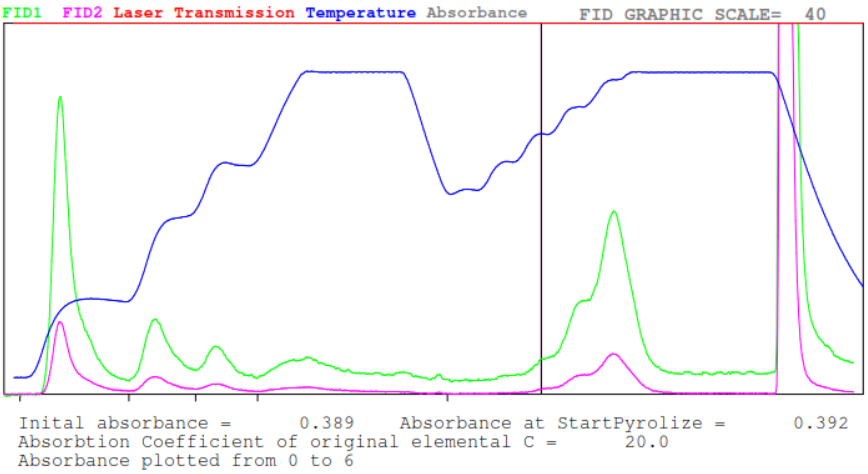

Figure A.113: 11.06.2017 unit 1 field sample thermogram.

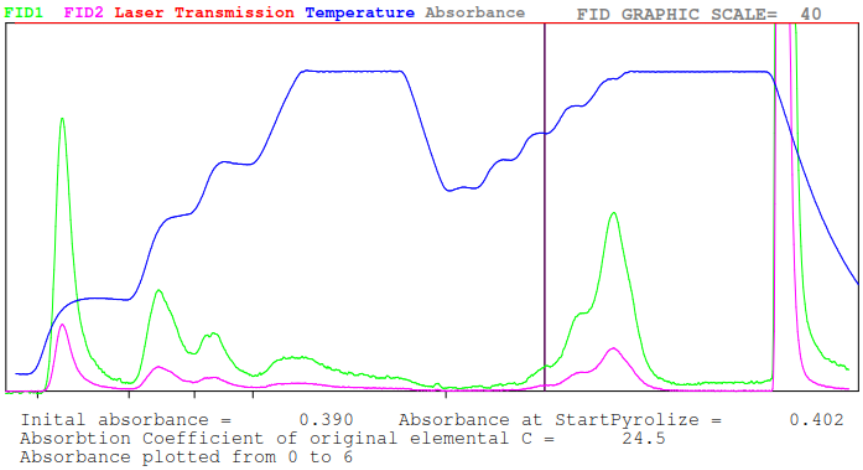

Figure A.114: 11.06.2017 unit 2 field sample thermogram. Second punch analysis used.

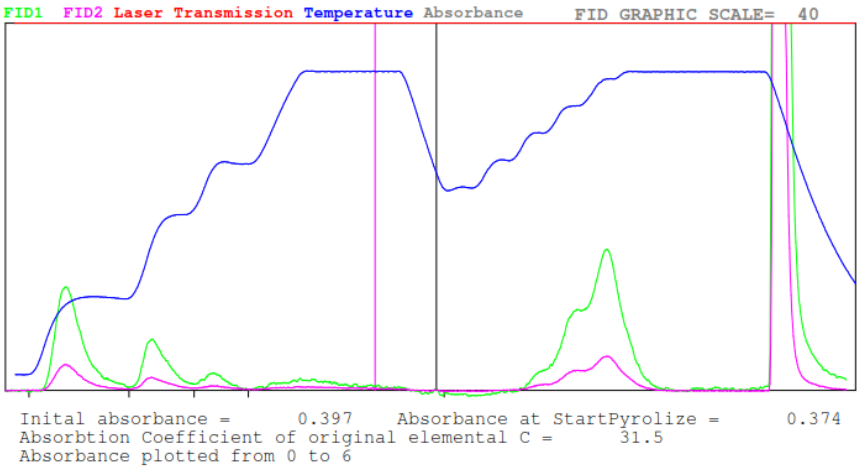

Figure A.115: 11.06.2017 unit 3 field sample thermogram.

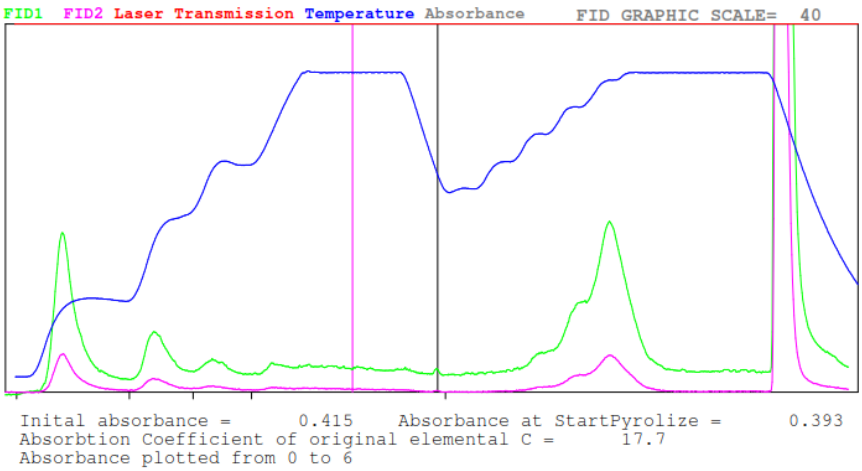

Figure A.116: 11.10.2017 unit 1 field sample thermogram.

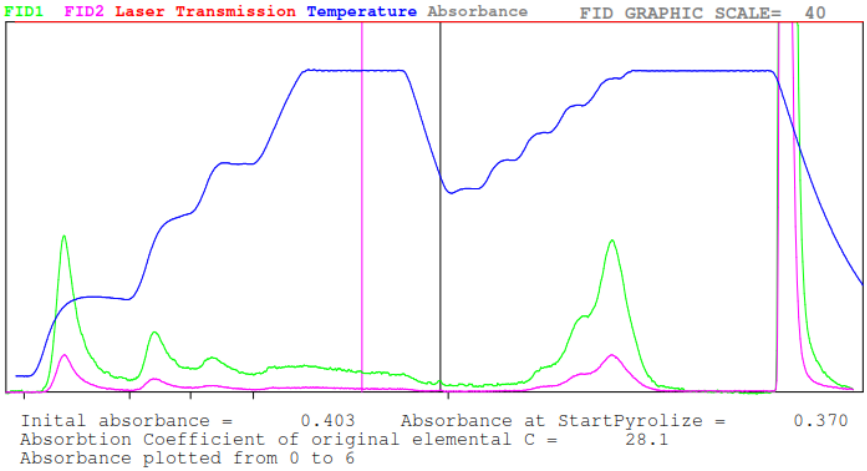

Figure A.117: 11.10.2017 unit 2 field sample thermogram.

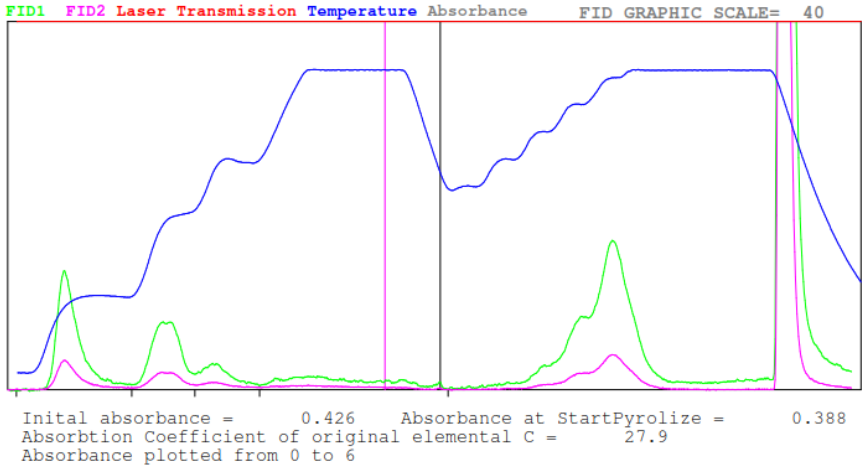

Figure A.118: 11.10.2017 unit 3 field sample thermogram.

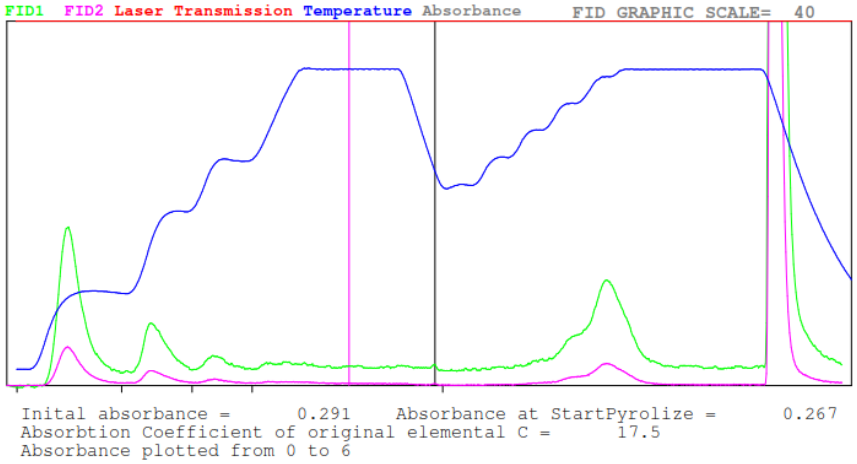

Figure A.119: 11.13.2107 unit 1 field sample thermogram.

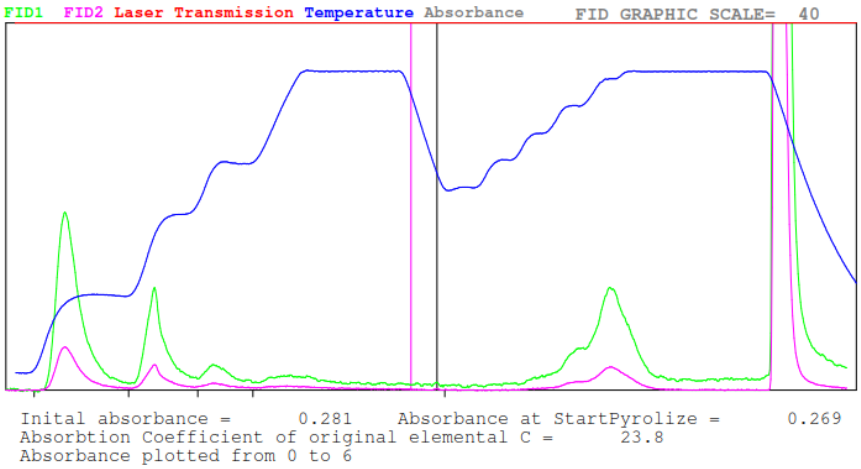

Figure A.120: 11.13.2017 unit 2 field sample thermogram.

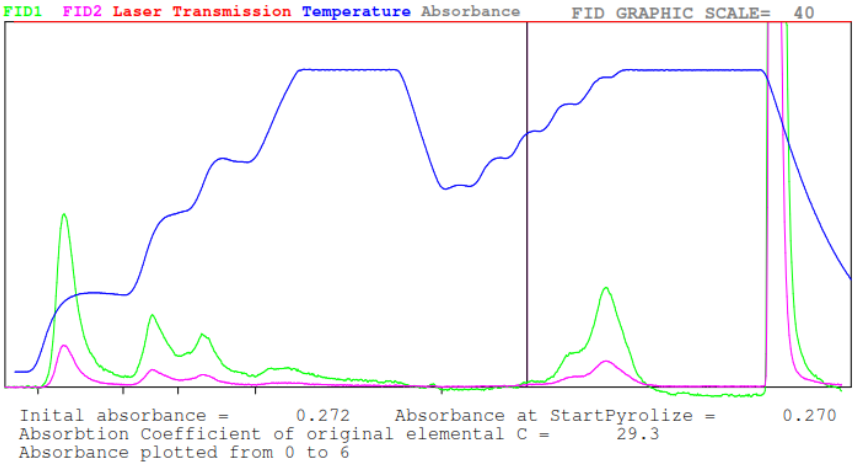

Figure A.121: 11.13.2017 unit 3 field sample thermogram.

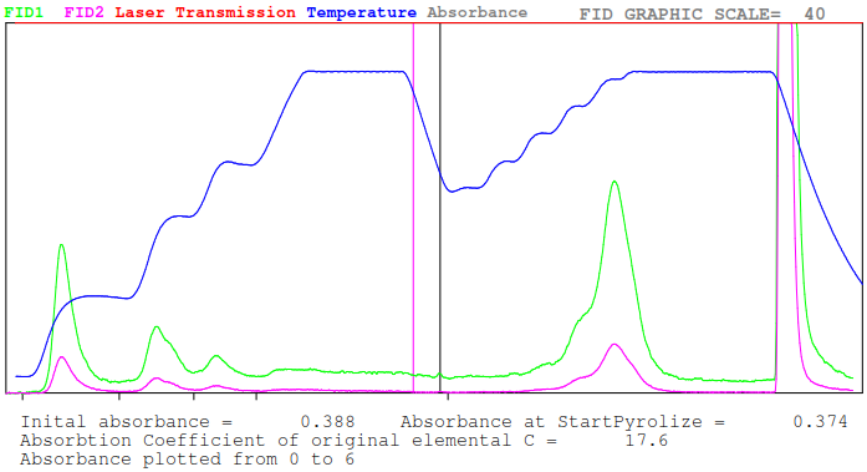

Figure A.122: 11.17.2017 unit 1 field sample thermogram.

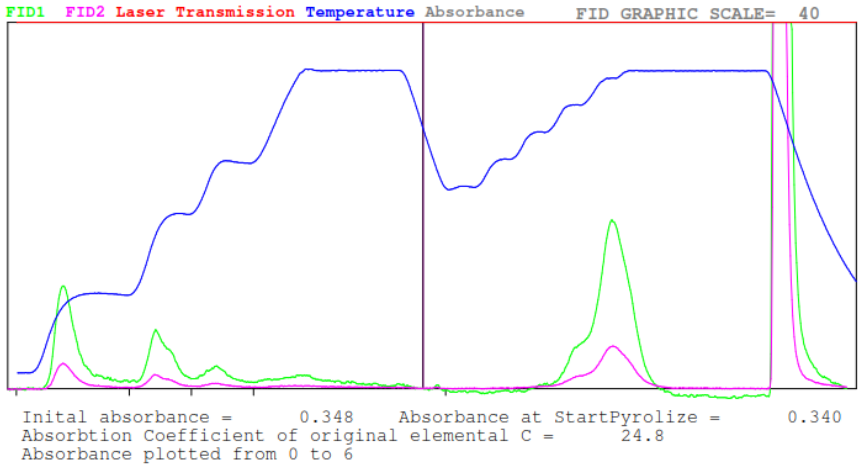

Figure A.123: 11.17.2017 unit 2 field sample thermogram.

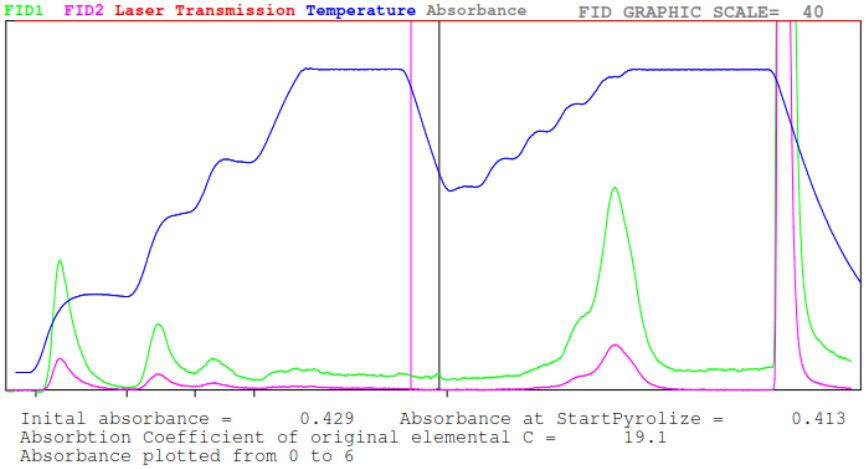

Figure A.124: 11.17.2017 unit 3 field sample thermogram.

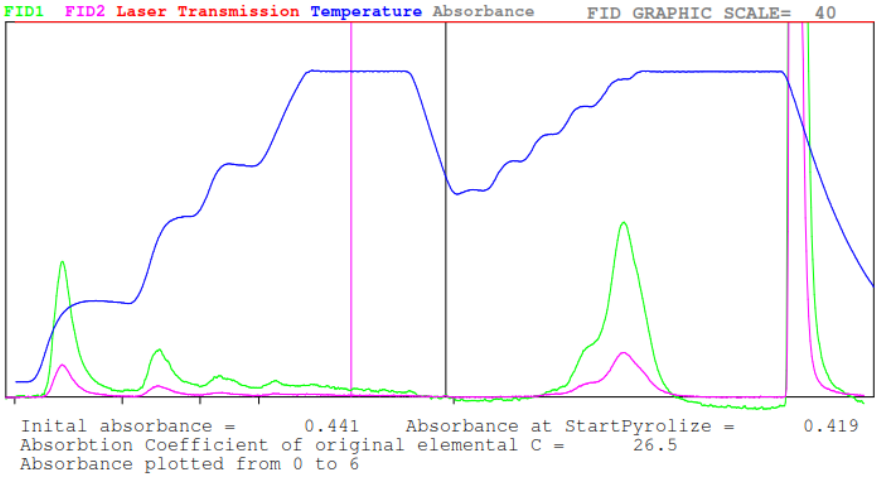

Figure A.125: 11.20.2017 unit 1 field sample thermogram.

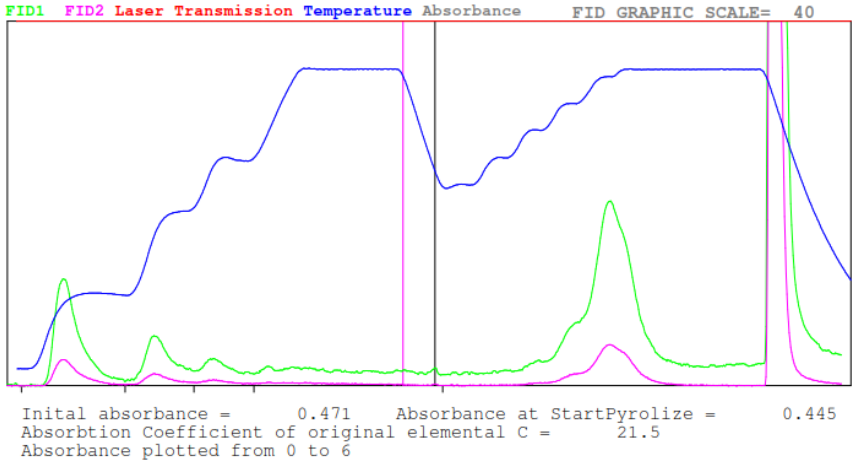

Figure A.126: 11.20.2017 unit 2 field sample thermogram.

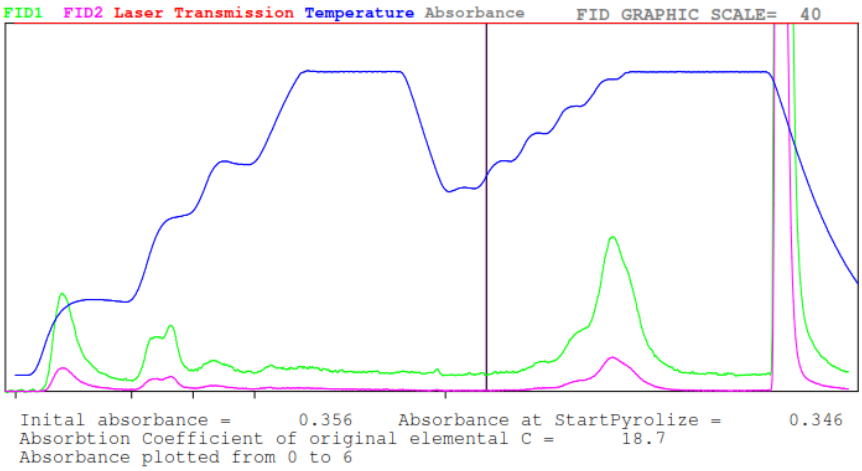

Figure A.127: 11.20.2017 unit 3 field sample thermogram.